

FILMWISE CONDENSATION IN A VERTICAL TUBE
IN COUNTER-CURRENT AND CO-CURRENT FLOW

By

SOMPORN KOMOLSIRIKUL

Bachelor of Science

Chulalongkorn University

Bangkok, Thailand

1988

Submitted to the Faculty of the
Graduate College of the
Oklahoma State University
in partial fulfillment of
the requirements for
the Degree of
MASTER OF SCIENCE
July, 1991

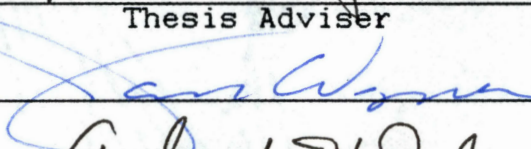
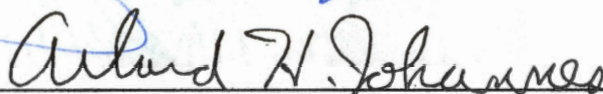
Theo12
1991
K816
cop. 2


FILMWISE CONDENSATION IN A VERTICAL TUBE
IN COUNTER-CURRENT AND CO-CURRENT FLOW

Thesis Approved:



Thesis Adviser


Dean of the Graduate College

PREFACE

Condensation of steam in a vertical reflux condenser was studied for both co-current and counter-current flow of the vapor and condensate. The condenser was composed of three sections in series. The cooling water flowed inside the annular jackets, while the steam was in the inner tube.

This was only a preliminary study of heat transfer, including the condensing heat transfer coefficient and the heat transfer coefficient in the annulus.

The present study covered a range of cooling water Reynolds numbers from 460 to 3,800 based on the equivalent diameter. Entering steam Reynolds numbers ranged from 4.1×10^5 to 1.2×10^6 , while the exit condensate Reynolds numbers ranged from 30 to 450. From experimental data, the condensing heat transfer coefficient, the annular heat transfer coefficient, and conduction heat transfer through the pyrex glass wall were calculated from heat transfer correlations, and then compared to the ones obtained from the Wilson Line Method applied to the data. In addition, for counter-current flow, the flooding point was also computed by the Diehl-Koppany and Wallis correlations.

I wish to express my sincere gratitude to Dr. Kenneth J. Bell for his advice and guidance throughout this work.

I am also thankful to the other committee members, Dr. Jan Wagner and Dr. Arland H. Johannes, for their valuable suggestions. Valuable suggestions from John Howell and help during the construction stage from Charles Baker are appreciated.

Special thanks are due to my parents, Puttichai and Ratchada Komolsirikul, for their encouragement throughout my graduate work.

TABLE OF CONTENTS

| Chapter | Page |
|--|------|
| I. INTRODUCTION..... | 1 |
| II. LITERATURE REVIEW..... | 3 |
| Basic Principles of Heat Transfer..... | 3 |
| Heat Transfer in Condensation..... | 6 |
| Calculation of the Condensing Film Coefficient..... | 8 |
| Heat Transfer in Annuli..... | 19 |
| Wilson Line Method..... | 22 |
| Flooding in Vertical Countercurrent Gas-Liquid or Condensing Flows..... | 24 |
| III. APPARATUS..... | 30 |
| General Description..... | 30 |
| Steam Supply System..... | 32 |
| The Reflux Condenser..... | 32 |
| The Auxiliary Condenser..... | 33 |
| The Cooling Water Supply System..... | 35 |
| The Lower Plenum..... | 35 |
| The Upper Plenum..... | 38 |
| Temperature Measurement..... | 38 |
| Pressure Measurement..... | 39 |
| Cooling Water Flow Rate Measurement..... | 39 |
| IV. EXPERIMENTAL PROCEDURE..... | 40 |
| Calibration of Rotameter and Thermocouples.. | 40 |
| Rotameter Calibration..... | 40 |
| Thermocouple Calibration..... | 40 |
| Prestart Up..... | 41 |
| Start Up..... | 41 |
| Operation and Data Acquisition..... | 45 |
| Shut Down Procedure..... | 46 |
| V. DATA ANALYSIS AND DISCUSSION..... | 48 |
| Experimental Data Analysis..... | 48 |
| Reduction of Experimental Data..... | 48 |

| Chapter | Page |
|---|------|
| Heat Balance..... | 49 |
| Overall Heat Transfer Coefficient..... | 49 |
| Individual Heat Transfer Coefficient... | 50 |
| Calculation Based on Literature Correlations | 55 |
| Comparison between Experimental Data and LiteratureCorrelation..... | 55 |
| Overall Heat Transfer Coefficient..... | 55 |
| Cooling Water Side Heat Transfer Coefficient..... | 58 |
| Film Side Heat Transfer Coefficient.... | 61 |
| Visual Observation..... | 61 |
| Flooding Point..... | 65 |
| VI. CONCLUSIONS AND RECOMMENDATIONS..... | 70 |
| Conclusions..... | 70 |
| Recommendations..... | 72 |
| BIBLIOGRAPHY..... | 73 |
| APPENDIX A - ROTAMETER CALIBRATION..... | 77 |
| APPENDIX B - THERMOCOUPLE CALIBRATION..... | 81 |
| APPENDIX C - SAMPLE CALCULATIONS..... | 83 |
| APPENDIX D - ERROR ANALYSIS..... | 112 |

LIST OF TABLES

| Table | Page |
|---|------|
| I. Rotameter Calibration Data..... | 78 |
| II. Thermocouple Calibration Data..... | 82 |
| III. Error Associated with the Calculated Quantities... | 114 |

LIST OF FIGURES

| Figure | Page |
|---|------|
| 1. Diagram of Conduction through a Cylindrical Wall.... | 4 |
| 2. Temperature Profile for Heat Transfer During Condensation..... | 7 |
| 3. Nusselt Condensation on a Plane Vertical Surface.... | 9 |
| 4. Idealized Vertical Film Condensation..... | 14 |
| 5. Correlation for Condensation on a Vertical Surface (no vapor shear)..... | 16 |
| 6. Value of m as a Function of N_L | 27 |
| 7. Value of c as a Function of N_L | 27 |
| 8. Tube Geometries..... | 28 |
| 9. Schematic Diagram of the Experimental Apparatus.... | 31 |
| 10. Reflux Condenser..... | 34 |
| 11. Auxiliary Condenser..... | 36 |
| 12. Lower Plenum..... | 37 |
| 13. Upper Plenum..... | 37 |
| 14. Schematic of Counter-current Flow Tests..... | 43 |
| 15. Schematic of Co-current Flow Tests..... | 44 |
| 16. Comparison of Overall Coefficients for Normal and Reflux Operation..... | 51 |
| 17. Effect of Vapor Flow Rate on $U_{o,TOT}$ for Normal Operation..... | 52 |
| 18. Wilson Line Plot at 1.0 Psig for Reflux Operation at the Bottom Section..... | 53 |

| Figure | Page |
|--|------|
| 19. Comparison between $U_{O,TOT}$ (literature) and $U_{O,TOT}$ (experiment): steam fed at the top section of the reflux condenser..... | 56 |
| 20. Comparison between $U_{O,TOT}$ (literature) and $U_{O,TOT}$ (experiment): steam fed at the bottom section of the reflux condenser..... | 57 |
| 21. Comparison between h_o (literature) and h_o (Wilson line method) for Normal Operation at the Top Section..... | 59 |
| 22. Comparison between h_o (literature) and h_o (Wilson line method) for Reflux Operation at the Bottom Section..... | 60 |
| 23. Comparison between h_c (literature) and h_c (Wilson line method) for Normal Operation at the Top Section..... | 62 |
| 24. Comparison between h_c (literature) and h_c (Wilson line method) for Reflux Operation at the Bottom Section..... | 63 |
| 25. General Pattern of a Condensing Flow in Co-current Flow..... | 64 |
| 26. Flooding Flow Pattern..... | 66 |
| 27. Comparison of Flooding Curve: experiment and Diehl and Koppany Method..... | 67 |
| 28. Comparison of Flooding Curve: experiment and Wallis Method..... | 68 |
| 29. Rotameter Calibration Curve..... | 80 |

NOMENCLATURE

Roman

| | |
|----------|---|
| A | heat transfer area, ft^2 (m^2) |
| A_i | inside surface area, ft^2 (m^2) |
| A_o | outside surface area, ft^2 (m^2) |
| a | specific heat transfer area, ft^2/ft (m^2/m) |
| c_p | heat capacity at constant pressure, Btu/lb_m $^{\circ}\text{F}$ (KJ/Kg K) |
| D_{eq} | equivalent diameter of annulus, ft (m) |
| D_1 | outer diameter of annulus, ft (m) |
| D_2 | inner diameter of annulus, ft (m) |
| d_i | inside diameter of the inner column, ft (m) |
| d_o | outside diameter of the inner column, ft (m) |
| G_T | mass velocity of the entire flow, lb_m/hr ft^2 (Kg/s m^2) |
| G_l | liquid mass flow rate, lb_m/hr (Kg/s) |
| G_v | vapor mass flow rate, lb_m/hr (Kg/s) |
| g | local gravitational acceleration, ft/s^2 (m/s^2) |
| h | film coefficient, Btu/hr ft^2 $^{\circ}\text{F}$ (KJ/s m^2 K) |
| h_c | mean condensing heat transfer coefficient for a surface, Btu/hr ft^2 $^{\circ}\text{F}$ (KJ/s m^2 K) |
| h_x | heat transfer coefficient at point x, Btu/hr ft^2 $^{\circ}\text{F}$ (KJ/s m^2 K) |
| h_o | heat transfer coefficient of cooling water, Btu/hr ft^2 $^{\circ}\text{F}$ (KJ/s m^2 K) |

| | |
|-----------|--|
| J_l^* | non-dimensional superficial liquid velocity |
| J_v^* | non-dimensional superficial vapor velocity |
| k | thermal conductivity of fluid, Btu/hr ft °F (KJ/s m K) |
| k_w | thermal conductivity of solid, Btu/hr ft °F (KJ/s m K) |
| L | length of a condensing surface, ft (m) |
| LMTD1 | logarithmic mean temperature difference, at the top section of reflux condenser, °F (°C) |
| LMTD2 | logarithmic mean temperature difference, at the middle section of reflux condenser, °F (°C) |
| LMTD3 | logarithmic mean temperature difference, at the bottom section of reflux condenser, °F (°C) |
| LMTDT | logarithmic mean temperature difference, evaluated for the whole reflux condenser, °F (°C) |
| m_c | mass flow rate of condensate, lb _m /s (Kg/s) |
| m_w | mass flow rate of cooling water, lb _m /s (Kg/s) |
| P | absolute inlet steam pressure, psi (KPa) |
| P_{atm} | absolute atmospheric pressure, psi (KPa) |
| P_{pg} | pressure gauge reading for inlet steam, psig (KPa) |
| P_t | perimeter for condensate drainage per tube, ft (m) |
| Pr_l | Prandtl number for the liquid, dimensionless |
| Q_1 | amount of heat transferred to cooling water at the top section of reflux condenser, Btu/hr (KJ/s) |
| Q_2 | amount of heat transferred to cooling water at the middle section of reflux condenser, Btu/hr (KJ/s) |
| Q_3 | amount of heat transferred to cooling water at the bottom section of reflux condenser, Btu/hr (KJ/s) |
| Q_{con} | total heat of condensation, Btu/hr (KJ/s) |
| Q_{TOT} | total amount of heat transferred to cooling water, Btu/hr (KJ/s) |
| q | heat load, Btu/hr (KJ/s) |

| | |
|------------------------|---|
| r_1 | outer radius of the inner tube, ft (m) |
| r_2 | inner radius of the outer tube, ft (m) |
| r_o | outer radius of tube, ft (m) |
| r_i | inner radius of tube, ft (m) |
| Re_c | Reynolds number of the condensate film, dimensionless |
| Δt | the difference between inlet and outlet cooling water temperature at one section, °F (°C) |
| ΔT | the difference between average wall and average cooling water temperature at one section, °F (°C) |
| T_{1F} - T_{6F} | temperature reading of thermocouple # 1 to 6, °F (°C) |
| TR_1 - TR_6 | true temperature of thermocouple # 1 to 6, °F (°C) |
| T_i | temperature at the inner wall, °F (°C) |
| T_o | temperature at the outer wall, °F (°C) |
| T_f | bulk fluid temperature, °F (°C) |
| T_{sat} | saturated temperature of vapor, °F (°C) |
| T_w | wall temperature, °F (°C) |
| U_o | overall heat transfer coefficient, Btu/hr ft ² °F KJ/s m ² K) |
| V_v^* | superficial flooding velocity of the vapor, ft/s (m/s) |
| V_v | vapor velocity, ft/s (m/s) |
| V_l | liquid velocity, ft/s (m/s) |
| V | velocity of cooling water, ft/s (m/s) |
| w | mass flow rate, lb _m /hr (Kg/s) |
| x | coordinate, usually taken parallel to heat transfer surface, ft (m) |
| x_i | inlet quality, dimensionless |
| x_o | outlet quality, dimensionless |

Greek

| | |
|-----------|--|
| β | coefficient of cubical expansion, $1/^{\circ}\text{F}$ ($1/^{\circ}\text{C}$) |
| δ | average thickness of film, ft (m) |
| Γ | weight flow rate of condensate per unit of tube drainage perimeter, $\text{lb}_m/\text{ft hr}$ (kg/m s) |
| λ | latent heat of condensation, Btu/lb_m (KJ/Kg) |
| μ | viscosity evaluated at bulk fluid temperature, $\text{lb}_m/\text{hr ft}$ (Kg/s m) |
| μ_v | viscosity of vapor, $\text{lb}_m/\text{hr ft}$ (Kg/s m) |
| μ_l | viscosity of liquid, $\text{lb}_m/\text{hr ft}$ (Kg/s m) |
| μ_w | viscosity evaluated at the surface temperature, $\text{lb}_m/\text{hr ft}$ (Kg/s m) |
| ρ | density, lb_m/ft^3 (Kg/m^3) |
| ρ_v | density of vapor, lb_m/ft^3 (Kg/m^3) |
| ρ_l | density of liquid, lb_m/ft^3 (Kg/m^3) |
| σ | interfacial tension, lb_f/ft (N/m) |

CHAPTER I

INTRODUCTION

Condensation of a vapor to liquid is a common phenomenon in heat transfer processes in most industries. In designing a condenser, we need to calculate the overall heat transfer coefficient which includes the condensing heat transfer coefficient, cooling fluid heat transfer coefficient, and conduction heat transfer through the condenser wall. The heat transfer coefficients are very important because the higher the heat transfer coefficient, the smaller the surface area needed.

The present study of reflux condensing heat transfer mechanisms is the first step towards better apparatus design.

The objectives of this work are to:

1. Determine by experimental measurements and by visual observation the physical nature of the condensing heat transfer mechanism inside a vertical reflux steam condenser tube.
2. Determine the overall heat transfer coefficient.
3. Compare the results obtained from the experiment to those obtained from literature correlations.

4. Make a preliminary study of reflux condensing heat transfer mechanisms for better apparatus design.

This experiment is conducted in a pyrex glass vertical reflux condenser which comprises three sections in series. The water flows inside the annular jackets, while the steam is in the inner tube. In present work, both co-current and counter-current flow of the condensing vapor and the coolant are studied.

From the experimental data, the overall heat transfer coefficient is calculated for each section. The film heat transfer coefficient is calculated by using two approaches; the Wilson line method on the experimental data and Nusselt-Colburn-Boyko-Kruzhilin literature methods. The cooling water heat transfer coefficient is computed using two methods; the Wilson line method on the experimental data and the Chen-Hawkins-Solberg literature method. For counter-current flow of the vapor and condensate, the flooding point is also computed by using the Diehl-Koppany and Wallis correlations and compared to the experimental results.

The range of this study covers cooling water Reynolds numbers from 460 to 3,800 , entering steam Reynolds numbers from 4.1×10^5 to 1.2×10^6 , and exit condensate Reynolds numbers from 30 to 450 .

CHAPTER II

LITERATURE REVIEW

Basic Principles of Heat Transfer

Heat transfer occurs as a result of a temperature difference between a fluid and a wall or another fluid. There are three basic mechanisms of heat transfer.

The first mechanism is conduction. Heat can be conducted through solids, liquids, and gases. Heat in solid, liquid, or gaseous matter is the random kinetic energy of the electrons, atoms or molecules present; temperature is a measure of the average kinetic energy possessed by the assembly of electrons, atoms and/or molecules.

Heat conduction through a cylindrical solid wall (see Figure. 1) is given by:

$$q = 2\pi L k_w (T_i - T_o) / \ln(r_o / r_i) \quad (1)$$

The alternative way to write Equation (1) is

$$q = \frac{(T_i - T_o)}{\frac{\ln(r_o / r_i)}{2\pi L k_w}} = \frac{\text{Driving force}}{\text{Thermal Resistance}} \quad (2)$$

So we can say that the **wall resistance** for this case is

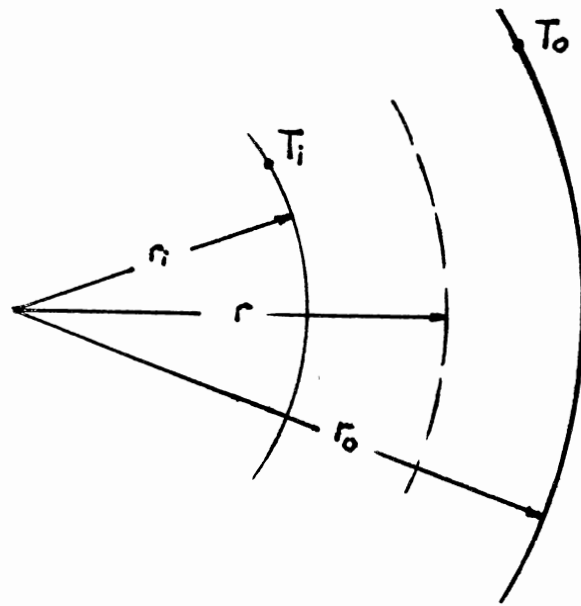


Figure. 1 Diagram of Conduction Through a Cylindrical Wall

$$\ln(r_o/r_i)/2\pi Lk_w.$$

The second mechanism of heat transfer is convection. Convection heat transfer is defined as the transport of heat from one point to another in a flowing fluid as a result of macroscopic motions of the fluid, the heat being carried as internal energy. Because motion of a fluid is involved, heat transfer by convection is largely governed by the laws of fluid mechanics. If convection is induced by density differences resulting from temperature differences within the fluid, it is said to be natural convection. However, if the motion of the fluid is the result of an outside force such as a pump, then the heat transfer mechanism is termed forced convection.

For many convective heat transfer processes, it is found that the local heat flux is approximately proportional to the temperature difference between the bulk of the fluid and the wall. Thus, we define the constant of this proportionality as the "film coefficient of heat transfer", which usually is denoted by h

$$q/A = h(T_f - T_w) \quad (3)$$

The value of h depends upon the geometry of the system, the physical properties of the fluid, and the velocity of flow. Computation of the film coefficient of heat transfer will be discussed later in this chapter.

The last heat transfer mechanism is radiation which has a great effect on the heat transfer rate only at

high temperatures. For the present study, this mechanism is not important and it will not be discussed here.

Heat Transfer in Condensation

Condensation of vapor to a liquid occurs only when there is a surface colder than the saturation temperature of the vapor at the pressure existing in the vapor phase, and this surface must be in contact with the vapor phase. During the condensation of a single component, two types of condensing mechanisms are commonly observed. These are dropwise and filmwise condensation. In dropwise condensation, the condensate forms drops on the surface and drains in the form of drops. In filmwise condensation the condensate forms a film on the surface and drains as a continuous film. In this study, we focus on filmwise condensation because it is the type that usually occurs in heat transfer equipment.

The various resistances to heat transfer during condensation of a pure saturated vapor are shown diagrammatically in Figure 2. In this case, the resistance at the vapor/liquid interface is small and, to an extremely good first approximation, may be neglected (6).

The latent heat of condensation appears at the interface and must be transferred through the condensate film to the wall and hence to the coolant. In the case of a pure saturated vapor, this temperature drop across the condensate film often represents the major resistance to

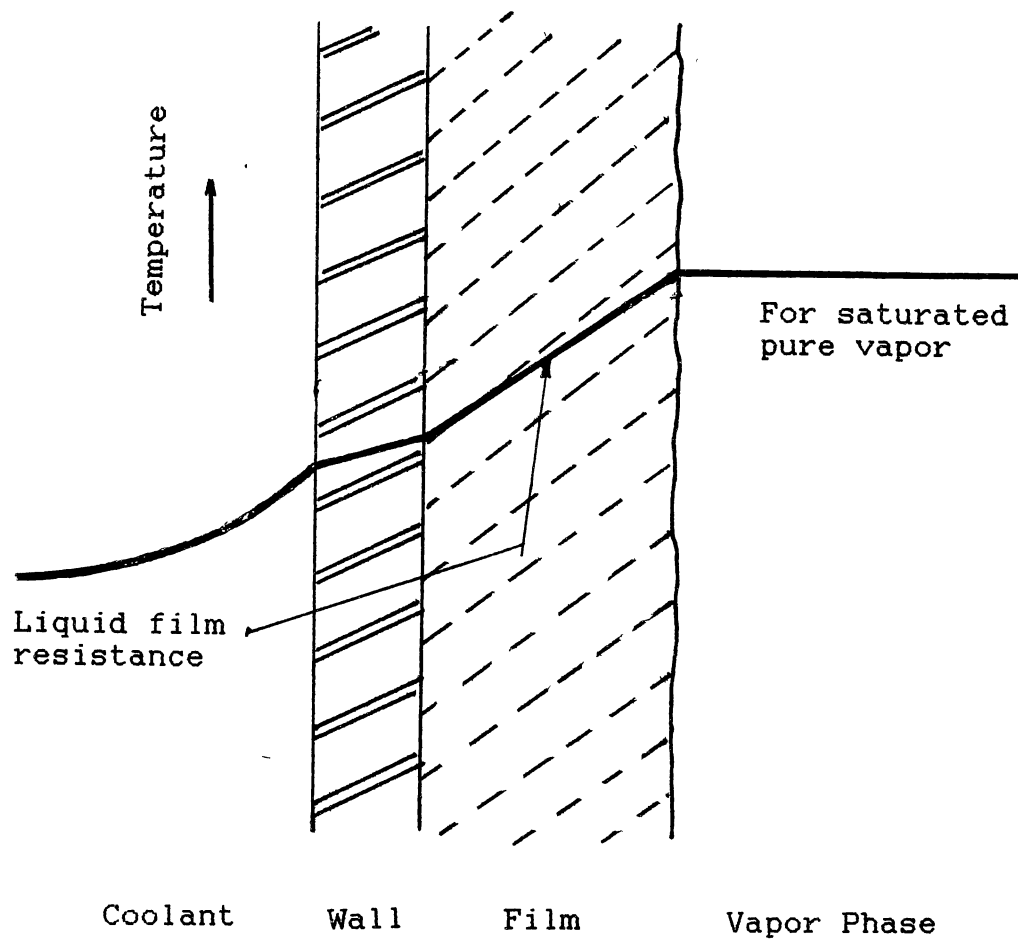


Figure 2. Temperature Profile for Heat Transfer During Condensation

heat transfer. However, in some cases, the resistance of the coolant is comparable to the resistance of the condensate film. Techniques which reduce the condensate film thickness in laminar flow or promote a higher "effective" conductivity e.g., turbulence, will therefore increase the condensing side heat transfer coefficient.

Considerable experimental work on condensation heat transfer coefficients has been reported over the years, and empirical correlations based on these experimental studies may differ from recent careful experimental results by from 50 to 500 % (19). For many years, however, even a fairly wide discrepancy made little practical difference, because in conventional process equipment the resistance to heat transfer on the condensate film side was often small compared with the other resistances. As a result, even a sizable error in the film side coefficient introduced only a small error in the overall resistance and heat transfer coefficient.

Calculation of the Condensing Film Coefficient

The classical work on the mechanics of thin films and heat transfer through these films was presented by Nusselt (35) in 1916. He made several assumptions as follows:

1. The liquid film (Figure 3) is in laminar flow.
2. The hydrodynamics of the film are controlled by the

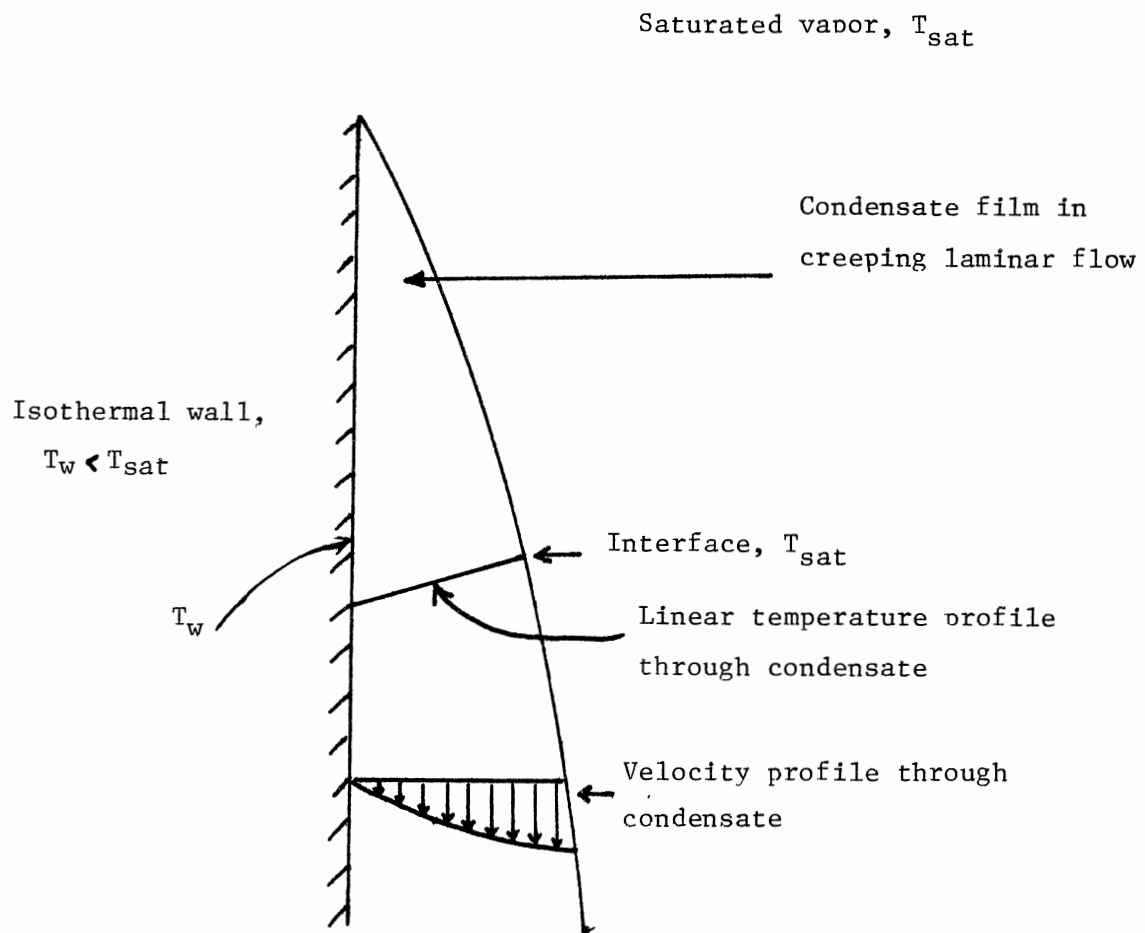


Figure 3. Nusselt Condensation on a Plane Vertical Surface

viscous terms in the Navier-Stokes equations.

3. The vapor is saturated.
4. The liquid and vapor have the same temperature (T_{sat}) at the interface, i.e., no interfacial resistance.
5. The sensible heat of subcooling the liquid is negligible compared to the latent heat load.
6. The temperature profile is linear through the liquid film.
7. The liquid and the solid surface are at the same temperature at their interface.
8. The solid surface is isothermal.
9. The liquid properties are not functions of temperature.
10. The liquid has zero velocity at the liquid-solid interface, i.e., the no-slip condition.

Nusselt found that the local value of the film heat transfer coefficient at a distance x from the start of condensation is

$$h_x = \left[\frac{k_l^3 \rho_l (\rho_l - \rho_v) \lambda g}{4 \mu_l (T_{\text{sat}} - T_w) x} \right]^{1/4} \quad (4)$$

A far more useful quantity is the average coefficient for a surface of length L , which is identified for convenience as the condensing coefficient h_c :

$$h_c = \frac{1}{L} \int_0^L h_x dx = 0.943 \left[\frac{k_l^3 \rho_l (\rho_l - \rho_v) \lambda g}{\mu_l L (T_{\text{sat}} - T_w)} \right]^{1/4} \quad (5)$$

The heat transfer coefficient predicted by Equation (5) decreases as L and $(T_{\text{sat}} - T_w)$ increase. This is due to the increased resistance to conduction offered by a thickened film. The total heat transfer however increases with L and $(T_{\text{sat}} - T_w)$ as may be seen by writing the rate equation

$$q = h_c a L (T_{\text{sat}} - T_w) \quad (6)$$

or

$$q \propto L^{3/4} (T_{\text{sat}} - T_w)^{3/4} \quad (7)$$

The derivation has been carried out in terms of a vertical plane surface. Since the condensate film is so thin compared to typical tube diameters, the result is applicable to condensation on the inside or the outside of vertical tubes [4]

A more convenient form of h_c is obtained if one first defines a tube loading per linear foot of tube drainage perimeter (Γ). That is, if w lb/hr are to be condensed on each tube,

$$\Gamma = \frac{w}{P_t} \quad (8)$$

where $P_t = \pi D$ for a vertical tube.

It is also desirable to define a condensate Reynolds number

$$\text{Re}_c = \frac{4\Gamma}{\mu_l} \quad (9)$$

Substituting Equations (8) and (9) into Equation (5) gives,

with the aid of a heat balance:

$$h_c = 1.47 \left[\frac{k_1^3 \rho_1 (\rho_1 - \rho_v) g}{\mu_1^2} \right]^{1/3} Re_c^{-1/3} \quad (10)$$

Nusselt equation has been experimentally checked a number of times. We may conclude that the general validity of the Nusselt equation is established within usual engineering standards. A major problem for designing a condenser for a new process is that the physical properties used in the calculations are often inaccurate or not well known.

Many workers have analytically and experimentally tested the effects of violation of Nusselt's assumptions. The results showed that in most cases in the laminar region, these assumptions can be safely applied. However some assumptions should be noticed.

The assumption concerning vapor shear on the condensate on a vertical surface was examined by Nusselt (36) and is described in detail in Jakob (29). If the vapor and the condensate flow together vertically downwards, vapor shear somewhat enhances the condensing coefficient in laminar flow. If the vapor and condensate flow are in opposite directions, the condensate film is thickened and resistance increases. However, in this case a probable and important consequence is that the film becomes rippled and/or turbulent, and entrainment, slugging, flooding, etc., occur. These will be

discussed later.

The assumption of an isothermal condensing surface is generally not realized in practice. However we can relax the assumption by dividing the condenser column into several sections and assuming that each section is isothermal. Even this in principle requires a reiterative calculation; assuming a surface temperature, etc.

The assumption of constant liquid properties is not truly valid, but is accepted because it is so difficult and tedious to account for temperature effects, especially upon the viscosity. The physical properties are generally taken at the arithmetic mean film temperature. By taking this method, Bell (4) states that significant errors in the final result are unlikely to arise unless the temperature difference is very great or the condensate has a very large temperature coefficient of viscosity. In case of doubt, the viscosity at the surface temperature is used in the Nusselt equations.

For cases where one or more of Nusselt's assumptions break down, numerous studies have been published. The effect of turbulent condensate film was studied by Colburn (14) and the effect of vapor shear was studied by Boyko and Kruzhilin (7) and Rohsenow (41).

Since Equations (5) or (10) are valid only for laminar flow of the condensate film in the vertical tube, we have to find other correlations to express the average film coefficient in turbulent flow. Even though the value of Re_c

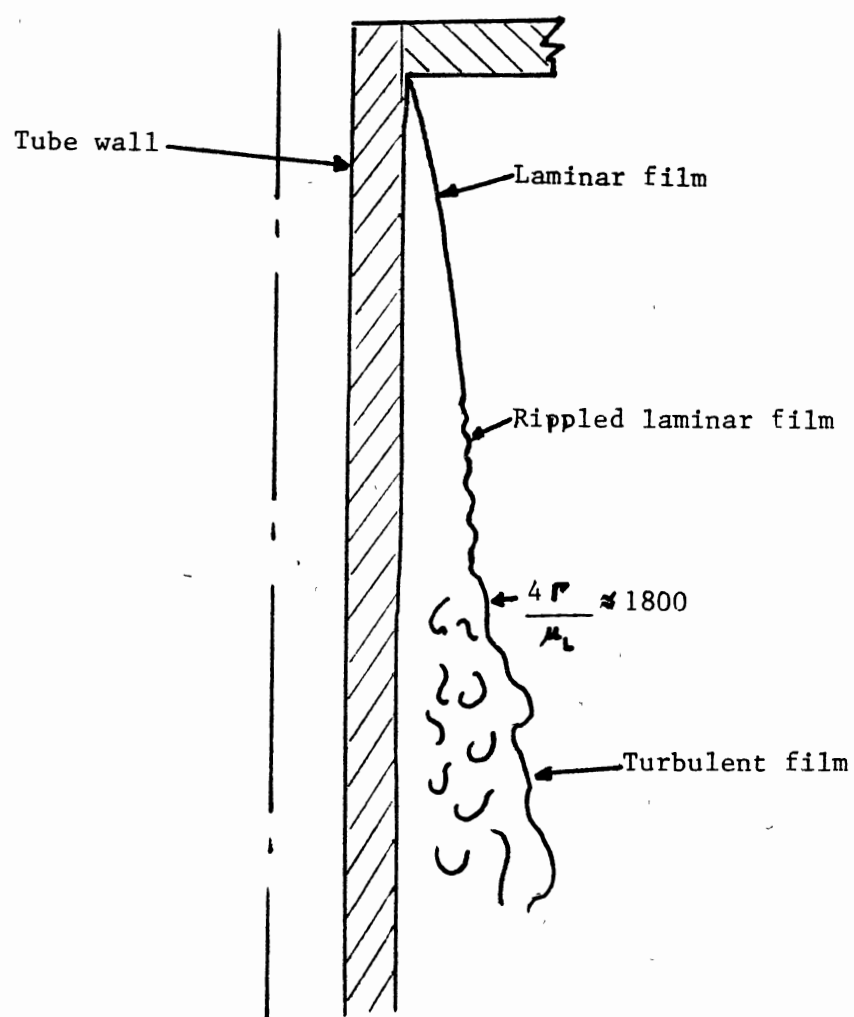


Figure. 4 Idealized Vertical Film Condensation [Bell, (4)]

is quite low, ripples can appear on the surface as shown in Figure 4 but these seem to have very little effect on the condensing coefficient (4).

In general, the critical Reynolds numbers for a falling film in the absence of vapor shear is approximately 1600-2000. However, something like turbulent flow might appear at lower Reynolds numbers near the bottom of a very long vertical wall, and whether a falling liquid film is inherently stable in laminar flow at any Reynolds number is still a question (4).

Condensation heat transfer coefficients under turbulent flow but low vapor shear conditions were studied by Kirkbride (34) who proposed an empirical correlation. Furthermore, Colburn (14) analyzed Kirkbride's data and developed a graphical representation of the final result. It was noted that the Nusselt solution, equation (10) can be plotted as

$$h_c \left[\frac{\mu_1^2}{k_1^3 \rho_1 (\rho_1 - \rho_v) g} \right]^{1/3} \quad \text{versus} \quad Re_c$$

with a slope of $-1/3$ on log-log coordinates and an intercept of 1.47 at $Re_c = 1$. The Colburn solution may also be plotted on these coordinates with Pr_1 as a parameter, giving the graph shown in Figure 5. Colburn assumed the flow become turbulent at $Re_c = 2100$ and used this value in his computation, and it is somewhat conservative. The correlation shown in Figure 5 has been reasonably well verified experimentally, and can be applied as long as the

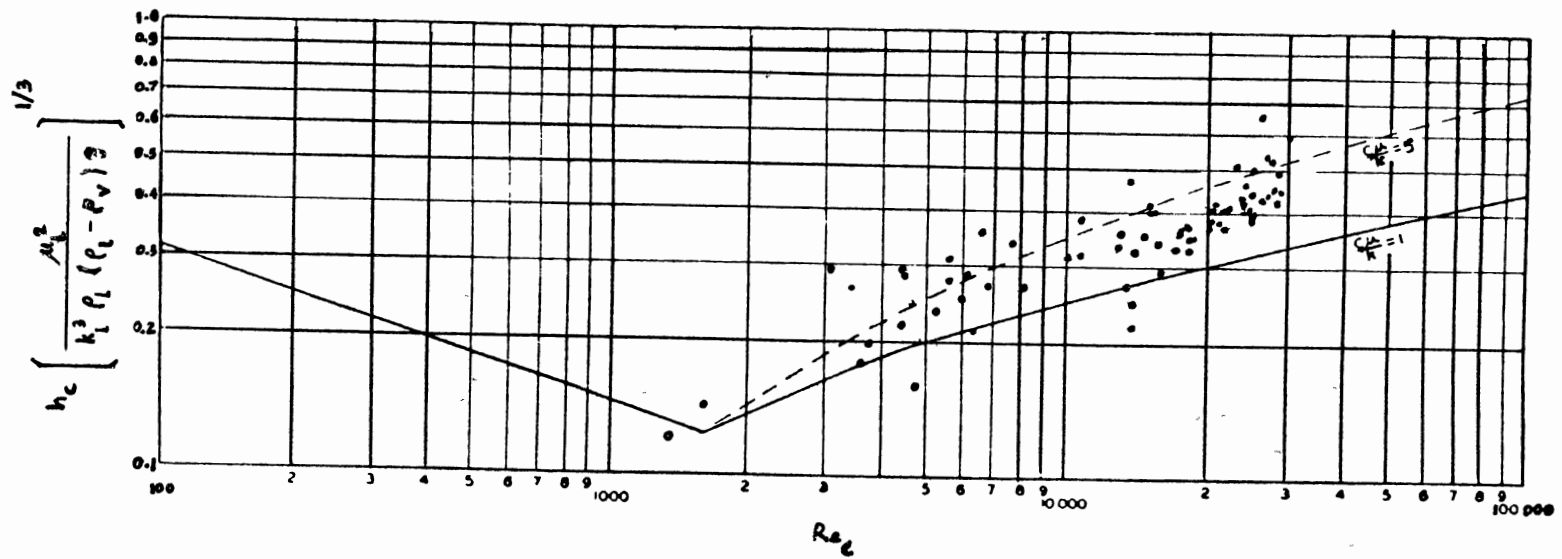


Figure. 5 Correlation for Condensation on a Vertical Surface
(no vapor shear), Colburn, (13).

Prandtl number does not exceed 5. For convenience, Bell (4) proposed the empirical equation for Colburn's graphical representation as:

$$h_c \left[\frac{\mu_1^2}{k_1^3 \rho_1 (\rho_1 - \rho_v) g} \right]^{1/3} \approx 0.0089 \text{Pr}_1^{-0.55} \text{Re}_c^{0.35} \text{Pr}_1^{0.2} \quad (12)$$

It is recommended that, if $\text{Pr}_1 > 5$, Equation (12) be evaluated at $\text{Pr}_1 = 5$.

If the value of h_c calculated by Equation (12) is less than h_c calculated from Equation (10), it means that the film is laminar rather than turbulent and that Equation (10) [or its graphical equivalent in Figure 5] is the correct equation to use. A simple way to select the proper coefficient is to calculate the condensing coefficient by both Equations (10) and (12) and choose the higher value.

The above procedures are for calculating the condensing coefficient under gravity control inside or outside a vertical tube only. Carpenter and Colburn (10) reported that the turbulence caused by the presence of vapor shear occurred at a Reynolds number as low as 250-300. In a practical heat transfer point of view, this is not a serious problem because the magnitude of the calculated coefficient itself indicates what flow regime exists.

In the case of a vapor-shear controlled condensing situation inside a vertical tube, we have several procedures to choose from such as the Carpenter and Colburn

correlation (10), the Boyko-Kruzhilin correlation (7), or the Traviss, Baron, and Rohsenow correlation (41).

Here we choose the Boyko-Kruzhilin correlation (7) because it is simpler to use and is supported by a large number of steam data. This correlation gives the mean condensing coefficient for a stream between inlet quality x_i and outlet quality x_o :

$$\frac{h_c d_i}{k_1} = 0.024 \left[\frac{d_i G_T}{\mu_1} \right]^{0.8} Pr_1^{0.43} \left[\frac{\sqrt{(\rho/\rho_m)_i} + \sqrt{(\rho/\rho_m)_o}}{2} \right] \quad (13)$$

where

$$(\rho/\rho_m)_i = 1 + \frac{(\rho_l - \rho_v)}{\rho_v} x_i \quad (13a)$$

and

$$(\rho/\rho_m)_o = 1 + \frac{(\rho_l - \rho_v)}{\rho_v} x_o \quad (13b)$$

If the entering steam is dry saturated vapor, $x_i = 1$, and if the stream is totally condensed, $x_o = 0$; for this special case, the bracketed term becomes equal to $\left[\frac{1 + \sqrt{(\rho_l/\rho_v)}}{2} \right]$

The Carpenter-Colburn, Boyko-Kruzhilin, and Rohsenow correlations are valid only under the conditions that vapor shear controls the liquid film hydrodynamics and hence heat transfer. These correlations will give unrealistically low

coefficients if vapor shear does not control. Therefore, the best procedure is to calculate condensing coefficients by both a gravity-controlled correlation and a vapor shear-controlled correlation and take the higher value.

Heat Transfer in Annuli

A survey of the literature reveals that in the last decade a number of successful investigations have been made on the heat transfer in annular spaces for the case of turbulent flow. However, very little has been done for the case of laminar flow in annular spaces.

For the case of uniform heating or cooling from outside, inside, or from both sides at the same time, Jakob and Rees (30) presented a mathematical theory of heat transfer between the walls of an annulus and a fluid passing through it in laminar flow. The range of Reynolds numbers of the experiments was $Re = 50$ to 1000 . They made the assumptions of fully developed velocity and temperature profiles. For uniform heating from inside and perfect insulation outside, the surface heat transfer coefficient was calculated using the following correlation:

$$h_o = \frac{k \psi'(r)_{r=r_1}}{\psi(r)_{r=r_2}} \quad (14)$$

where

$$\psi(r) = \left[\frac{r^2}{4} (r_1^2 - \frac{r^2}{4} + B \ln \frac{r}{r_1} - B) + \right. \\ \left. - \frac{r_2^2}{4} (r_2^2 - B) \ln \frac{r_1}{r} - \frac{r_1^2}{4} (\frac{3r_1^2}{4} - B) \right]$$

$$\psi'(r) = \left[\frac{r}{2} (r_1^2 - \frac{r^2}{2} + B \ln \frac{r}{r_1} - \frac{B}{2}) - \frac{r_2^2}{4r} (r_2^2 - B) \right]$$

$$B = (r_2^2 - r_1^2) / \ln (r_2/r_1)$$

Using ethylene, hydrogen and air as the test fluids, they found that the deviation of h_0 calculated from Equation (14) was up to ± 15.0 %. This deviation was noted due to the beginning of turbulence in the range of $Re = 600$ to 1000 .

In 1943, Davis (16) suggested a tentative dimensionless equation for determining heat-transfer coefficients in annuli for the case of laminar flow. Since there were no experimental data available, the constants of the equation were left as unknowns.

The criterion of flow is indicated by the Reynolds number, $\frac{VD\rho}{\mu}$. In case of flow in an annular space, usually an equivalent diameter is used for D . There are two methods of calculating the equivalent diameter of an annulus. The first method uses the wetted perimeter defined as $\Pi (D_1 + D_2)$ and the equivalent diameter in this case is:

$$D_{eq} = \frac{4 \times \frac{\pi}{4} (D_1^2 - D_2^2)}{\pi (D_1 + D_2)} = D_1 - D_2 \quad (15)$$

In the second method, the heated perimeter where heat transfer takes place at the inner wall is used. Therefore, the equivalent diameter is defined as:

$$D_{eq} = \frac{4 \times \frac{\pi}{4} (D_1^2 - D_2^2)}{\pi D_2} = \frac{D_1^2 - D_2^2}{D_2} \quad (16)$$

The second method was first suggested by Jordan (31) and later used by Nusselt (36).

Although both of these equivalent diameters have been used for correlation data dealing with heat transfer in annular spaces, the first method is recommended to use in the Reynolds number computation (10).

Chen, Hawkins, and Solberg (11) proposed an empirical correlation for heat transfer in annular spaces for the case of laminar flow of water as follows:

$$\frac{h_o D_{eq}}{k} = 1.02 \left[\frac{VD_{eq}\rho}{\mu} \right]^{0.45} \left[\frac{C_p \mu}{k} \right]^{1/3} \left[\frac{\mu}{\mu_w} \right]^{0.14} \left[\frac{D_{eq}}{L} \right]^{0.4} \left[\frac{D_1}{D_2} \right]^{0.8} \left[\frac{D_{eq}^3 \rho^2 \beta g \Delta T}{\mu^2} \right]^{0.05} \quad (17)$$

Here, h_o is the mean heat transfer coefficient of an annular section.

This correlation is valid only for water in the range of Reynolds number from 200 to 2000, but this equation may also hold for $Re < 200$. In order to get this correlation, they assumed that the exponent for Prandtl number is $1/3$. The average deviation of this correlation is ± 6.6 percent and the maximum deviation of ± 14.1 percent. This correlation gives slightly better results than the one proposed by Jakob and Rees. In addition, the assumption of fully developed flow proposed by Jakob and Rees is not proper for our case.

After wall resistance, average condensing film coefficient, and water side coefficient in an annulus are calculated, we are able to compute the overall heat transfer coefficient based on outside surface area (assuming no fouling), U_o , as:

$$U_o = \frac{1}{\frac{1}{h_o} + \frac{r_o \ln(r_o/r_i)}{k_w} + \frac{A_o}{h_c A_i}} \quad (18)$$

Wilson Line Method

The individual heat transfer coefficients were also determined from the experimental data by using the Wilson Method (47), and then compared to those found using literature correlations. Equation (17) shows that h_o is proportional to $V^{0.45}$ if everything else is held constant. In this case, Equation (17) might be written as:

$$h_o = b V^{0.45} \quad (19)$$

in which the constant b could be calculated by equating Equation (17) and (19) or determined from the results of Wilson line experiment described below.

Combining Equation (18) and Equation (19) results in the following expression:

$$\frac{1}{U_o} = \frac{1}{b V^{0.45}} + \frac{r_o \ln(r_o/r_i)}{k_w} + \frac{A_o}{h_c A_i} \quad (20)$$

The last two terms on the right-hand side are the resistances of the tube wall and the inside fluid, respectively. If they remain constant for a series of runs over a range of V , a linear relation should exist between $1/U_o$ and $1/V^{0.45}$.

If the straight line through the points is extrapolated to the ordinate at which $1/V^{0.45}$ equals zero, the intercept of the straight line on the ordinate axis gives the value of $1/U_o$ equal to the sum of the tube wall and inside fluid resistances.

$$\left[\frac{1}{U_o} \right]_{V=0} = \frac{r_o \ln(r_o/r_i)}{k_w} + \frac{A_o}{h_c A_i} \quad (21)$$

The quantity $r_o \ln(r_o/r_i)/k_w$ can be readily calculated, and the value of the convective coefficient for the inside fluid h_c obtained. A reasonable value of h_c will be obtained if we have good values of k_w and r_o/r_i and a good value of the

intercept.

The slope of the straight line is equal to $1/b$. Because the quantity of $1/h_o$ is equal to $\text{slope}/V^{0.45}$, h_o can be easily calculated for a given value of V .

Flooding in Vertical Countercurrent Gas-Liquid or Condensing Flows

The flooding phenomenon in counter-current two-phase flows has become a major concern in many engineering systems. It may occur in packed columns in various chemical processes, in the hypothetical mode of loss of coolant accident (LOCA) in nuclear reactors, in heat pipes, and in heat exchangers with vertical two-phase flows. Numerous researchers (1, 17, 22-23, 25-27, 39, 43-45) have performed flooding experiments with a wide range of flow properties and test-channel geometries. These researchers proposed expressions correlating their experimental results. There exists very little consistency in their formulations of flooding correlations. Consequently, the various correlations do not generally agree. One of the main causes for this confused situation lies in the fact that many existing correlations are all semi- or totally empirical and do not have a sound physical and analytical basis. Another contributing factor is the lack of a standard criterion or definition of the flooding phenomenon.

The flooding phenomenon is the result of flow instability. As the relative velocity between upwards vapor

flow and downwards liquid flow increases, flow instability appears in the form of waves at the interface. At an even higher relative velocity, the amplitude of waves grows exponentially with time and eventually the liquid film starts to break into small liquid droplets (entrainment). This entrainment phenomenon is an early signal of an unstable flow condition. This leads to the partial or total stoppage of downwards liquid flow and/or dry-out. Consequently, the continuous operation of counter-current flow is interrupted. This limiting flow behavior is called flooding.

There are many different ways of identifying the onset of flooding. The following definitions of the flooding phenomenon have been offered:

1. Reversal of flow motion from counter-current flow motion to co-current.
2. Channel wall dry out.
3. Appearance of large pressure drop fluctuations.
4. Appearance of slug flow motion near the gas flow exit and at the upper plenum.
5. Formation of dispersed annular flow or chugging flow in the channel.
6. Shaping of liquid film bridges in the channel.
7. The onset of entrainment of liquid droplets.

However, each definition is not completely independent of the others. Some items are identical with respect to the critical flow rate at the flooding condition.

Among various researchers, the most commonly used flooding correlation has been the Wallis correlation (45) which characterizes a balance of inertial forces and hydrostatic forces in connection with single-phase flow turbulent stresses:

$$\left[\frac{V_L}{\sqrt{g d_i}} \sqrt{\frac{\rho_L}{(\rho_L - \rho_V)}} \right]^{1/2} + m \left[\frac{V_V}{\sqrt{g d_i}} \sqrt{\frac{\rho_V}{(\rho_L - \rho_V)}} \right]^{1/2} = c \quad (22)$$

where m and c are given in Figures 6 and 7.

(i) When gravity forces are far more important than

$$\text{viscous forces, } N_L = \left[\frac{\rho_L g d_i^3 (\rho_L - \rho_V)}{\mu_L^2} \right]^{1/2} \text{ is high}$$

$$(N_L > 100).$$

$$m = 1$$

$$0.88 < c < 1 \text{ for round-edged tube (Figure 8a)}$$

$$c = 0.725 \text{ for sharp-edged (Figure 8b)}$$

(ii) When gravity forces can be neglected with respect to

$$\text{viscous forces, } N_L \text{ is small, } (N_L < 100)$$

$$m = 5.6 N_L^{-1/2}$$

$$c = 0.725 \text{ for round-edged tubes}$$

The other commonly used flooding correlation is the Diehl and Koppany correlation:

$$V_V^* = F_1 F_2 \left[\frac{\sigma}{\rho_V} \right]^{0.5} \quad \text{if } F_1 F_2 \left[\frac{\sigma}{\rho_V} \right]^{0.5} > 10 \quad (22)$$

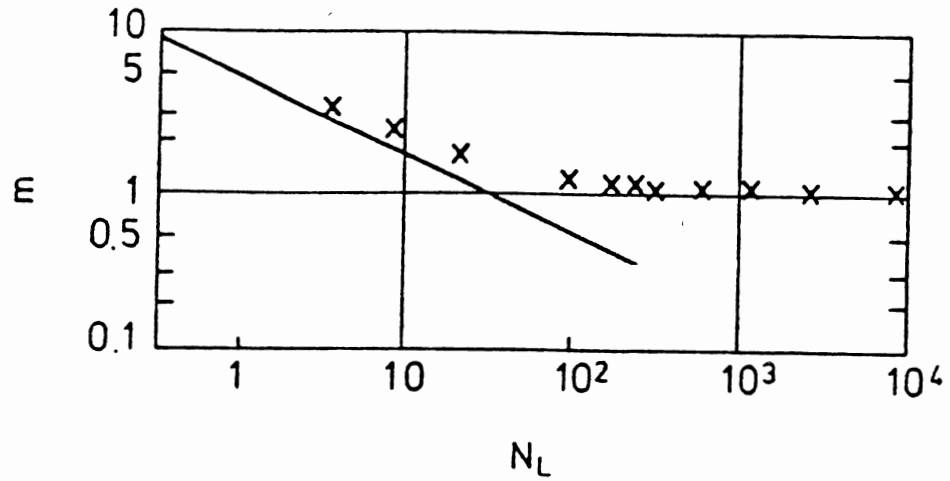


Figure 6. Value of m as a function of N_L (Wallis, 1969)

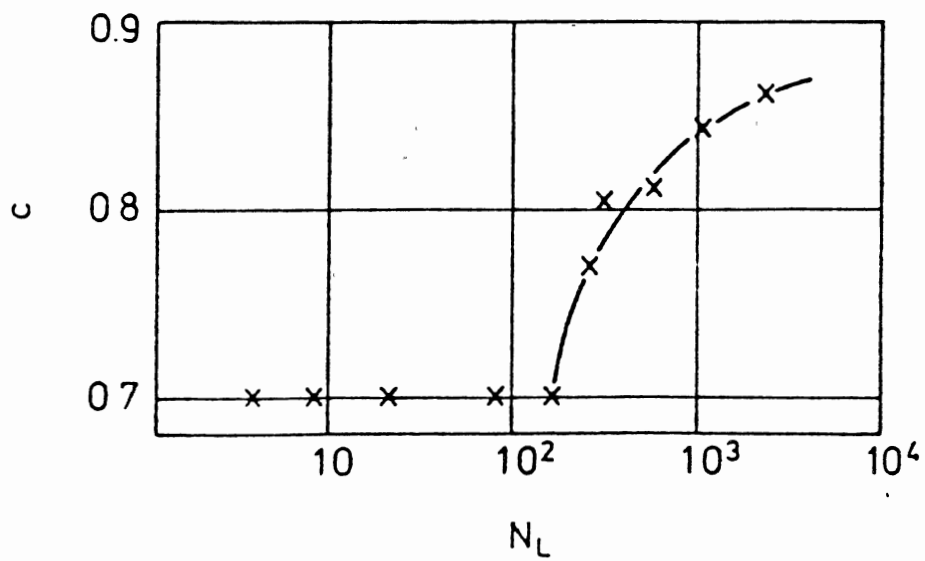


Figure 7. Value of c as a function of N_L (Wallis, 1969)

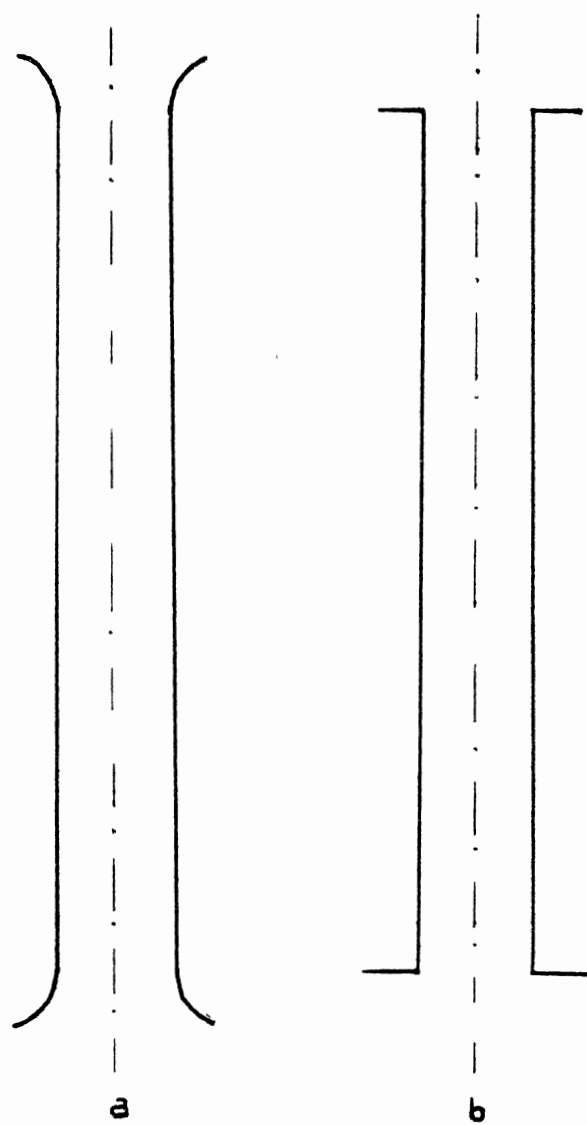


Figure 8. Tube geometries

(8a) Round-edged tube

(8b) Sharp-edged tube

$$V_v^* = 0.71 \left[F_1 F_2 \left[\frac{\sigma}{\rho_v} \right]^{0.5} \right]^{1.15} \quad \text{if } F_1 F_2 \left[\frac{\sigma}{\rho_v} \right]^{0.5} < 10$$

(23)

where

V_v^* = superficial flooding velocity of the vapor, ft/s

$F_1 = (12 d_i / (\sigma / 80))^{0.4}$ if $(12 d_i / (\sigma / 80)) < 1.0$

$= 1.0$ if $(12 d_i / (\sigma / 80)) \geq 1.0$

$F_2 = (V_v / V_l)^{0.25}$

V_v = vapor velocity (ft/s)

V_l = liquid velocity (ft/s)

ρ_v = vapor density (lb/ft³)

d_i = inside diameter of the inner tube (ft)

σ = surface tension (dyne/cm)

Therefore, in this work, we use these two correlations to compute the flooding points.

CHAPTER III

APPARATUS

General Description

Figure 9 is a schematic diagram of the experimental apparatus. The reflux condenser, upper plenum, and lower plenum are made of pyrex glass to permit visual observation of the flow pattern. The reflux condenser comprises three sections in series. The water flows inside the annular jacket while steam flows in the inner tube.

The wet steam is fed through the pressure regulator and separator in order to obtain dry steam. In this apparatus, the steam flows in 1/2 in. OD copper tube. The apparatus is designed for both co-current and counter-current flows of the condensate and the condensing vapor. For the case of counter-current flow of steam and condensate, steam is fed at the lower plenum and flows into the inner tube of the reflux condenser, while cooling water is pumped through the rotameter and then to the jacket of the lowest section of the reflux condenser. After transferring heat to the cooling water, steam is condensed and the condensate flows down to the lower plenum.

In the case of incomplete condensation, uncondensed steam is fed through the auxiliary condenser and exchanges

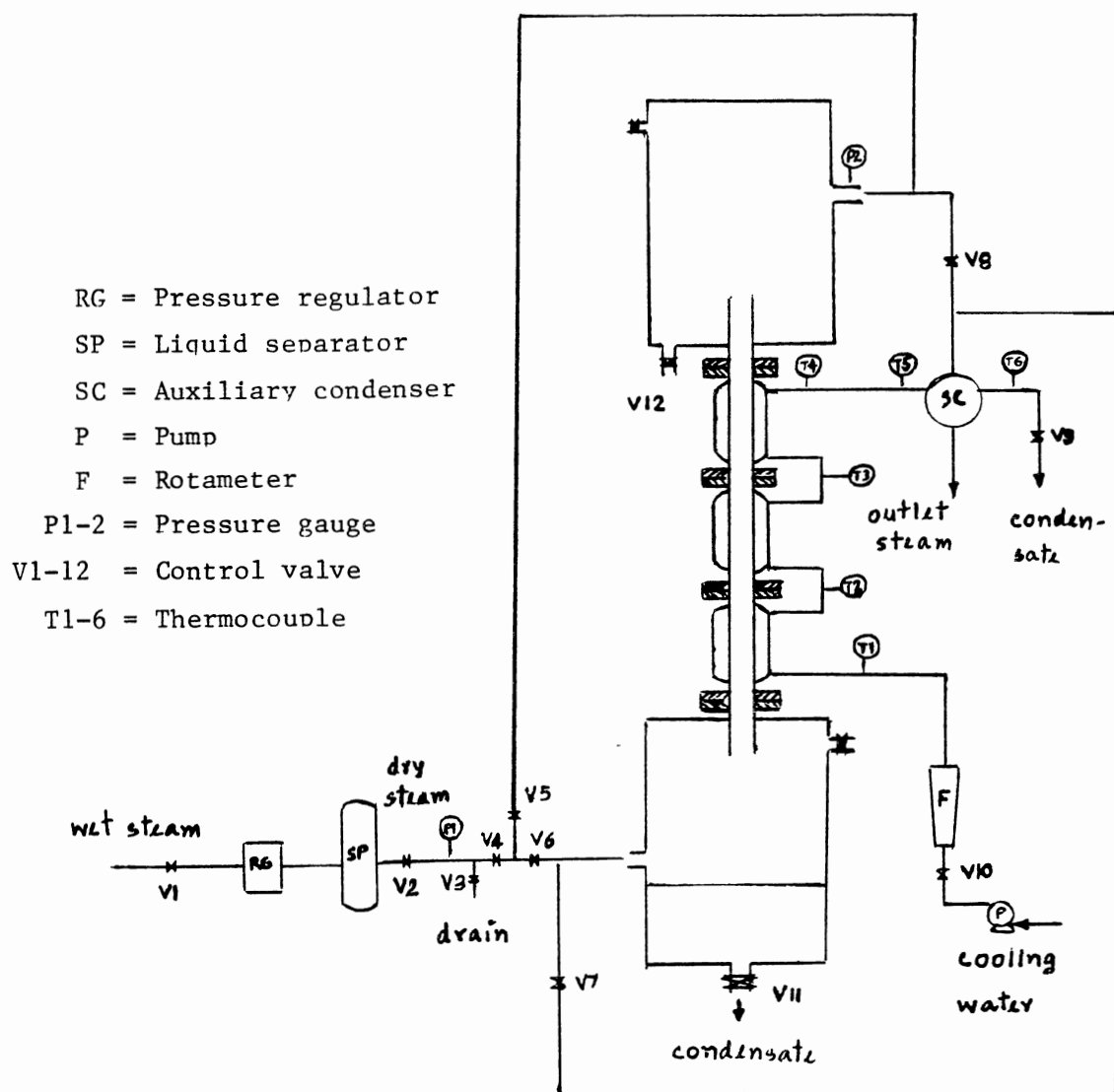


Figure 9. Schematic Diagram of the Experimental Apparatus

heat with cooling water that exits from the top section of the reflux condenser.

For co-current flow of steam and condensate, steam is fed at the upper plenum while water is still fed at the lowest section of the reflux condenser. A detailed description of all the components is given below.

A plexiglass protective shield was mounted on the reflux condenser. These shields were employed to intercept any hot fluid splashing in case of an accident.

The water and steam used in the experiment were locally supplied from the laboratory mains.

Steam Supply System

Pressure of the laboratory supply steam is about 60 psig. The 60 psig steam flows through a pressure regulator in order to reduce the pressure to about 15 psig, and then flows through the liquid separator to eliminate the water mixed with the steam. The steam flow is controlled by control valve V1, and the pressure of steam entering the apparatus is measured by pressure gauge P1 (counter-current flow) or P2 (co-current flow). In this experiment, inlet steam pressure is in the range of 1 to 4 psig, and the inlet temperature is in the range of 100.9 - 105.9 °C.

The Reflux Condenser

The reflux condenser (see Figure 10) is made of pyrex glass so that the flow phenomena can be observed. The

reflux condenser is composed of three sections in series. Cooling water flows inside an annular jacket and steam is in the inner tube.

The dimensions of the reflux condenser are as follows: inside and outside diameters of the inner tube are 25 and 28 mm. respectively, and the inside and outside diameters of the annular jacket are 37 and 41 mm. respectively. Each section of the reflux condenser is 0.657 m. in length.

The condensate is collected in the lower plenum, and the condensate flow rate is measured by keeping the level of liquid in the lower plenum constant at a certain level. This is done by marking a red line somewhere below the entrance of entering/exiting steam on the lower plenum. Control valve V-11 is used to maintain the level of condensate at that red line. The condensate exit from valve 11 is collected during a certain time increment and the amount of condensate is measured by volumetric cylinder. Thus the flow rate of condensate can be obtained by dividing the amount of condensate collected (in cm^3) by the collection time (in seconds).

The Auxiliary Condenser

The auxiliary condenser (see Figure 11) is constructed of a coiled tube inside a Schedule 40 carbon steel pipe, 8.625 in. OD. x 7.981 in. ID., 2 ft long. The cooling coil is a 1/2 in. OD. x 0.436 in. ID. copper tube with several feet of coil length inside the cylinder. The vapor to be

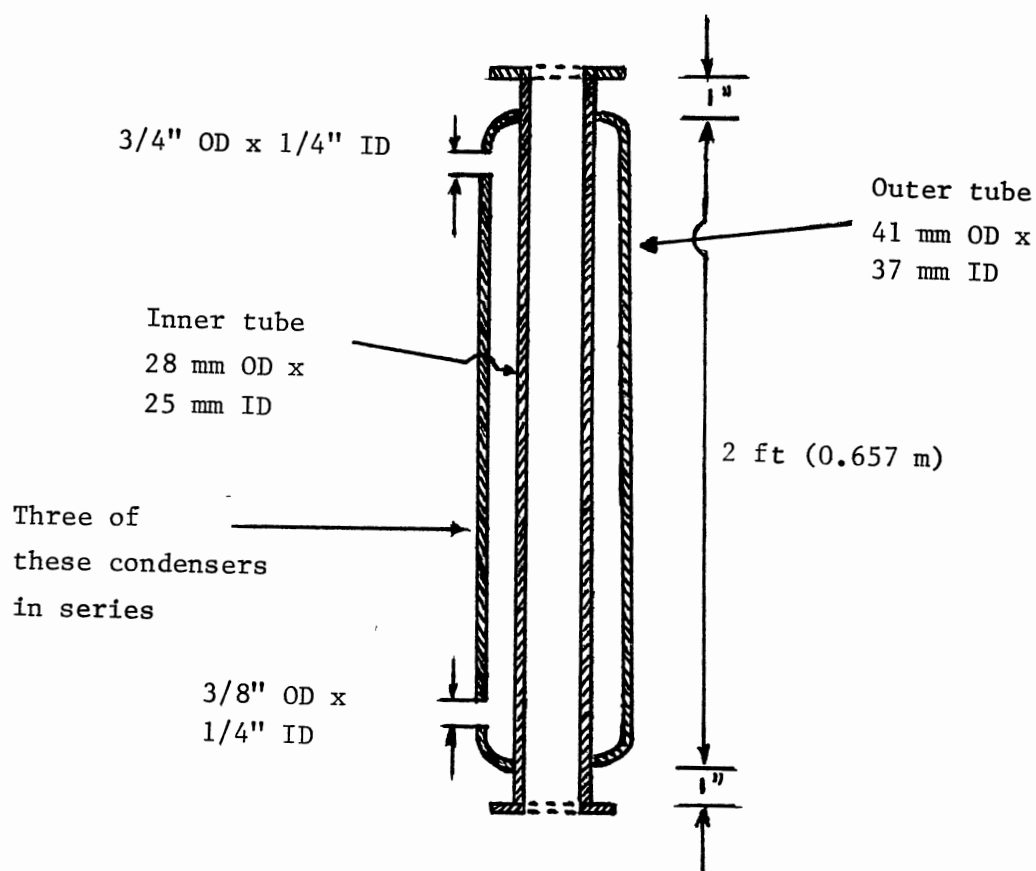


Figure 10. Reflux Condenser (one section)

condensed enters the shell side from the side, near the top. The condensate is drained from the bottom using a 1/4 in. diameter tube, and the flow rate is measured.

The Cooling Water Supply System

The cooling water line is connected directly to the annular jacket through a flow control valve, and the flow rate is measured by a rotameter. A 1/2 in. diameter copper tube is used throughout for the water flow. The cooling water flow rate used is in the range of 1.85×10^{-2} to 1.40×10^{-1} Kg/s or 4.06×10^{-2} to $3.08 \times 10^{-1} \text{ lb}_m/\text{s}$ (4.03×10^{-2} to 3.06×10^{-1} m/s in terms of velocity in the annulus).

After exchanging heat with steam in the reflux condenser, this cooling water is used as the coolant in the auxiliary condenser. This is done to assure complete condensation of the steam.

The Lower Plenum

The lower plenum tank (see Figure 12) is used to collect the condensate from the reflux condenser, and to allow the steam to enter the inner tube of the reflux condenser. This plenum is made of pyrex glass 143 mm. inside diameter. The plenum has four connections: one for inlet steam (3/4" O.D., 11/16" I.D.), one for condensate drain (1/2" O.D., 7/16" I.D.), one connected to the reflux condenser (28 mm. O.D., 25 mm. I.D.), and the last one for pressure relief (1/4" O.D., 7/32" I.D.).

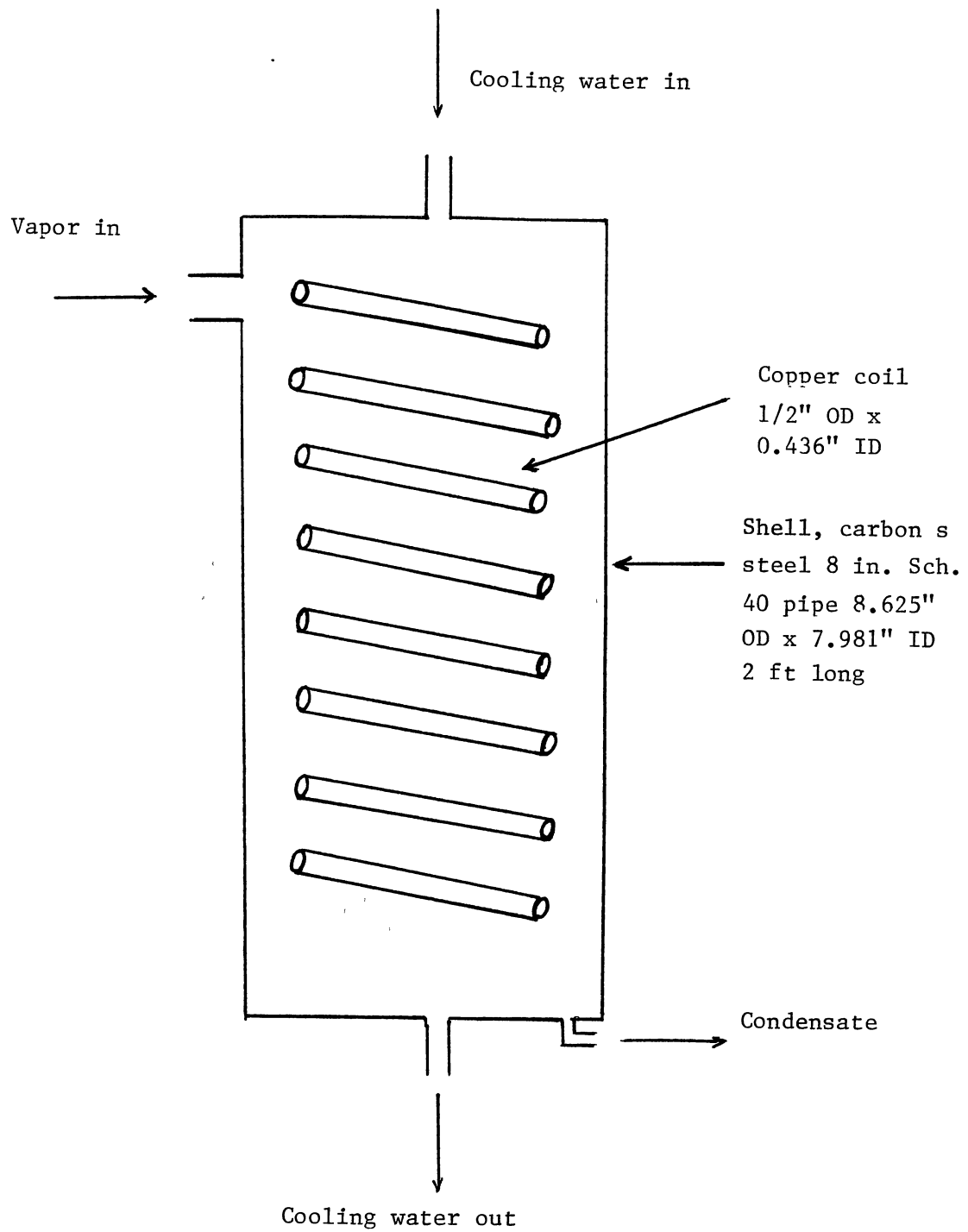


Figure 11. Auxiliary Condenser

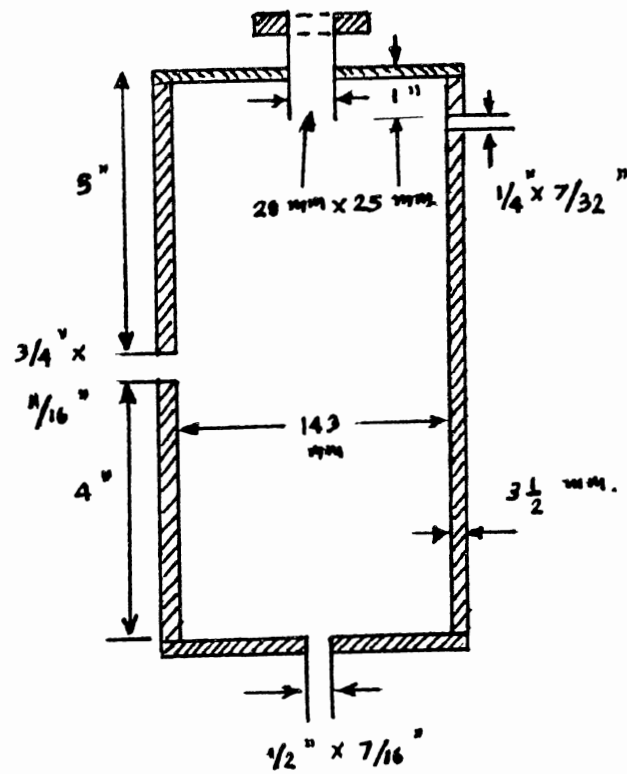


Figure 12. Lower Plenum

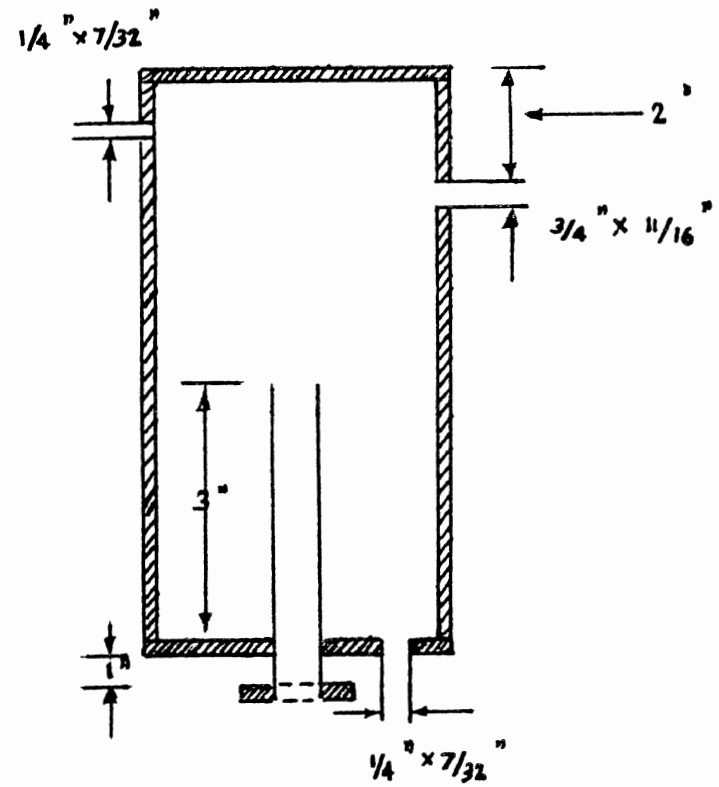


Figure 13. Upper Plenum

The Upper Plenum

The purpose of the upper plenum (see Figure 13) is to separate the steam and water exiting the top of the reflux condenser (flooding condition) or separating the water from the supplied steam in case the steam is not really dry (co-current flow). The upper plenum is 143 mm inside diameter and also has four connections as follows: 1/4" O.D., 7/32" I.D. connection for pressure relief, 3/4" O.D., 11/16" I.D. connection for outlet (counter-current flow) or inlet (co-current flow) steam, 28 mm x 25 mm for steam flowing down to or flowing up from the reflux condenser, and 1/4" O.D., 7/32" I.D. connection for entrainment drain in case flooding occurs.

Temperature Measurements

There are six thermocouples used in temperature measurement. All are made of copper-constantan junctions (type T). Four thermocouples are used for cooling water inlet and outlet temperature measurement in the reflux condenser, while the other two thermocouples are used for cooling water inlet and outlet temperature measurement in the auxiliary condenser.

A multijunction switch was used to connect one thermocouple at a time to the Omega type T digital temperature readout.

Pressure Measurement

A Bourdon tube pressure gauge is used to indicate the inlet steam pressure. In this apparatus, there are two pressure gauges, P1 for counter-current flow and P2 for co-current flow. These gauges have a pressure measuring range of 105-198 KPa absolute.

Cooling Water Flow Rate Measurement

Cooling water is measured by using rotameter which can measure the flow rate up to 300 cc/sec. Calibration of the rotameter is required in order to get the actual flow rate of cooling water.

Rotameter was calibrated by varying the flow rate, reading the rotameter scale and measuring the amount of water passing through the rotameter in a certain interval of time. The results were plotted as a calibration curve between the rotameter scale and measured volumetric flow rate. The details of rotameter calibration are described in Chapter IV.

CHAPTER IV

EXPERIMENTAL PROCEDURE

Calibration of Rotameter and Thermocouples

Rotameter Calibration

The rotameter was calibrated by varying the flow rate, reading the rotameter scale and measuring the amount of water passing through the rotameter in a certain interval of time. The results were plotted as a calibration curve between the rotameter scale and measured volumetric flow rate. The calibration data and calibration curve are shown in Appendix A. The accuracy of this calibration curve is ± 3.15 cc/sec.

Thermocouples Calibration

The thermocouples were calibrated in a constant temperature oil bath against an NBS calibrated platinum resistance thermometer. The thermocouples were calibrated by reading the temperature from digital thermocouple indicator model DS 350-T3 and reading the voltage of the thermocouple via a null detector galvanometer. The calibration data and calibration equations are presented in

Appendix B. The maximum error in each thermocouple was found to be equal to or less than 0.86°C .

Pre-start up

All experimental tests were run with water flowing in the system first; then the steam was fed into the condenser. The feed steam pressure was no more than 4 psig, and the cooling water flow rates were varied from 1.85×10^{-2} to 1.04×10^{-1} Kg/s.

Before start up, the following steps were conducted:

1. Valve V-10 was opened to let the cooling water flow into the lowest jacket. The valve was adjusted to the desired flow rate.
2. Valves V-4, V-5, V-6, V-7 were closed and valves V-2 and V-3 were opened.
3. Then the main steam valve V-1 was opened.
4. The quality of the steam was observed by checking the drain from the steam trap connected to the liquid separator. If there was no evidence of water coming out, the steam was assumed to be dry and the experiment was ready to start.

Start Up

The procedure to start the experiment depends on whether we want to operate for counter-current flow (steam enters the bottom plenum) or co-current flow (steam enters

the top plenum).

For counter-current flow (see Figure 14), valves V-4, V-6, and V-8 were opened first, and then valves V-3, V-5, and V-7 were closed. The steam rose to the top section of the reflux condenser, but some steam was condensed by exchanging heat with the cooling water in the annular jacket. The condensate flowed down against the steam rising, the condensate was collected in the lower plenum and the flow rate was measured as described in Chapter 3.

The exit steam from the upper plenum entered the auxiliary condenser by valve V-8 and exchanged heat with the cooling water from the top section of the annular jacket. All of the vapor was condensed and collected in the auxiliary condenser. After a certain interval of time the valve V-9 was opened and the amount of condensate collected in the auxiliary condenser was measured by volumetric cylinder (in term of cc). The condensate flow rate in the auxiliary condenser then was calculated by dividing the amount of collected condensate by the interval of time (in term of seconds). In case flooding occurred, the entrained liquid in the upper plenum was also measured.

For co-current flow (see Figure 15), valves V-4, V-5, and V-7 were opened first, and valves V-3, V-6, and V-8 were closed. The steam entered the upper plenum and then flowed down to the lower plenum, exchanging heat with the cooling water which still entered at the lowest section of

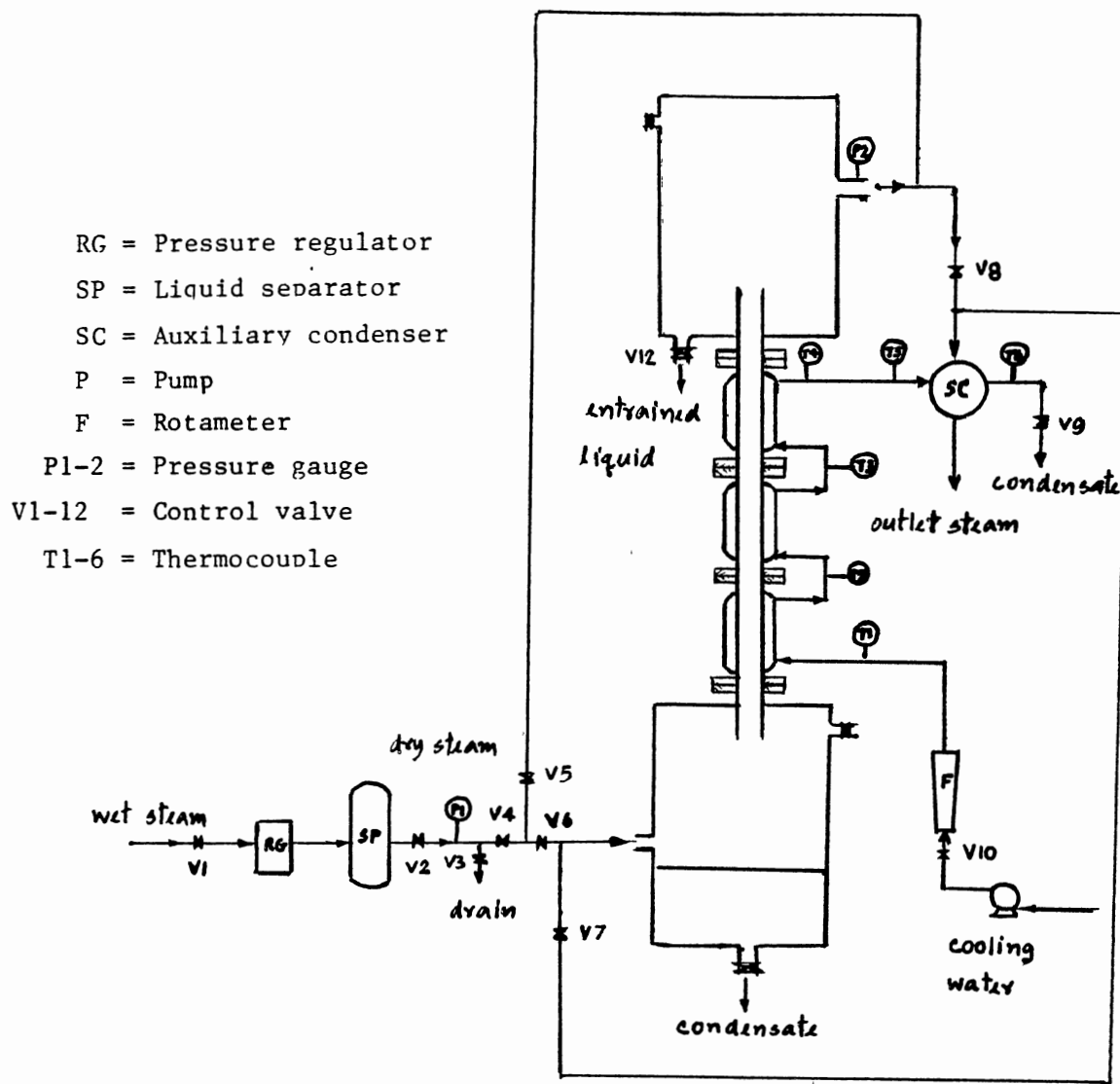


Figure 14. Schematic of Counter-current Flow Tests

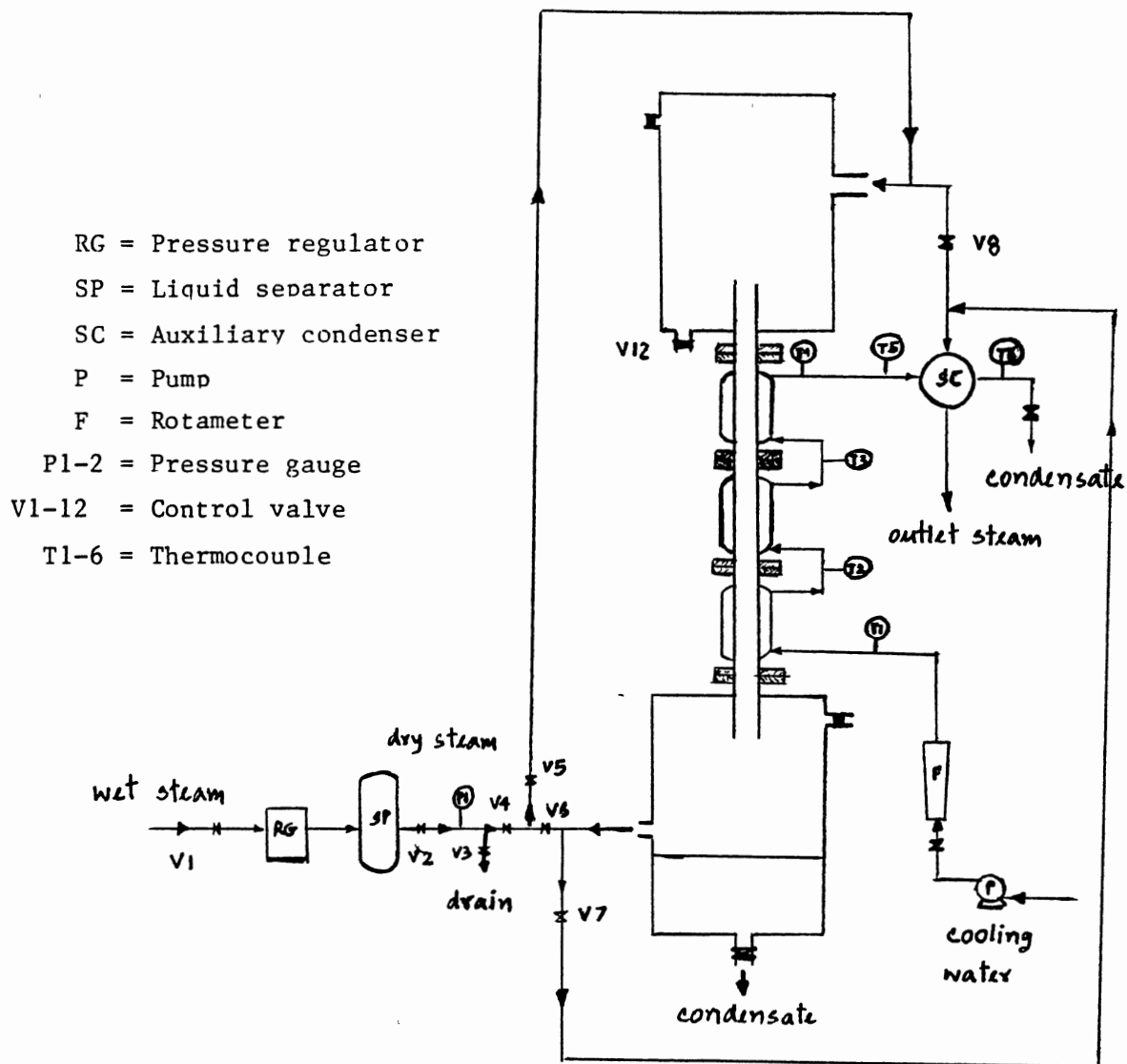


Figure 15. Schematic of Co-current Flow Tests

the annular jacket. The condensate flowed down to the lower plenum in the same direction as the steam, and the condensate flow rate was measured as before.

The steam exited the lower plenum through valve V-7 to the auxiliary condenser to exchange heat with the cooling water from the top section of the annular jacket. Then, the secondary condensate flow rate was measured.

Operation and Data Acquisition

Approximately 30 minutes were allowed for the process to achieve steady state. During this period, the inlet steam pressure, cooling water flow rate, and the inlet and outlet temperature of cooling water at each location were constantly watched for variations. The pressure in the apparatus was kept below 5.0 psig.

The following sequence was performed for acquiring data for a particular run:

The pressure gauge was read for the steam line pressure. A mercury barometer was read to record the barometric pressure. The cooling water flow rate was recorded. The six thermocouple temperatures were recorded one by one using the digital readout meter. The condensing flow patterns were observed visually through the transparent reflux condenser in order to indicate whether flooding phenomena occurred. In this case, the existence of entrainment was used to determine whether flooding occurred.

The condensate flow rates from the reflux condenser and the auxiliary condenser were measured. If flooding occurred, the entrained liquid in the upper plenum was also measured. The experiment was operated further for 15-20 minutes in order to get another set of data under the same vapor and cooling water flow rate. After this, operating parameters such as the cooling water flow rate or the inlet pressure could be changed, and the system was allowed to run for approximately 30 minutes to achieve another steady state and another set of data were obtained.

Shut Down Procedure

In normal shut down after obtaining data, the steam valve V-1 is shut off to stop steam entering to the reflux condenser. For counter-current flow, valves V-3, V-8, V-9, and V-11 are opened to drain all the condensate left in the line and apparatus, and valves V-4, V-5, V-6, and V-7 are closed. For co-current flow, open valves V-3, V-7, V-9, and V-11, and close valve V-4, V-5, V-6, and V-8. The cooling water flow is continued for another 10 minutes. The condensation surface should be cooled substantially by then. When the hottest temperature at any of the four stations is less than 80°F, the cooling water flow can be safely shut off. This completes the normal shut down procedure.

An emergency shut down may be necessary for several reasons such as loss of electrical power in the building, or

a sudden leak in the system. The first procedure in such cases is to shut off the steam valve V-1. In case of leaks, these then should be isolated, and flow towards these be stopped. The cooling water, if not leaking, should continue to flow through the system until the system is cooled down.

CHAPTER V

DATA ANALYSIS AND DISCUSSION

Experimental Data Analysis

Reduction of Experimental Data

At each section of the annular jacket, the inlet and outlet cooling water temperatures and cooling water flow rate were used to compute the amount of heat that the cooling water received from steam (Q_{TOT}), and to calculate the Reynolds number of the cooling water. From the inlet steam pressure and the condensate flow rate, saturation temperature and latent heat, total heat of condensation (Q_{con}), steam velocity and the Reynolds numbers of steam and condensate were computed for each section of the reflux condenser. Q_{TOT} was compared to Q_{con} to check the heat balance consistency.

From the inlet and outlet cooling water temperatures and the steam temperature, the LMTD was calculated for each section of the reflux condenser. From Q_{TOT} and LMTD, the overall heat transfer coefficient based on the outside surface area was calculated. The condensate film side and cooling water side heat transfer coefficients were calculated by using the Wilson line method.

In this study, the occurrence of entrainment is used as a criterion to determine whether flooding occurs (Bell, personal communication). The entrained liquid can be observed along the reflux condenser and is accumulated in the upper plenum. The entrained liquid flow rate can be measured after a certain interval of time.

All the data and the results are presented in a separate report which can be obtained from Dr. Bell.

Heat Balance

Heat balance was checked by comparing Q_{TOT} with Q_{con} . It was found that in general Q_{TOT} is less than Q_{con} in the range of 0 - 15 %. This is because some amount of heat is lost to the atmosphere, especially at the upper plenum, without transferring heat to the cooling water. Higher deviations (from 17 to 50 %, based on Q_{con}) are obtained when flooding occurs.

Overall Heat Transfer Coefficient

The sample calculations for Run No. 68 are given in Appendix C. The results of the overall heat transfer coefficient (U_o) obtained from experimental data are presented in the separate report which can be obtained from Dr. Bell. Because of the errors associated with the calculations of Q_{TOT} and LMTD, the error in calculating $U_{o,TOT}$ [based on Equation (D1) and (D2)] is quite high (36 %, see Appendix D). Comparison between $U_{o,TOT}$ for normal

and reflux operation under the same conditions except the direction of steam feed (Figure 16) shows that the first is about 20 % higher than the latter. This is probably the result of the thinner film and therefore less heat transfer resistance when steam is fed at the top section of the reflux condenser. When the steam is fed at the top section, vapor shear on the film makes the film become thinner.

Vapor flow rate increases when the operating pressure increases. The increasing of vapor flow rate may result in enhancing the effect of vapor shear, and under this condition increasing vapor flow rate will result in better heat transfer coefficient. Comparison between U_o at various vapor flow rates presented in Figure 17 shows this tendency.

Individual Heat Transfer Coefficient

The cooling water side (h_o) and film side (h_c) heat transfer coefficients were computed from the experimental data using the Wilson line method. The sample calculations for Run No. 68 are given in Appendix C. The results of h_o and h_c were presented in a separate report which can be obtained from Dr. Bell.

Since h_o was calculated from slope of the Wilson plot, the uncertainty of h_o depends on the uncertainty of the slope. Figure 18 illustrates how the uncertainty in obtaining the slope affects the calculation of h_o . When linear regression was used on all of the data points,

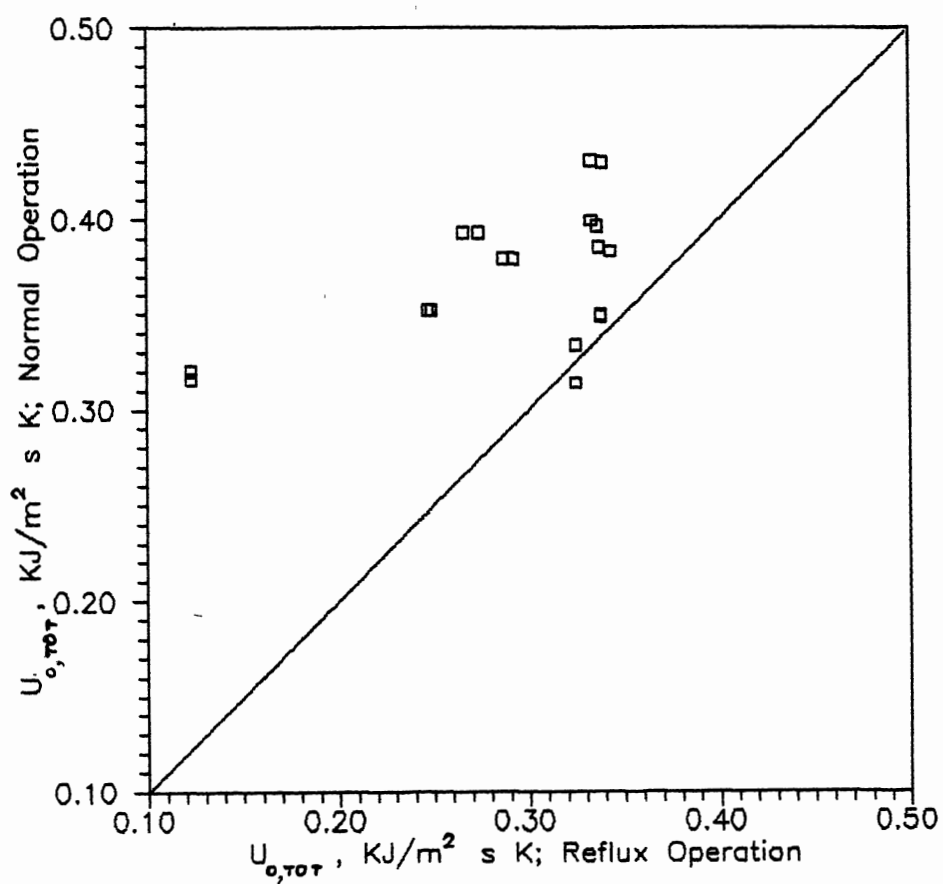


Figure 16. Comparison of Overall Coefficients ($U_{o,tot}$) for Normal and Reflux Operation Under the Same Conditions.

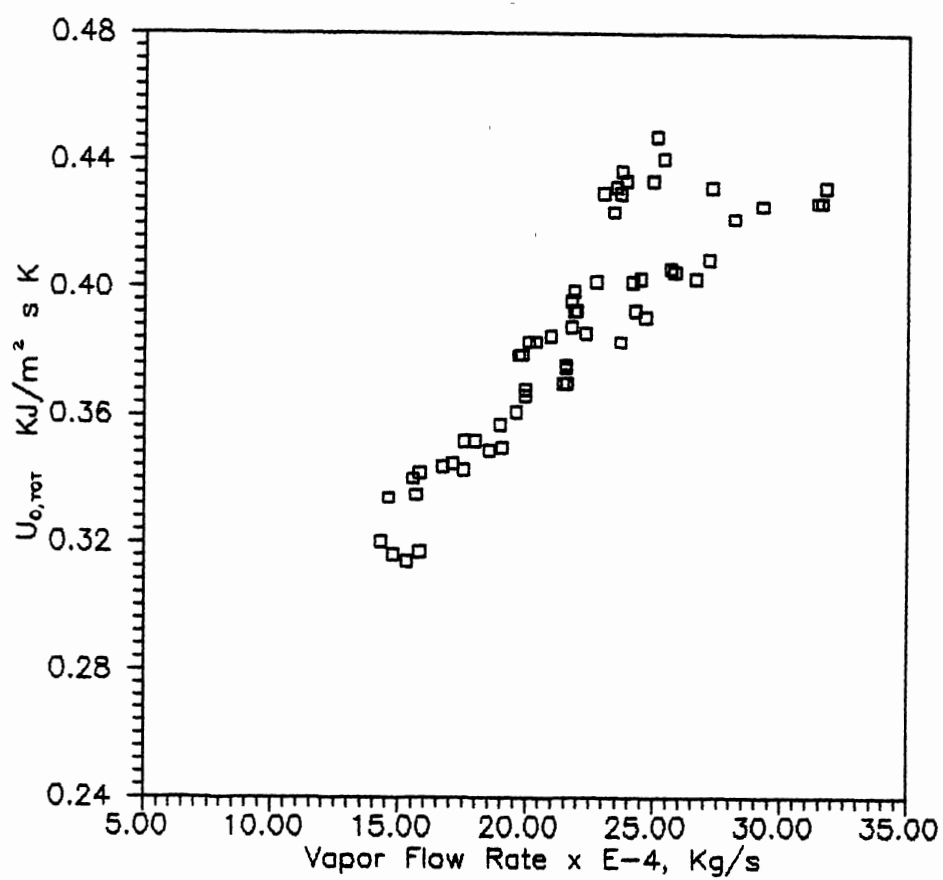


Figure 17. Effect of Vapor Flow Rate on $U_{o,tot}$ for Normal Operation

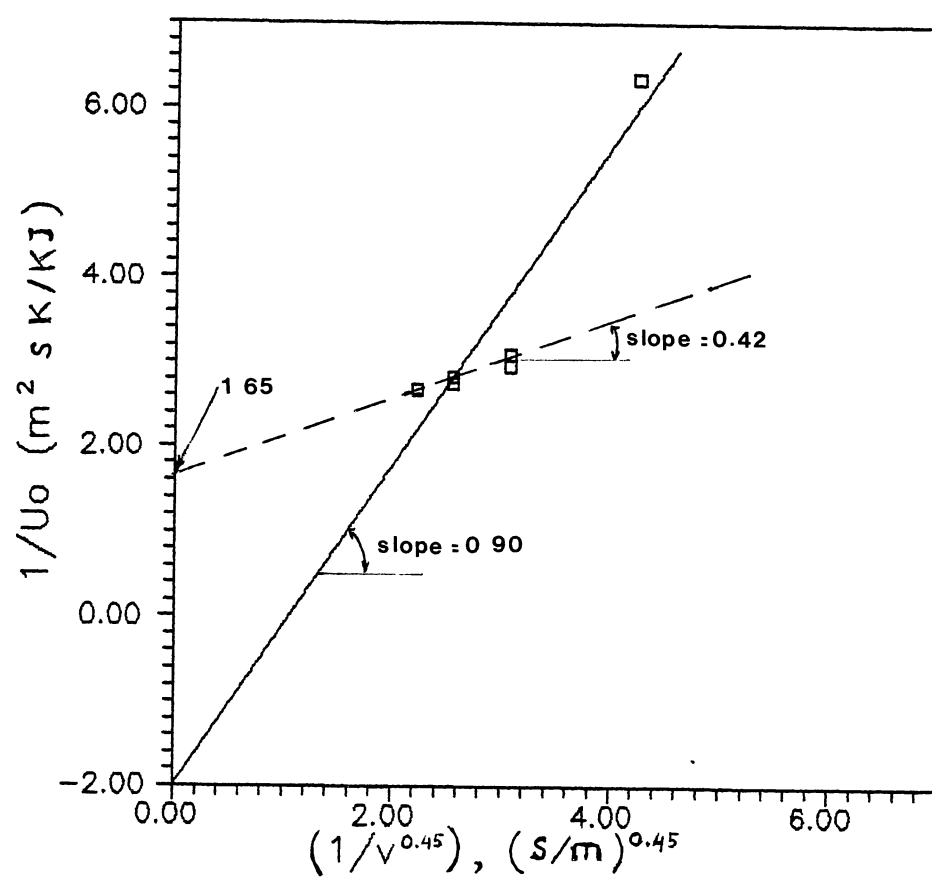


Figure 18. Wilson Line Plot at 1.0 Psig for Reflux Operation at the Bottom Section.

slope = 0.90 was obtained. Using this value at V (cooling water velocity) = 0.041 m/s, and applying Equation (19), h_o was obtained equal to $7.980 \text{ KJ/m}^2\text{s K}$. However if the last point was neglected, the Wilson plot became the dashed line. In this case the slope was 0.42 and $h_o = 1.764 \text{ KJ/m}^2\text{s K}$ was obtained (about 78 % less than the previous calculation). Probably this high uncertainty arises because the assumption that h_o is proportional to $V^{0.45}$ [11] does not really fit the experimental data.

The intercept of the Wilson plot is the combination of wall resistance and film side heat transfer coefficient. Therefore, the uncertainty of h_c is dependent on the uncertainty of wall resistance and the uncertainty of the intercept obtained from the Wilson line method. High uncertainty in obtaining h_c using the Wilson line method is exemplified by using Figure 18. In this case, linear regression of the points results in a negative intercept (-2.0). Using this number and applying Equation (21) to calculate h_c gives negative value ($-0.339 \text{ KJ/m}^2\text{s K}$) which is unrealistic. However, if the last point is neglected, the intercept = 1.65 and $h_c = 3.207 \text{ KJ/m}^2\text{s K}$. Moreover, the high uncertainty in calculating wall resistance (about 50 %, see Appendix D) makes h_c obtained from this method become more uncertain.

Calculations Based on Literature Correlations

From inlet and outlet cooling water temperatures and cooling water velocity, the cooling water side heat transfer coefficient was calculated for each section of the reflux condenser by using the Chen-Hawkins-Solberg correlation. From the steam saturation temperature, wall temperature, and the Reynolds number of the condensate film, the condensate film side heat transfer was computed for each section of the reflux condenser by using the Nusselt, Colburn, and Boyko-Kruzhilin correlations.

From the condensate film side and cooling water side heat transfer coefficients and wall resistance, the overall heat transfer coefficient was computed for each section of the reflux condenser.

Comparison between Experimental Data and Literature Correlations

Overall Heat Transfer Coefficient

The results of the overall heat transfer coefficient (U_o) obtained from experimental data and from literature methods are presented in the separate report. The comparisons between $U_{o,tot}$ evaluated from the experimental data and from literature are given in Figure 19 and 20 for steam fed at the top and bottom section of the reflux condenser, respectively. Both figures show that $U_{o,tot}$ evaluated from the experimental data is about 20 % lower

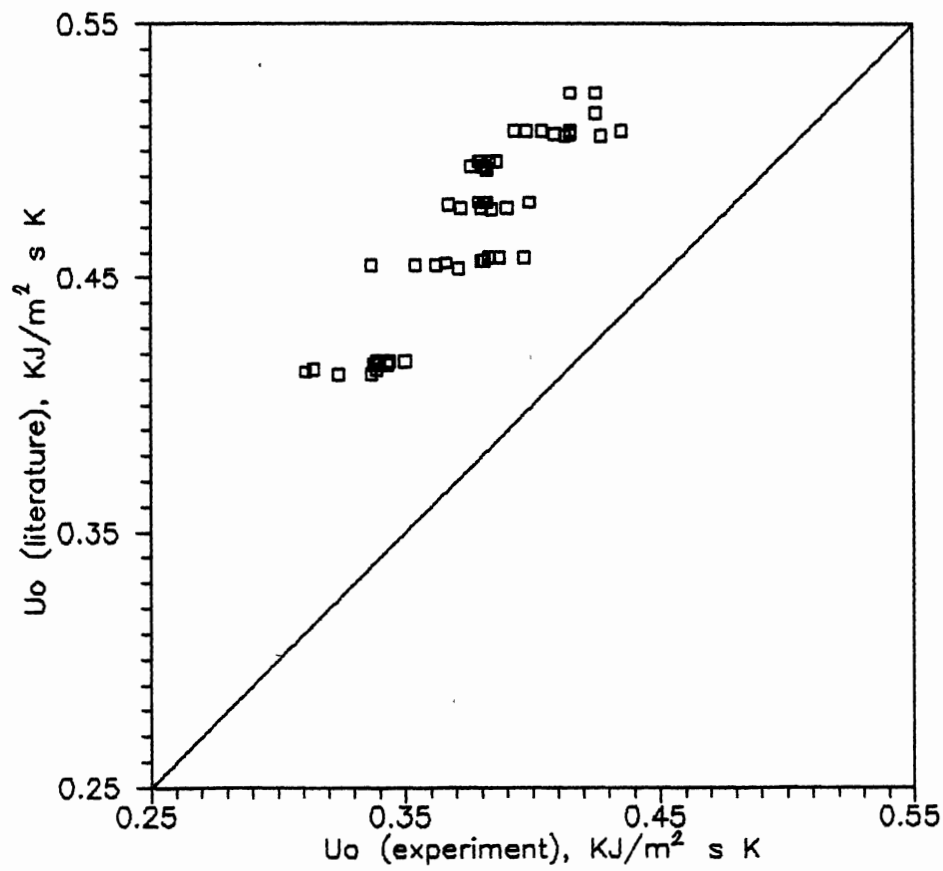


Figure 19. Comparison Between $U_{o,TOT}$ (literature) and $U_{o,TOT}$ (experiment): steam fed at the top section of the reflux condenser.

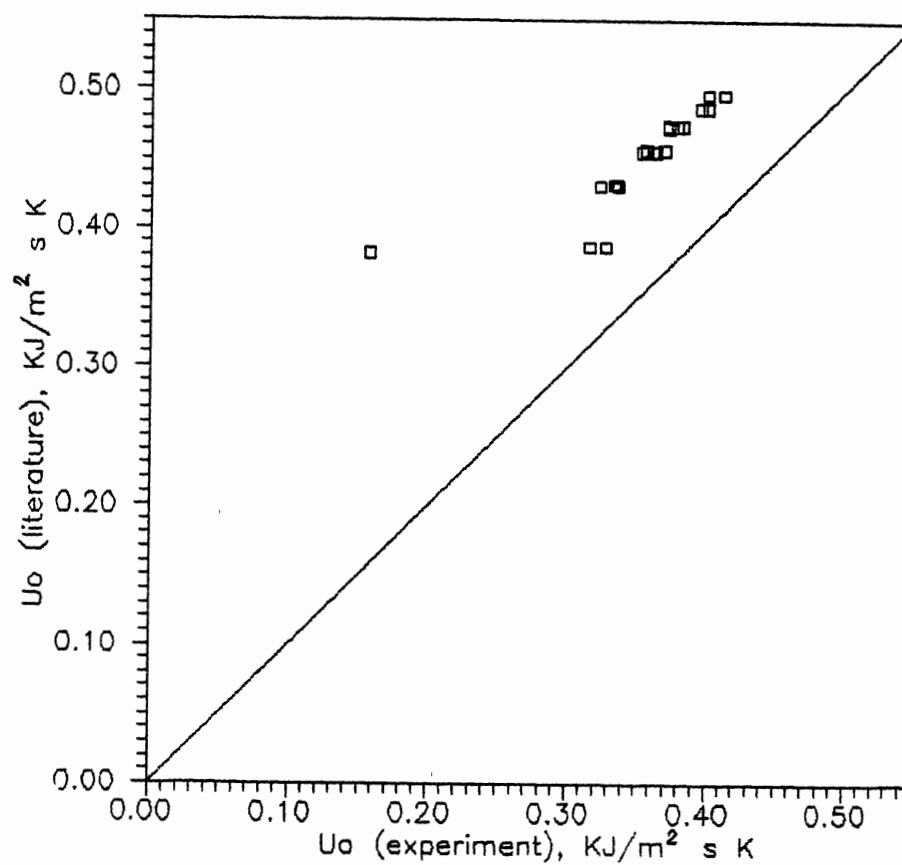


Figure 20. Comparison Between $U_{o,TOT}$ (literature) and $U_{o,TOT}$ (experiment): steam fed at the bottom section of the reflux condenser.

than $U_{O,TOT}$ evaluated from literature. This deviation is probably because of the uncertainty in calculating $U_{O,TOT}$ from the experimental data (estimated about $\pm 36 \%$, see Appendix D) and the high uncertainty in calculating wall resistance.

Wall resistance has a great effect on U_O . It was found that the wall constitutes about half of the total resistance to heat transfer in this apparatus. Consequently, the higher the uncertainty in calculating the wall resistance, the higher the uncertainty in calculating U_O . In all cases considered in this study, the uncertainty of wall resistance is approximately 50 % (see Appendix D).

Cooling Water Side Heat Transfer Coefficient (h_O)

The results of the water side heat transfer coefficient (h_O) calculated using the Wilson line method and using the literature methods are presented in a separate report. Figure 21 shows the comparison between h_O (literature) and h_O (Wilson line method) for normal operation at the top section. The deviation between h_O (Wilson line method) and h_O (literature) varies from - 45 % to + 13 % [evaluated based on h_O (literature)]. At the middle section, the deviation is between - 20 % and + 21 % and at the bottom section, the deviation is between - 12 % and + 11 % (the comparison graphs for these two section are not presented here). The same comparison is shown in Figure 22 for reflux operation at the bottom section. The deviation [based on

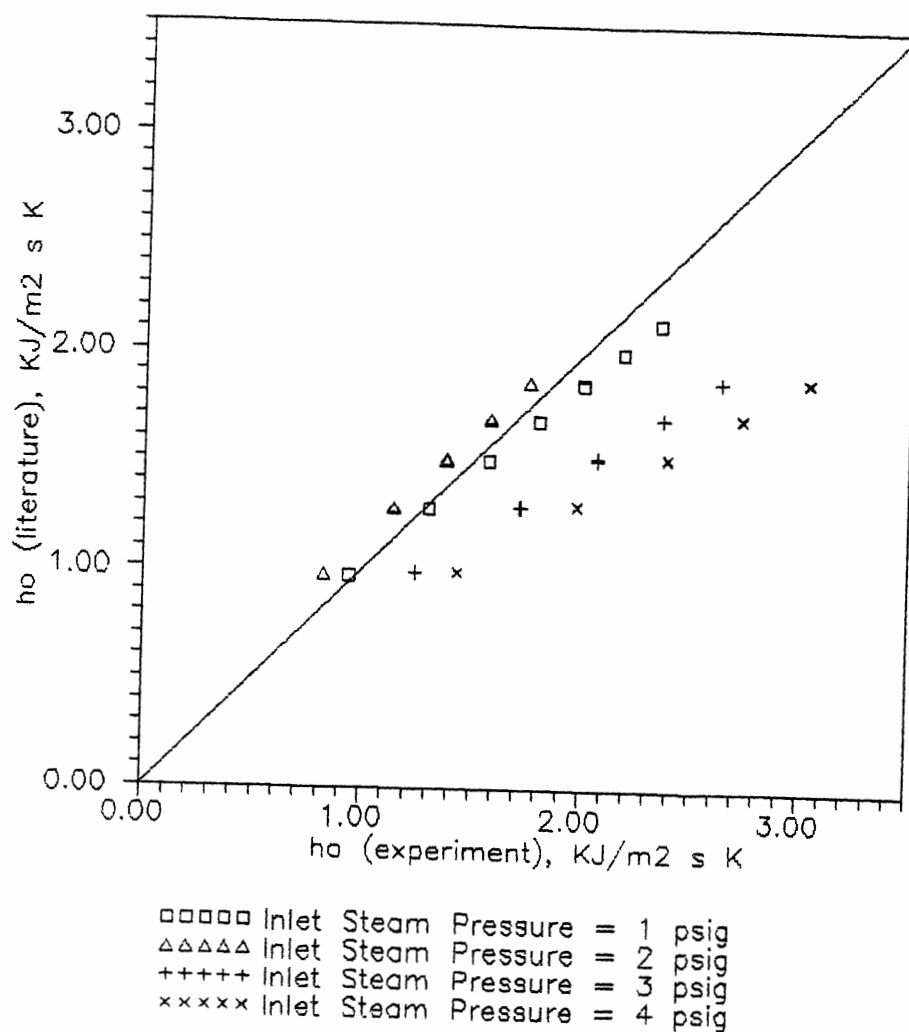


Figure 21. Comparison between h_o (literature) and h_o (Wilson line method) for Normal Operation at the Top Section.

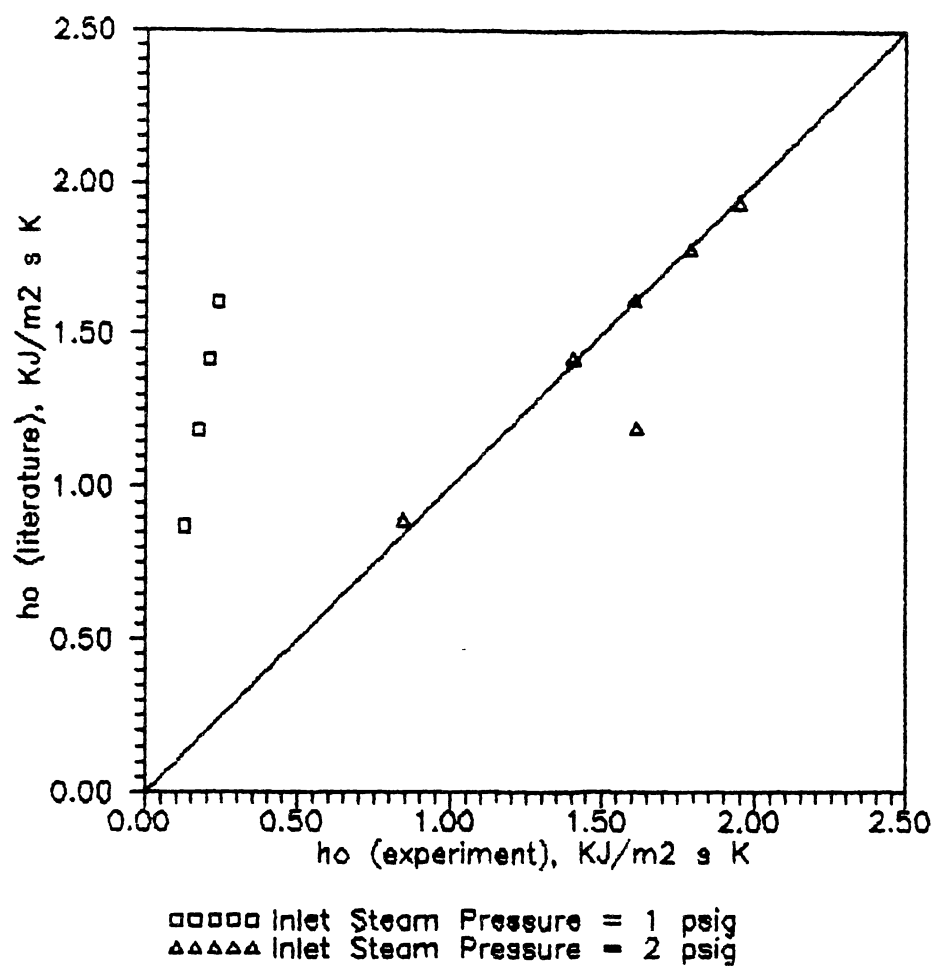


Figure 22. Comparison between h_o (literature) and h_o (Wilson line method) for Reflux Operation at the Bottom Section.

h_o (literature)] is in the range of -5 % to +97 %.

At the top section, the deviation is about - 33 % to + 116 % and at the middle section, the deviation is about + 38 %.

The difference of % deviation between normal and reflux operation (at the same section) is still a question, but this might be caused by the high uncertainty in calculating h_o using the Wilson line method.

Film Side Heat Transfer Coefficient (h_c)

The results of the film side heat transfer coefficient (h_c) calculated using the Wilson line method and using literature methods are presented in the separate report. Figures 23 and 24 show the comparison between h_c (literature) and h_c (Wilson line method) for normal operation at the top section and for reflux operation at the bottom section, respectively. For normal operation, h_c obtained from the Wilson line method is approximately 80 % lower than the one predicted from literature. An even worse result is obtained for reflux operation (about 90 % lower). This significant deviation is because of the high uncertainty of h_c obtained from experimental data as discussed in the experimental data analysis section.

Visual Observation

The general pattern of a condensing flow may be illustrated in Figure 25. At the top section of the condenser the condensing film pattern is distinguished by

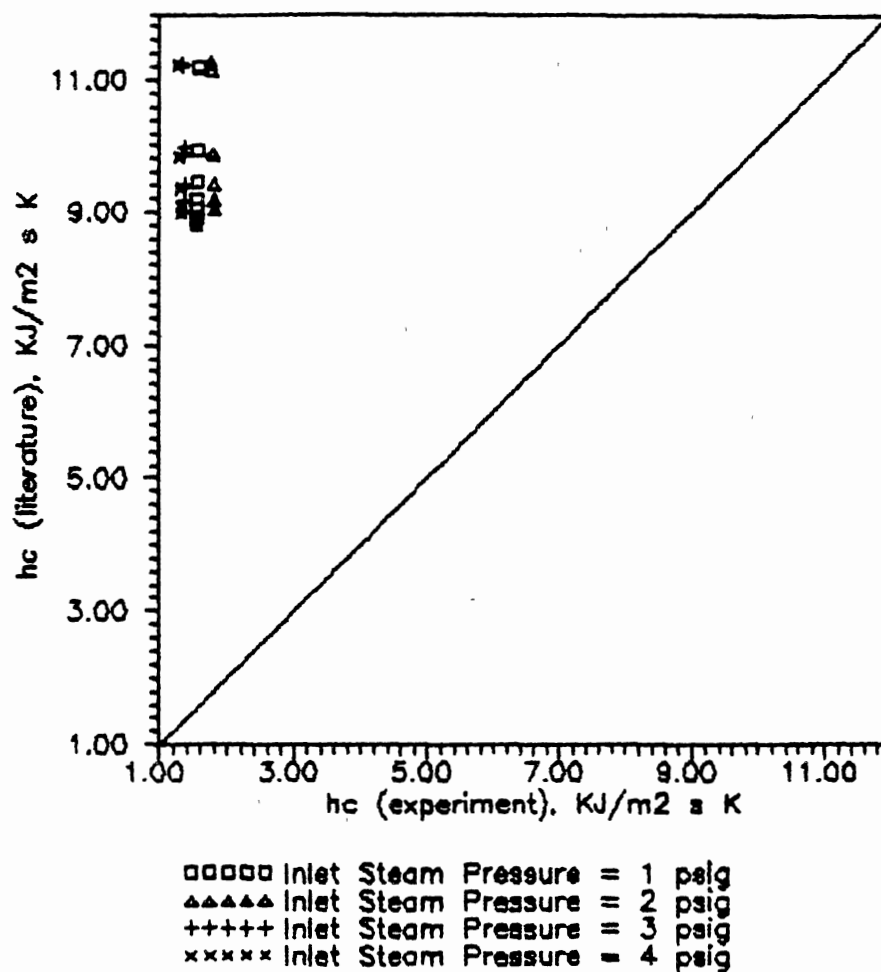


Figure 23. Comparison between h_c (literature) and h_c (Wilson line method) for Normal Operation at the Top Section.

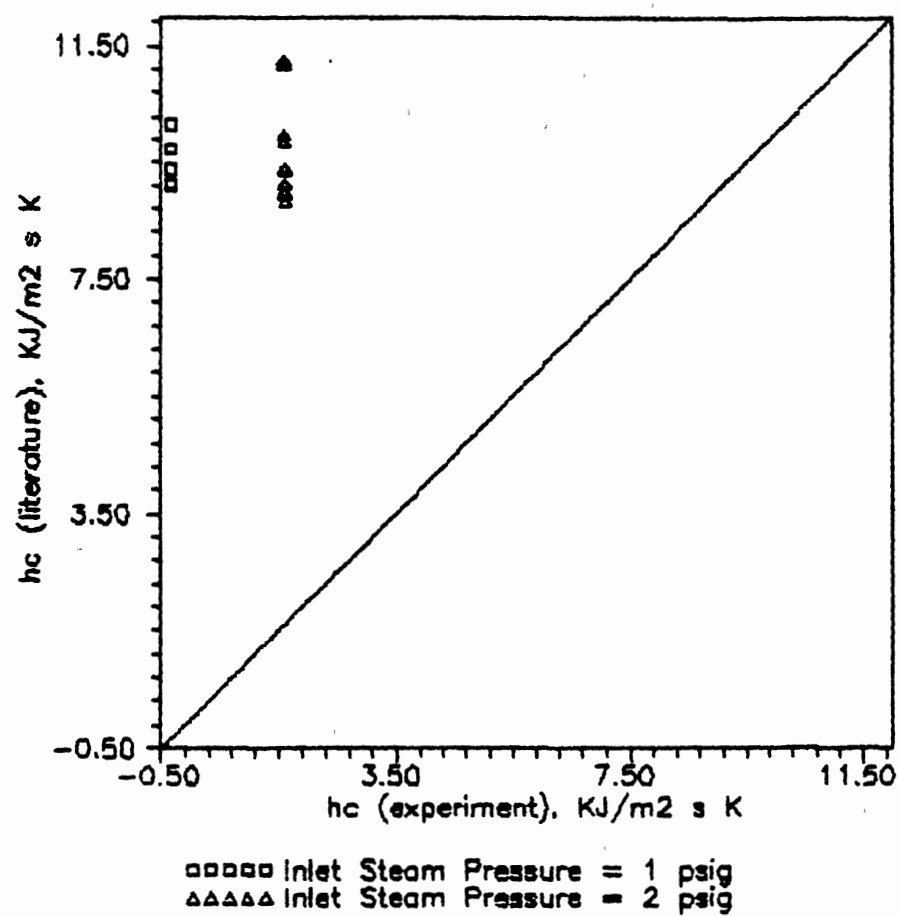


Figure 24. Comparison Between h_c (literature) and h_c (Wilson line method) for Reflux Operation at the Bottom Section.

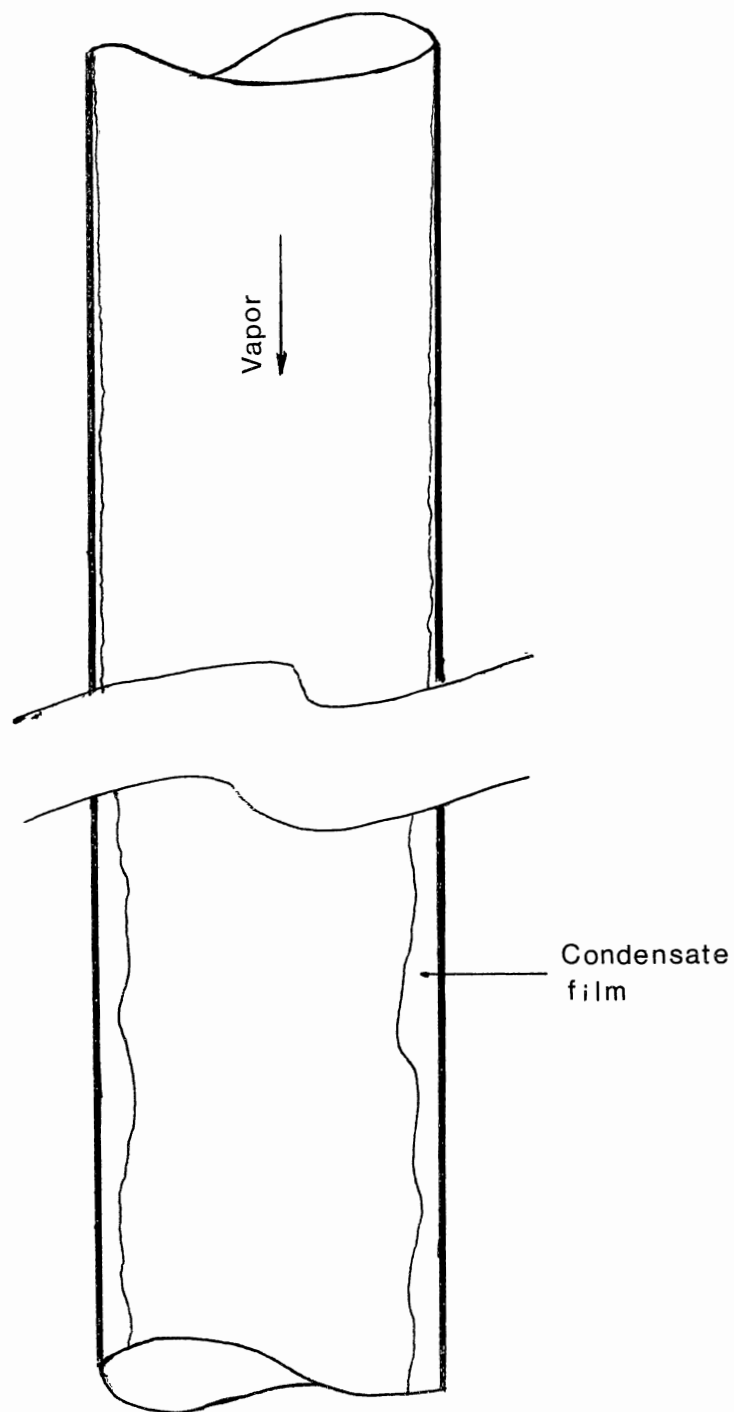


Figure 25. General Pattern of a Condensing Flow
in Co-current Flow.

small waves, thin film and creeping movement. As the condensate moves down, the condensate film becomes thicker, has larger waves and becomes more turbulent.

When steam is fed at the bottom, flooding is observed at a steam flow rate equal or greater than 2.23 E-3 Kg/s (flooding point will be discussed further in the next section). This flooding phenomenon is indicated by the existence of entrainment. Figure 26 illustrates the flow pattern when this flooding occurs.

Figures 25 and 26 are only rough illustrations of the flow pattern in the system considered. Additional equipment including a high speed camera is required to observe this flow pattern behavior.

Flooding Point

The most obvious indication of flooding phenomena is the occurrence of entrainment which can be observed along the reflux condenser and, more clearly, is distinguished by the existence of accumulated liquid in the upper plenum. Therefore this was used as a criterion to determine whether flooding occurs.

Estimation curves representing flooding points are shown in Figure 27 and 28. Flooding occurs when the condition is above the curves. Figure 27 shows the comparison between the flooding curve observed in this experiment and that predicted from Diehl & Koppany correlation. Figure 28 shows the comparison between the

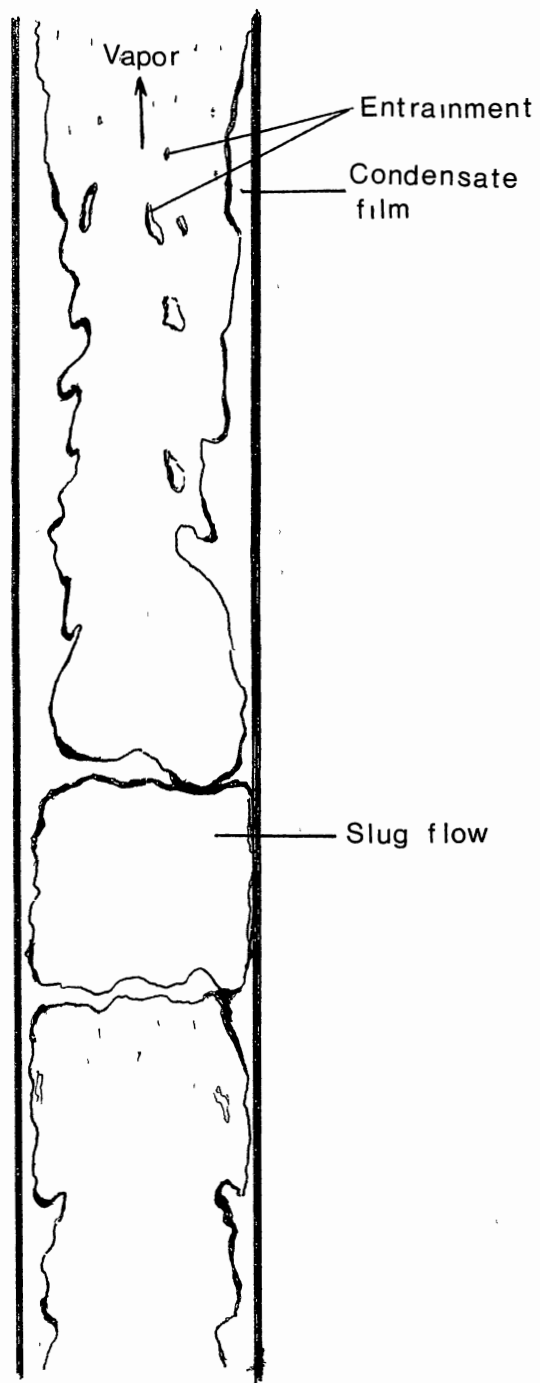


Figure 26. Flooding Flow Pattern

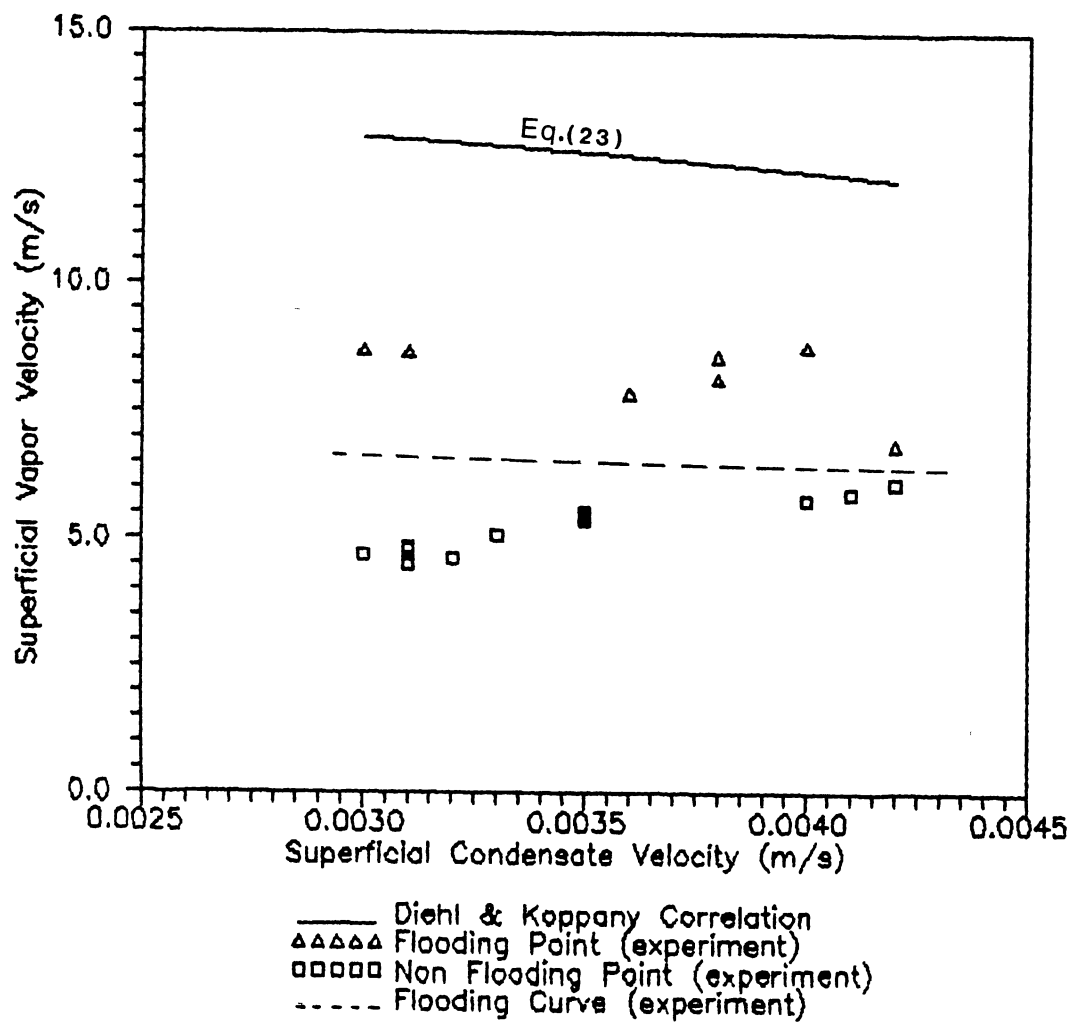


Figure 27. Comparison of Flooding Curve: experiment and Diehl & Koppany Method

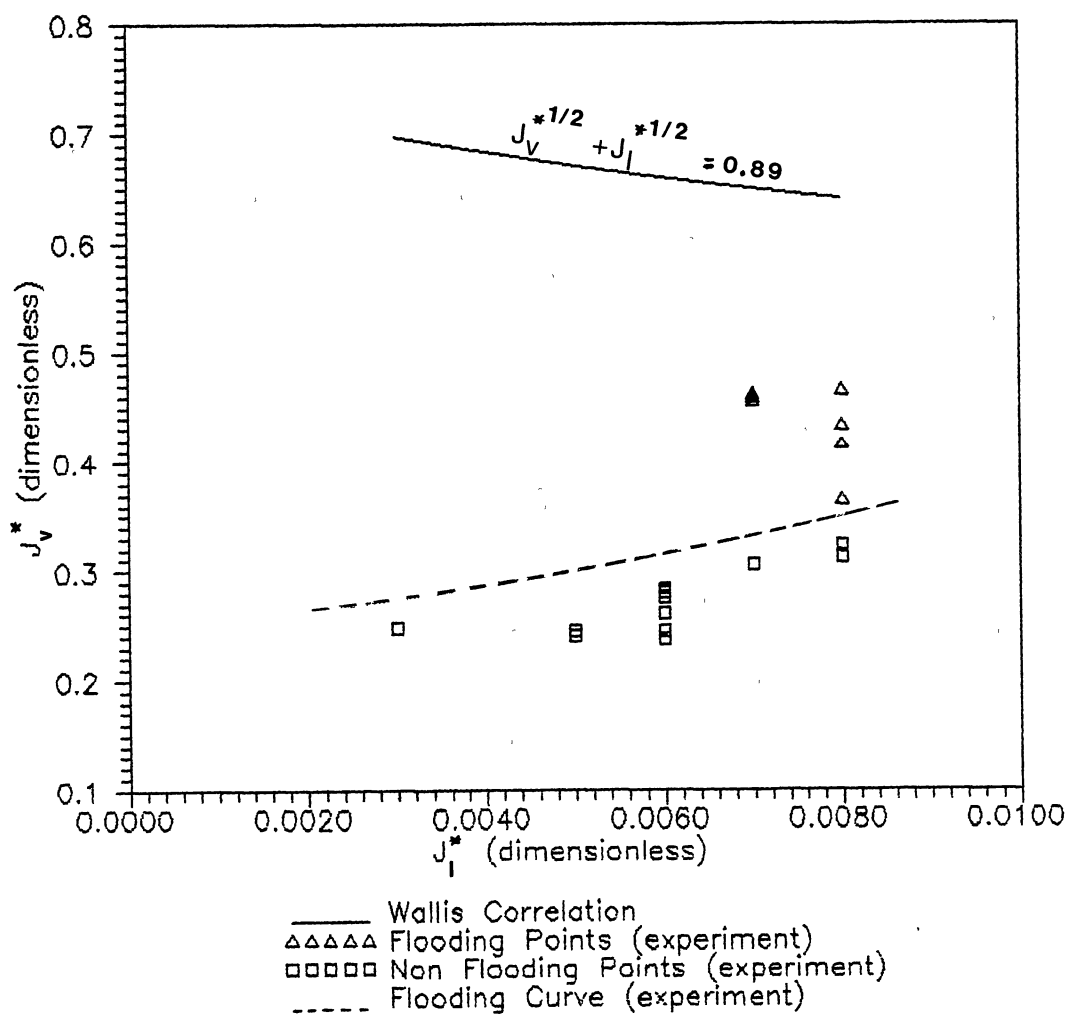


Figure 28. Comparison of Flooding Curve:
experiment and Wallis Method

estimated flooding curve obtained from this experiment and that calculated from the Wallis correlation. The flooding point curve obtained from Diehl & Koppany correlation is closer to the curve obtained from experiment than the one obtained from the Wallis correlation. However, both figures show that the curves predicted from literature are higher than the ones obtained from experimental data.

CHAPTER VI

CONCLUSIONS AND RECOMMENDATIONS

Conclusions

1. Overall heat transfer coefficients in a pyrex glass vertical reflux condenser have been measured in the range of cooling water Reynolds numbers from 460 to 3800, entering steam Reynolds numbers from 4.1×10^5 to 1.2×10^6 , and exit condensate Reynolds numbers from 30 to 450.

2. $U_{O,TOT}$ evaluated from the experimental data is about 20 % lower than $U_{O,TOT}$ calculated from literature. This deviation is probably caused by the high uncertainty of calculating $U_{O,TOT}$ (experiment) which is about ± 36 % and the uncertainty in calculating the wall resistance (± 50 %).

3. $U_{O,TOT}$ obtained from experimental data when steam is fed at the the top section is about 20 % higher than one when steam is fed at the bottom section. This is the result of the thinner film and thus less heat transfer resistance when steam is fed at the top.

4. The results of h_o and h_c obtained from the Wilson line method have high uncertainties because of the high uncertainty in obtaining the slopes and intercepts. In addition, high uncertainty in the wall resistance also plays

a role in calculating h_c .

5. In general, the deviation between h_o calculated from literature [11] and h_o calculated from the Wilson line method varies from -45 % to +21 % (based on literature) for normal operation. For reflux operation, the deviation is in between - 33 % and 116 %. These high deviations are probably because of the high uncertainty in obtaining h_o from the Wilson line method.

6 For normal operation, h_c calculated by the Wilson line method is about 80 % higher than the one calculated from literature [4] and for reflux operation, h_c calculated by the Wilson line method is about 90 % higher. These deviations are also because of the high uncertainty in obtaining h_c from the Wilson line method.

7. Increasing vapor flow rate results in a better heat transfer coefficient. This is probably because of the increasing vapor shear effect.

8 The general pattern of the condensing flow is a thin film, small waves and creeping flow at the top section of the condenser. As the condensate moves down, the condensate film becomes thicker, has larger waves, and become more turbulent.

9. When steam is fed at the bottom section of the condenser, flooding is observed at steam flow rates above $4.54 \text{ Kg/m}^2\text{s}$.

10. The estimated flooding point curve obtained from experimental data shows significant deviation from the

literature predictions (Diehl & Koppany and Wallis correlations), especially as the steam flow rate increased.

Recommendations

1. Improved steam temperature and pressure measurements are needed for the inlet steam.
2. Pyrex glass should be replaced by another material such as metal to improve heat transfer coefficients if we are not interested in making visual observations.
3. Wall temperature should be measured by adding a thermocouple placed at the wall surface.
4. Additional instrumentation such as a high speed camera is needed to make better visual observations.
5. A sight gauge should be added to the lower plenum to make controlling liquid level easier.
6. The accuracy of condensate flow rate measurement might be improved by accumulating the condensate over a longer period of time.

BIBLIOGRAPHY

1. Alekseev, V.P., Poberezkin, A.E., and Gerasimov, P.V. (1972) "Determination of Flooding Rates in Packing," Heat Trans. Soviet Res., 4: 159-163.
2. Balekjian, G., and Katz, D.L. (1958) "Heat Transfer from Superheated Vapors to a Horizontal Tube," AIChE J., No. 1, 4: 43.
3. Bell K.J. (1989) Notes on Process Heat Transfer, School of Chemical Engineering, Oklahoma State University.
4. Bell, K.J. (1989) Notes on Condensation Heat Transfer, School of Chemical Engineering, Oklahoma State University.
5. Bennett, C.O., and Myers, J.E. (1962) Momentum, Heat, and Mass Transfer, Second Ed., 458-460.
6. Bergles, A.E., Collier, J.G., Delhay, J.M., Hewitt, G.F., and Mayinger, F. (1981) Two-phase Flow and Heat Transfer in the Power and Process Industries, Hemisphere Publishing Corporation, Washington, New York: 27-34, 330-334.
7. Boyko, L.D., and Kruzhilin, G.N. (1967) "Heat Transfer and Hydraulic Resistance During Condensation of Steam in a Horizontal Tube in a Bundle of Tubes," Int. J. Heat Mass Transfer, 10: 361.
8. Bromley, L.A. (1952) "Effect of Heat Capacity of Condensate," Ind. Eng. Chem., 44: 2966.
9. CRC Handbook of Chemistry and Physics (1987), 68th Ed., CRC Press: E-6.
10. Carpenter, E.F., and Colburn, A.P. (1951) "The Effect of Vapor Velocity on Condensation Inside Tubes" Proceedings of General Discussion on Heat Transfer, London, ASME, New York.

11. Chen, C.Y., Hawkins, G.A., and Solberg, H.L. (1946)
"Heat Transfer in Annuli," Trans. ASME: 99-106.
12. Chung, K.S. (1978) Flooding Phenomenon in Counter-current Two-phase Flow Systems, Ph.D.
Dissertation, University of California, Berkeley.
13. Clift, R., Pritchard, C.L., and Nedderman, R.M. (1966)
"The Effect of Viscosity on the Flooding
Conditions in Wetted Wall Columns," Chem. Eng.
Sci., 21: 87-95.
14. Colburn, A.P. (1934) "Note on the Calculation of
Condensation When a Portion of Condensate Layer
is in Turbulent Motion," Trans. AIChE, 30: 187.
15. Colburn, A.P., Millar, L.L., and Westwater, J.W. (1942),
"Condenser-subcooler Performance and Design,:"
Trans. AIChE, 38: 447.
16. Davis, E.S. (1943) "Heat Transfer and Pressure Drop in
Annuli," Trans. ASME, 65: 755-760.
17. Diehl, J.E., and Koppany, C.R. (1977) "Flooding
Velocity Correlation for Gas-liquid Counterflow
in Vertical Tubes," Chem. Eng. Prog. Symp. Series,
65(92): 77.
18. Dietrich, C.F. "Uncertainty, Calibration and
Probability," The Statistics of Scientific and
Industrial Measurement, John Wiley, New York.
19. Dukler, A.E. (1960) "Fluid Mechanics and Heat Transfer
in Vertical Falling-film Systems," Chem. Eng.
Symp. Series, 56(30): 1.
20. Dukler, A.E., and Smith, L. (1967) "Two Phase
Interactions in Countercurrent Flow Studies of
the Flooding Mechanism," US NRC Contract AT (49 -
24) 0194, Summary Report, No.1.
21. Edwin, M.B. (1966) Statistical Methods in Engineering
Experiments, U. of Alabama in Huntsville, Charles
E. Merrill Books, Inc., Columbus, Ohio: 83-97,
108-130.
22. English, K.G., Jones, W.T., Spiller, R.C., and Orr V.
(1963) "Flooding in a Vertical Updraft Partial
Condenser," Chem. Eng. Prog. 59: 51.
23. Feind, K. (1960) "Stromungsuntersuchungen bei Gegenstrom
von Rivselfilmen und Gas in lotrechten Rohren,"
VDI-Forschungsheft, 481.

24. George, W.M. (1954) "Properties of Glass," American Chemical Society, Monograph Series, Second Ed., Reinhold Publishing Corp. Washington, D.C.
25. Grolmes, M.A., Lambert, G.A., and Fauske, H.K. (1974) "Flooding in Vertical Tubes," Symp on Multi-phase Flow System, Inst. Chem. Eng. Symp., 38: A4
26. Hewitt, G.F., Lacey, P.M.C., and Nicholls, B. (1965) "Transitions in Film Flow in a Vertical Tube," AERE-R4614, Symp. on Two Phase Flow, Paper No. B4, University of Exeter.
27. Hewitt, G.F., and Wallis, G.B. (1963) "Flooding and Associated Phenomena in Falling Film Flow in a Tube," AERE-R4022.
28. Imura, H., Kusuda, H., and Funtasu S. (1977) "Flooding Velocity in a Counter-current Annular Two-phase Flow," Chem. Eng. Sci., 32: 79-87.
29. Jakob, M. (1949) Heat Transfer, Hohn Wiley and Sons, New York.
30. Jakob, M., and Rees. K.A. (1941) "Heat Transfer to a Fluid in Laminar Flow Through an Annular Space," Trans. AIChE, 37: 619-648.
31. Jordan, H.P. (1909) "On the Rate of Heat Transmission Between Fluids and Metal Surfaces," Proceedings of the Institution Mechanical Engineers, London, England, Part 4: 1317-1357.
32. Kamei S., Oishi, J., and Okane, T. (1954) "Flooding in a Wetted Wall Tower," Chem. Eng. (Japan), 18: 364.
33. Katz, J.G., and Knudsen, D.L. (1958) Fluid Dynamics and Heat Transfer, McGraw-Hill, New York.
34. Kirkbride, C.G. (1934) "Heat Transfer by Condensing Vapor on Vertical Tube," Trans. AIChE, 30: 170.
35. Minkowycz, W.J., and Sparrow, E.M. (1966) "Condensation Heat Transfer in the Presence of Non-condensable, Interfacial Resistance, Superheating, Variable Properties and Diffusion" Int. J. Heat Mass Transfer, 9: 1125.
36. Nusselt, W. (1916) "Die oberflächen kondensation des Wasserdampfes" ZVDI, 60: 541, 569.
37. Nusselt, W. (1913) "Über Wärmeübergang auf ruhige Oder Bewegte Luft," ZVDI, 57: 197-199.

38. Pioneering Research Division U.S Army Natick Laboratories (1966), Project Ref. IP014501B11A, Series: Thermal Cond. -1, Natick, Massachusetts.
39. Pushkina, O.L., and Sorokin, Y.L. (1969) "Breakdown of Liquid Film Motion in Vertical Tubes," Heat Trans. Soviet Res., 1: 56.
40. Rohsenow, W.M. (1956) "Heat Transfer and Temperature Distribution in Laminar Film Condensation," Trans. ASME, 78: 1645.
41. Rohsenow, W.M., Webber, J.H., and Ling, A.T. (1956) "Effect of Vapor Velocity on Laminar and Turbulent Film Condensation," Trans. ASME, 78: 1637.
42. Schrage, R.W. (1953) A Theoretical Study of Interphase Mass Transfer, Columbia University Press, New York.
43. Shires, G.L., and Pichering, A.R. (1965) "The Flooding Phenomena in Counter-current Two-phase Flow" Symp.on Two Phase Flow, Exeter: b501.
44. Tobilevich, N.Y., Sagan, I.I., and Porzhezinskii, Y.G. (1968) "The Downward Motion of a Liquid Film in Vertical Tubes in an Air-Vapor Counter Flow," Inzhenesno-Fizicheskii Zhurnal, 15: 855.
45. Wallis, G.B. (1961) "Flooding Velocities for Air and Water in Vertical Tubes," UKAEA Report AEEW-R123.
46. Wallis, G.B. (1969) One-dimensional Two-phase Flow, McGraw-Hill, New York: 339.
47. Wilson, E.E. (1915) "A Basis of Rational Design of Heat Transfer Apparatus" Trans Am. Soc. Mech. Eng., 37: 47.

APPENDIX A

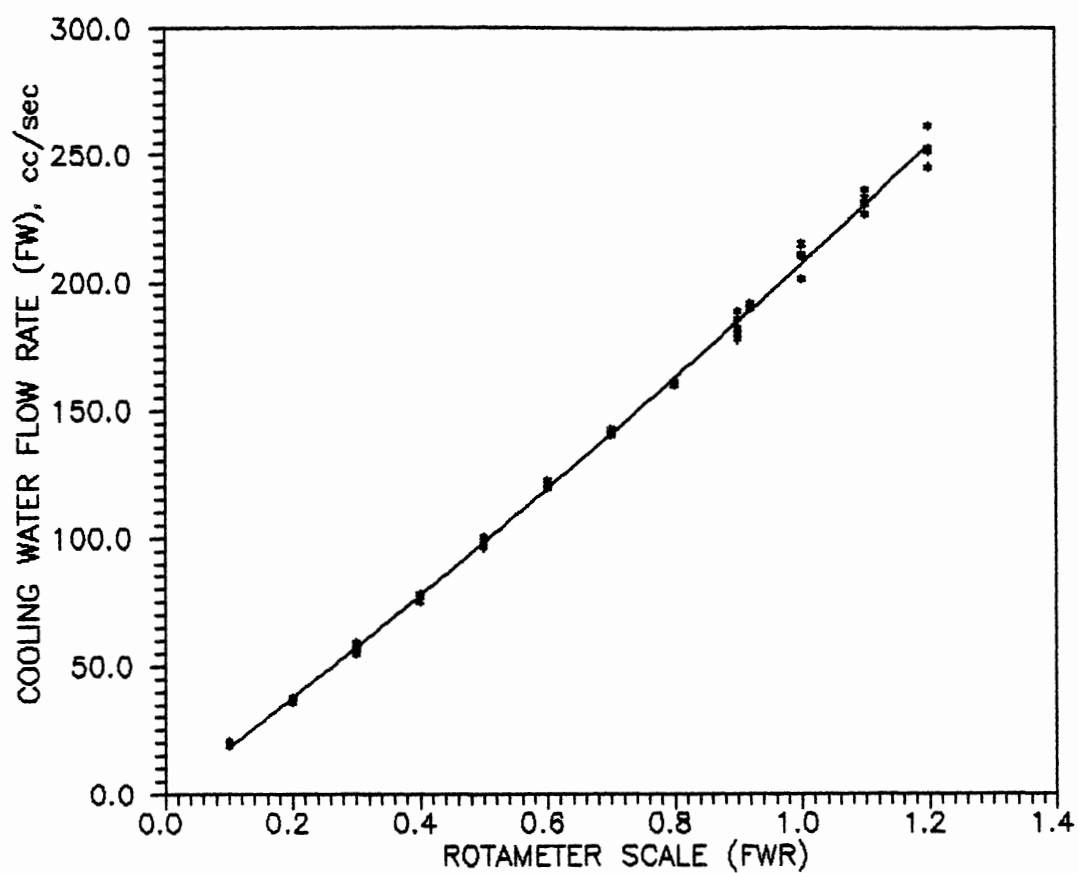
ROTAMETER CALIBRATION

TABLE I
ROTAMETER CALIBRATION DATA

| Run No. | Rotameter Scale | Measured Volumetric Flow Rate of Cooling Water, cc/s |
|---------|-----------------|---|
| 1 | 0.1 | 18.78 |
| 2 | | 20.03 |
| 3 | | 19.57 |
| 4 | | 20.07 |
| 5 | | 20.50 |
| 6 | 0.2 | 37.93 |
| 7 | | 37.13 |
| 8 | | 37.32 |
| 9 | | 36.08 |
| 10 | | 36.07 |
| 11 | | 35.91 |
| 12 | 0.3 | 59.03 |
| 13 | | 58.37 |
| 14 | | 51.92 |
| 15 | | 56.30 |
| 16 | | 55.09 |
| 17 | 0.4 | 78.15 |
| 18 | | 78.37 |
| 19 | | 77.29 |
| 20 | | 77.24 |
| 21 | | 75.54 |
| 22 | 0.5 | 100.55 |
| 23 | | 100.52 |
| 24 | | 99.34 |
| 25 | | 96.52 |
| 26 | 0.6 | 120.26 |
| 27 | | 122.39 |
| 28 | | 119.43 |
| 29 | | 120.00 |
| 30 | 0.7 | 140.41 |
| 31 | | 140.86 |
| 32 | | 141.01 |
| 33 | | 140.30 |
| 34 | 0.8 | 160.09 |
| 35 | | 161.04 |
| 36 | | 161.29 |
| 37 | 0.9 | 182.90 |
| 38 | | 188.90 |
| 39 | | 185.62 |
| 40 | | 178.03 |
| 41 | | 180.24 |
| 42 | 0.92 | 191.96 |

TABLE I (Continued)

| Run No. | Rotameter Scale | Measured Volumetric Flow Rate of Cooling Water, cc/s |
|---------|-----------------|---|
| 43 | | 190.38 |
| 44 | | 190.42 |
| 45 | 1.0 | 201.77 |
| 46 | | 215.17 |
| 47 | | 210.62 |
| 48 | | 210.88 |
| 49 | 1.1 | 230.84 |
| 50 | | 236.39 |
| 51 | | 227.04 |
| 52 | | 232.92 |
| 53 | 1.2 | 251.66 |
| 54 | | 252.60 |
| 55 | | 261.55 |
| 56 | | 245.38 |



$$FW = 21.5734FWR^2 + 186.297FWR - 0.320556$$

Average Standard Error = ± 3.15 cc/second

Figure 29 . Rotameter Calibration Curve

APPENDIX B

THERMOCOUPLE CALIBRATION

TABLE II
THERMOCOUPLE CALIBRATION DATA

| Run No. | Temperature Reading of Thermocouple No., °F | | | | | | True Temperature, °F |
|------------|--|-------|-------|-------|-------|-------|----------------------------|
| | 1 | 2 | 3 | 4 | 5 | 6 | |
| 1 | 79.2 | 79.1 | 77.8 | 79.6 | 80.7 | 80.4 | 79.1 |
| 2 | 79.2 | 79.7 | 80.0 | 79.4 | 80.1 | 79.7 | 78.4 |
| 3 | 86.7 | 86.8 | 86.8 | 88.0 | 85.5 | 85.0 | 86.3 |
| 4 | 94.7 | 95.5 | 95.4 | 97.3 | 95.2 | 94.5 | 95.0 |
| 5 | 104.9 | 105.4 | 105.1 | 107.1 | 105.7 | 104.2 | 104.7 |
| 6 | 116.9 | 117.3 | 117.1 | 118.1 | 117.2 | 117.6 | 116.3 |
| 7 | 128.3 | 128.6 | 128.8 | 129.5 | 128.8 | 128.0 | 127.1 |
| 8 | 139.2 | 139.5 | 139.6 | 140.1 | 139.4 | 139.5 | 139.9 |
| 9 | 150.0 | 150.1 | 150.1 | 150.7 | 150.1 | 150.0 | 148.7 |
| 10 | 159.7 | 159.8 | 159.8 | 160.2 | 159.7 | 159.9 | 158.6 |
| 11 | 170.0 | 170.0 | 170.0 | 170.4 | 169.9 | 170.0 | 169.7 |
| 12 | 181.6 | 181.6 | 181.7 | 182.2 | 181.7 | 181.6 | 180.6 |
| 13 | 192.4 | 192.4 | 192.4 | 193.0 | 192.5 | 192.2 | 191.5 |
| 14 | 204.1 | 203.9 | 204.2 | 204.7 | 204.3 | 204.2 | 204.3 |
| 15 | 214.8 | 214.8 | 215.0 | 215.4 | 215.0 | 214.6 | 213.9 |
| 16 | 225.0 | 224.9 | 225.0 | 225.5 | 225.2 | 225.1 | 224.3 |
| 17 | 233.7 | 233.6 | 233.7 | 234.3 | 234.0 | 233.7 | 233.3 |
| 18 | 245.2 | 245.2 | 245.3 | 245.7 | 245.5 | 245.5 | 244.8 |
| 19 | 258.8 | 258.8 | 259.0 | 259.3 | 259.1 | 259.1 | 258.0 |
| 20 | 267.8 | 267.8 | 267.9 | 268.3 | 268.2 | 268.3 | 267.4 |

The calibration equations of each thermocouple are:

1. $T1F = 0.9983 TR1 - 0.29178$, standard error = ± 0.51 °F
2. $T2F = 1.0007 TR2 - 0.81919$, standard error = ± 0.49 °F
3. $T3F = 0.9980 TR3 - 0.34001$, standard error = ± 0.68 °F
4. $T4F = 1.0027 TR4 - 1.85328$, standard error = ± 0.60 °F
5. $T5F = 0.9994 TR5 - 0.70000$, standard error = ± 0.86 °F
6. $T6F = 0.9965 TR6 - 0.03446$, standard error = ± 0.62 °F

APPENDIX C

SAMPLE CALCULATIONS

SAMPLE CALCULATIONS

All of these calculations use the data for Run No. 68

Input Data

Vapor enters at the bottom section of the reflux condenser

$$P_{\text{atm}} = 29.04 \text{ in Hg} = 98.35 \text{ KPa (absolute)}$$

$$P_{\text{pg}} = 2.0 \text{ psig} = 13.79 \text{ KPa (gauge)}$$

$$P = 98.35 + 13.79 = 112.13 \text{ KPa (absolute)}$$

$$\text{Cooling water flow rate} = 1.85 \times 10^{-5} \text{ m}^3/\text{s} \text{ (corresponding to } 0.1 \text{ in rotameter scale)}$$

$$\begin{aligned} \text{Condensate flow rate from the reflux condenser (measured)} \\ = 1.56 \times 10^{-6} \text{ m}^3/\text{s} \end{aligned}$$

$$\begin{aligned} \text{Condensate flow rate from the auxiliary condenser} \\ = 0.00 \text{ m}^3/\text{s} \end{aligned}$$

$$\text{Flow rate of entrained liquid} = 0.00 \text{ m}^3/\text{s}$$

$$\text{Thermocouple \#1, at the inlet bottom section} = 81.7 \text{ }^{\circ}\text{F}$$

$$\text{Thermocouple \#2, at the outlet bottom section} = 110.6 \text{ }^{\circ}\text{F}$$

$$\text{Thermocouple \#3, at the outlet middle section} = 113.2 \text{ }^{\circ}\text{F}$$

$$\text{Thermocouple \#4, at the outlet top section} = 152.9 \text{ }^{\circ}\text{F}$$

$$\text{Thermocouple \#5, at the inlet auxiliary condenser} = 152.9 \text{ }^{\circ}\text{F}$$

$$\text{Thermocouple \#6, at the outlet auxiliary condenser} = 148.5 \text{ }^{\circ}\text{F}$$

Dimensions of apparatus

The inside diameter of the inner column(d_i) = 0.025 m

The outside diameter of the inner column(d_o) = 0.028 m

The inside diameter of the annular jacket(D_2) = 0.037 m

The outside diameter of the annular jacket(D_1) = 0.041 m

The length of each section of the reflux condenser = 0.657 m

Calculations from the Experimental Data

1. Saturated Temperature(T_{sat})

By fitting the data from a steam table, saturated temperature ($^{\circ}\text{C}$) and pressure (KPa) are correlated as follows:

$$\begin{aligned} T_{sat} &= -4.65382 \times 10^{-4} * P^2 + 0.349967 * P + 69.1549 \\ &= -4.65382 \times 10^{-4} * (112.13)^2 + 0.349967 * (112.13) + 69.1549 \\ &= 102.6 \text{ }^{\circ}\text{C} = 216.6 \text{ }^{\circ}\text{F} \end{aligned}$$

2. The Real Values of Temperature

$$\begin{aligned} T1F &= 0.9983 * TR1 - 0.291782 = 0.9983(81.7) - 0.291782 \\ &= 81.3 \text{ }^{\circ}\text{F} = 27.4 \text{ }^{\circ}\text{C} \end{aligned}$$

$$\begin{aligned} T2F &= 1.00074 * TR2 - 0.819189 = 1.00074(110.6) - 0.819189 \\ &= 109.9 \text{ }^{\circ}\text{F} = 43.3 \text{ }^{\circ}\text{C} \end{aligned}$$

$$\begin{aligned} T3F &= 0.997961 * TR3 - 0.340013 = 0.997961(113.2) - 0.340013 \\ &= 132.6 \text{ }^{\circ}\text{F} = 55.9 \text{ }^{\circ}\text{C} \end{aligned}$$

$$\begin{aligned} T4F &= 1.00274 * TR4 - 1.85328 = 1.00274(152.9) - 1.85328 \\ &= 151.5 \text{ }^{\circ}\text{F} = 66.4 \text{ }^{\circ}\text{C} \end{aligned}$$

Note: TR1, TR2, TR3 and TR4 are thermocouples # 1, 2, 3 and 4 (in $^{\circ}\text{F}$).

3. Flow Rate of Cooling Water

The calibration equation of the rotameter is:

$$\text{FW} = (21.5734 \cdot \text{FWR}^2 + 186.297 \cdot \text{FWR} - 0.320556) \cdot 10^{-6}$$

where FW = volumetric flow rate (m^3/s)

FWR = rotameter scale

at FWR = 0.1, $\text{FW} = 1.85 \cdot 10^{-5} \text{ m}^3/\text{s} = 2.35 \text{ ft}^3/\text{hr}$

Density of water is obtained based on the following fitting equation:

$$\rho_1 = (-6.85715 \cdot 10^{-5} \cdot T^2 + 2.66668 \cdot 10^{-3} \cdot T + 62.4024) (16.0185)$$

where ρ_1 (density of water) is in Kg/m^3 and T is in $^{\circ}\text{F}$

At 81.3°F , the density of water is $995.8 \text{ Kg}/\text{m}^3$

(= $62.16 \text{ lb}_m/\text{ft}^3$).

Mass flow rate of cooling water is

$$\begin{aligned} (1.85 \cdot 10^{-5} \text{ m}^3/\text{s}) (995.8 \text{ Kg}/\text{m}^3) &= 1.85 \cdot 10^{-2} \text{ Kg/s} \\ &= 146.83 \text{ lb}_m/\text{hr} \end{aligned}$$

The cross section area for an annulus is

$$\begin{aligned} A &= (\pi/4) (D_2^2 - D_1^2) = (\pi/4) (0.037^2 - 0.028^2) \\ &= 4.59 \cdot 10^{-4} \text{ m}^2 = 4.94 \cdot 10^{-3} \text{ ft}^2 \end{aligned}$$

Velocity of cooling water is

$$\begin{aligned} (1.85 \cdot 10^{-5} \text{ m}^3/\text{s}) / (4.59 \cdot 10^{-4} \text{ m}^2) &= 4.03 \cdot 10^{-2} \text{ m/s} \\ &= 0.13 \text{ ft/s} \end{aligned}$$

4. Flow Rate of Condensate

Volumetric flow rate of condensate (measured)

$$= 1.56 \times 10^{-6} \text{ m}^3/\text{s} = 0.2 \text{ ft}^3/\text{hr}$$

Density of saturated water (ρ_1) at $P = 112.13 \text{ KPa}$ is

$$956.1 \text{ Kg/m}^3 = 59.7 \text{ lb}_m/\text{ft}^3$$

Mass flow rate of condensate = $(1.56 \times 10^{-6})(956.1)$

$$= 1.49 \times 10^{-3} \text{ Kg/s}$$

$$= 11.83 \text{ lb}_m/\text{hr}$$

5. Amount of Heat Transferred to Cooling Water

At the Top Section

$$Q_1 = m_w \cdot c_p \cdot \Delta t$$

m_w = mass flow rate of cooling water = $1.85 \times 10^{-2} \text{ Kg/s}$

c_p = 4.19 KJ/Kg K (assumed constant)

$$\Delta t = 66.4 - 55.9 = 10.5 \text{ }^\circ\text{C}$$

$$Q_1 = (1.85 \times 10^{-2})(4.19)(10.49) = 0.810 \text{ KJ/s} = 2764 \text{ Btu/hr}$$

At the Middle Section

$$\begin{aligned} Q_2 &= (1.85 \times 10^{-2})(4.19)(55.88 - 43.26) = 0.975 \text{ KJ/s} \\ &= 3327 \text{ Btu/hr} \end{aligned}$$

At the Bottom Section

$$\begin{aligned} Q_3 &= (1.85 \times 10^{-2})(4.19)(43.26 - 27.37) = 1.227 \text{ KJ/s} \\ &= 4187 \text{ Btu/hr} \end{aligned}$$

$$\begin{aligned} Q_{\text{TOT}} &= Q_1 + Q_2 + Q_3 = 0.810 + 0.975 + 1.227 = 3.012 \text{ KJ/s} \\ &= 10278 \text{ Btu/hr} \end{aligned}$$

6. Heat of Condensation

$$Q_{\text{con}} = m_c \lambda$$

m_c = mass flow rate of first condensate

$$= 1.49 \times 10^{-3} \text{ Kg/s}$$

$$\lambda = 1.14384 \times 10^{-3} (112.13)^2 - 0.914073 (112.13) + 2338.29$$

$$= 2250 \text{ KJ/Kg}$$

$$Q_{\text{con}} = (1.49 \times 10^{-3}) (2250) = 3.356 \text{ KJ/s} = 11452 \text{ Btu/hr}$$

7. Overall Heat Transfer Coefficient Calculated from Experimental Data

At the Top Section

$$\text{LMTD1} = \frac{(66.4 - 55.9)}{\ln \frac{(102.6 - 55.9)}{(102.6 - 66.4)}} = 41.2 \text{ }^{\circ}\text{C} = 74.2 \text{ }^{\circ}\text{F}$$

$$U_{o,1} = Q_1 / \text{LMTD1} \cdot A_o$$

where

$$A_o = \text{outside area of heat transfer per section}$$

$$= \pi d_o L = \pi (0.028) (0.657) = 0.058 \text{ m}^2$$

So,

$$U_{o,1} = (0.810) / (41.2 \times 0.058) = 0.339 \text{ KJ/m}^2 \text{ s K}$$

$$= 339.0 \text{ W/m}^2 \text{ K}$$

$$= 59.7 \text{ Btu/ft}^2 \text{ hr }^{\circ}\text{F}$$

At the Middle Section

$$\text{LMTD}_2 = \frac{(55.9-43.3)}{\ln \frac{(102.6-43.3)}{(102.6-55.9)}} = 52.7^\circ\text{C} = 94.9^\circ\text{F}$$

$$\begin{aligned} U_{o,2} &= Q_2 / \text{LMTD}_2 * A_o = (0.975) / (52.73 * 0.058) \\ &= 0.319 \text{ KJ/m}^2\text{S K} = 319.0 \text{ W/m}^2\text{K} = 56.1 \text{ Btu/ft}^2\text{hr } ^\circ\text{F} \end{aligned}$$

At the Bottom Section

$$\text{LMTD}_3 = \frac{(43.3-27.4)}{\ln \frac{(102.6-27.4)}{(102.6-43.3)}} = 66.9^\circ\text{C} = 120.4^\circ\text{F}$$

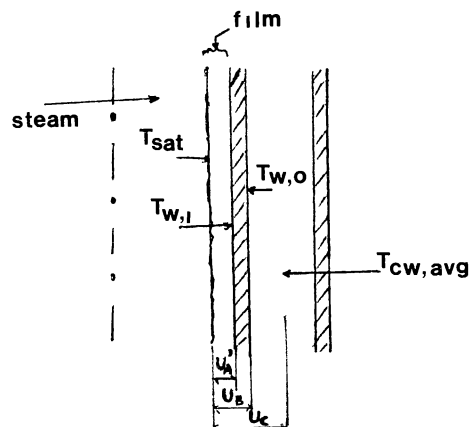
$$\begin{aligned} U_{o,3} &= Q_3 / \text{LMTD}_3 * A_o = (1.227) / (66.9 * 0.058) \\ &= 0.316 \text{ KJ/m}^2\text{S K} = 316.0 \text{ W/m}^2\text{K} = 55.7 \text{ Btu/ft}^2\text{hr } ^\circ\text{F} \end{aligned}$$

For the Whole Condenser

$$\text{LMTDT} = \frac{(66.4-27.4)}{\ln \frac{(102.6-27.4)}{(102.6-66.4)}} = 53.3^\circ\text{C} = 95.9^\circ\text{F}$$

$$\begin{aligned} U_{o,T} &= Q_{\text{TOT}} / \text{LMTDT} * 3 * A_o = (3.012) / (55.3 * 3 * 0.058) \\ &= 0.325 \text{ KJ/m}^2\text{S K} = 325.0 \text{ W/m}^2\text{S K} = 57.1 \text{ Btu/ft}^2\text{hr } ^\circ\text{F} \end{aligned}$$

8. Wall Temperature



Let U'_A = the heat transfer coefficient from the condensate film to the inner wall of the inner tube based on the outside area of the inner tube.

$$U'_A = 1/[A_o/A_i * h_c] = 1/[d_o/d_i * h_c] = (0.025 * h_c)/0.028$$

Let U_B = the heat transfer coefficient from the vapor-condensate interface to the outer wall of the inner tube based on the outside area of the inner tube.

$$U_B = \frac{1}{\frac{0.028}{0.025 * h_c} + \frac{0.014 \ln (0.028/0.025)}{k_w}}$$

The term $\frac{0.014 \ln (0.028/0.025)}{k_w}$ is the wall

resistance (WR)

Let U_c = the overall heat transfer coefficient from the condensate film to the cooling water in the annular jacket

$$U_c = \frac{1}{\frac{0.028}{0.025 h_c} + WR + \frac{1}{h_o}}$$

However, the amount of heat passing through each surface is the same. Consequently

$$U_c * (T_{sat} - T_{cw,avg}) = U_B (T_{sat} - T_{w,o})$$

or

$$T_{w,o} = T_{sat} - \frac{U_c (T_{sat} - T_{cw,avg})}{U_B}$$

in which

$T_{cw,avg}$ = average temperature of inlet and outlet
cooling water temperature in the top section
of the reflux condenser, °C

$T_{w,o}$ = outer wall temperature, °C

And

$$U_c (T_{sat} - T_{cw,avg}) = U'_A (T_{sat} - T_{w,i})$$

or

$$T_{w,i} = T_{sat} - \frac{U_c (T_{sat} - T_{cw,avg})}{U'_A}$$

in which

$T_{w,i}$ = inner wall temperature, °C

This is an trial and error process, first just simply guess that both the inner and outer wall temperature are the average temperature of T_{sat} and $T_{cw,avg}$, then use these temperature to calculate h_c , h_o , and wall resistance. Thus the new $T_{w,o}$ and $T_{w,i}$ are computed, if $|T_{new} - T_{old}| < 0.01$, this new value is the correct temperature and h_c , h_o , and WR will be calculated from these new temperatures. If not reiterate until $|T_{new} - T_{old}| < 0.01$. Repeat the same process for each section of the reflux condenser.

After trial and error, we find that:

At the Top Section

$$T_{w,o} = 78.8 \text{ } ^\circ\text{C} = 173.8 \text{ } ^\circ\text{F}$$

$$T_{w,i} = 100.8 \text{ } ^\circ\text{C} = 213.5 \text{ } ^\circ\text{F}$$

$$T_{w,avg} = 89.8 \text{ } ^\circ\text{C} = 193.6 \text{ } ^\circ\text{F}$$

At the Middle Section

$$T_{w,o} = 72.5^{\circ}\text{C} = 162.4^{\circ}\text{F}$$

$$T_{w,i} = 100.2^{\circ}\text{C} = 212.4^{\circ}\text{F}$$

$$T_{w,avg} = 86.3^{\circ}\text{C} = 187.4^{\circ}\text{F}$$

At the Bottom Section

$$T_{w,o} = 65.2^{\circ}\text{C} = 149.3^{\circ}\text{F}$$

$$T_{w,i} = 99.5^{\circ}\text{C} = 211.1^{\circ}\text{F}$$

$$T_{w,avg} = 82.3^{\circ}\text{C} = 180.2^{\circ}\text{F}$$

9. Thermal Conductivity of Pyrex Glass

By a curve fit, the correlation for thermal conductivity of pyrex glass in terms of temperature ($^{\circ}\text{C}$) is

$$k_w = (-0.00005 \cdot T^2 + 0.045 \cdot T + 26) \cdot (4.181 \times 10^{-5}) \text{ KJ/m s K}$$

$$T = T_{w,avg} = \text{average wall temperature, } ^{\circ}\text{C}$$

At the Top Section, $T_{w,avg} = 89.8^{\circ}\text{C}$

So

$$\begin{aligned} k_w &= [(-0.00005)(89.8)^2 + (0.045)(89.8) + 26] (4.181 \times 10^{-5}) \\ &= 1.24 \times 10^{-3} \text{ KJ/m s K} = 0.72 \text{ Btu/ft hr } ^{\circ}\text{F} \end{aligned}$$

At the Middle Section, $T_{w,avg} = 86.3^{\circ}\text{C}$

So

$$\begin{aligned} k_w &= [(-0.00005)(86.3)^2 + (0.045)(86.3) + 26] (4.181 \times 10^{-5}) \\ &= 1.23 \times 10^{-3} \text{ KJ/m s K} = 0.71 \text{ Btu/ft hr } ^{\circ}\text{F} \end{aligned}$$

At the Bottom Section, $T_{w,avg} = 82.3^{\circ}\text{C}$

So

$$\begin{aligned} k_w &= [(-0.00005)(82.3)^2 + (0.045)(82.3) + 26] (4.181 \times 10^{-5}) \\ &= 1.23 \times 10^{-3} \text{ KJ/m s K} = 0.71 \text{ Btu/ft hr } ^{\circ}\text{F} \end{aligned}$$

10. Wall Resistance

$$\text{wall resistance} = [r_o \ln (r_o/r_i)]/k_w$$

where

$$r_o = \text{outside radius of the inner column} = 0.014 \text{ m}$$

$$r_i = \text{inside radius of the inner column} = 0.0125 \text{ m}$$

So

$$\text{wall resistance} = [0.014 \ln (0.014/0.0125)]/k_w$$

$$\text{At the Top Section, wall resistance} = 1.28 \text{ m}^2 \text{ s K/KJ}$$

$$= 7.27 \times 10^{-3} \text{ ft}^2 \text{ s } ^\circ\text{F/Btu}$$

$$\text{At the Middle Section, wall resistance} = 1.29 \text{ m}^2 \text{ s K/KJ}$$

$$= 7.33 \times 10^{-3} \text{ ft}^2 \text{ s } ^\circ\text{F/Btu}$$

$$\text{At the Bottom Section, wall resistance} = 1.29 \text{ m}^2 \text{ s K/KJ}$$

$$= 7.33 \times 10^{-3} \text{ ft}^2 \text{ s } ^\circ\text{F/Btu}$$

11. Wilson Line Method

$$\frac{1}{U_o} = \frac{1}{h_o} + \frac{r_o \ln (r_o/r_i)}{k_w} + \frac{A_o}{h_c A_i}$$

In the annulus, $h_o \propto V^{0.45}$ where V = cooling water velocity (m/s). The value of $1/U_o$ ($\text{m}^2 \text{ s K/KJ}$) was plotted with respect to $1/V^{0.45}$ ($\text{s/m}^{0.45}$) resulting in a straight line with the slope m and intercept, $\{[r_o \ln (r_o/r_i)]/k_w + (A_o/A_i h_c)\}$. Thus,

$$1/h_o = m/V^{0.45}$$

or

$$h_o = V^{0.45}/m$$

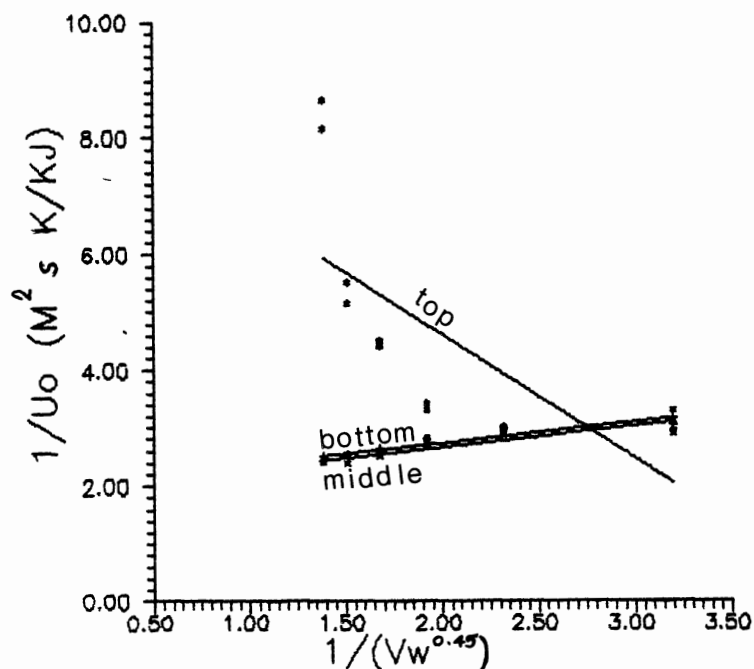
and

$$h_c = A_o/[A_i (\text{intercept} - \text{wall resistance})]$$

(based on outside surface area of the inner tube)

At the Top Section

In this section, the Wilson line method results in negative value of h_o which is impossible (see the following figure). This is probably because all vapor has already condensed so that in some part of the wall of the top section is dry and effectively transferring no heat.



At the Middle Section

From the linear curve, we get

$$1/U_{o,2} = 0.285425(1/V^{0.45}) + 1.90832$$

So

$$\begin{aligned} h_o &= V^{0.45}/\text{slope} = (40.32 \times 10^{-3})^{0.45}/0.285415 \\ &= 0.826 \text{ KJ/m}^2 \text{ s K} \end{aligned}$$

$$\begin{aligned} h_c &= (0.014/0.0125) * [1/(1.90832 - 1.2339)] \\ &= 1.661 \text{ KJ/m}^2 \text{ s K} \end{aligned}$$

At the Bottom Section

From the linear curve., we get

$$1/U_{o,3} = 0.279753(1/V^{0.45}) + 1.99675$$

So

$$\begin{aligned} h_o &= V^{0.45}/\text{slope} = (40.32 \times 10^{-3})^{0.45}/0.279753 \\ &= 0.843 \text{ KJ/m}^2 \text{ s K} \end{aligned}$$

$$\begin{aligned} h_c &= (0.014/0.0125) * [1/(1.99675 - 1.2922)] \\ &= 1.590 \text{ KJ/m}^2 \text{ s K} \end{aligned}$$

Calculations from the Literature Methods

1. Water Side Heat Transfer Coefficient

In an annulus, the calculation of h_o is performed according to the Chen, Hawkins, and Solberg (7) correlation:

$$\frac{h_o D_{eq}}{k} = 1.02 (Re)^{0.45} (Pr_1)^{1/3} (\mu/\mu_w)^{0.14} (D_{eq}/L)^{0.4} (D_1/D_2)^{0.8} Gr^{0.05}$$

In this case, D_{eq} is an equivalent diameter calculated as:

$$\begin{aligned}
 D_{eq} &= \text{outer diameter of an annulus (D1)} - \\
 &\quad \text{inner diameter of an annulus (D2)} \\
 &= 0.037 - 0.028 = 9 \times 10^{-3} \text{ m}
 \end{aligned}$$

At the Top Section

The average temperature of cooling water in this section is 61.1°C or 142.0°F

The physical properties at 142.0°F are as follows:

$$\rho_1 = 983.5 \text{ Kg/m}^3$$

$$\nu = 4.66 \times 10^{-7} \text{ m}^2/\text{s}$$

$$\mu = 4.58 \times 10^{-4} \text{ Kg/m s}$$

$$\text{Re} = (9 \times 10^{-3}) (4.03 \times 10^{-2}) / (4.66 \times 10^{-7}) = 779$$

$$\text{Pr}_1 = 2.96$$

$$k = 6.61 \times 10^{-4} \text{ KJ/m s K}$$

$$\beta = 5.27 \times 10^{-4} \text{ 1/}^\circ\text{C}$$

$$\Delta T = T_{w, \text{avg}} - T_{cw, \text{avg}} = 89.8.6 - 61.1 = 28.7^\circ\text{C}$$

$$\begin{aligned}
 \text{Gr} &= (D_{eq}^3 \rho_1^2 \beta g \Delta T) / \mu^2 \\
 &= \frac{[(9 \times 10^{-3})^3 (983.5)^2 (5.27 \times 10^{-4}) (9.81) (28.7)]}{(4.58 \times 10^{-4})^2} \\
 &= 5.0 \times 10^5
 \end{aligned}$$

$$\text{At } T_{w, o} = 78.8^\circ\text{C},$$

$$\rho_v = 973.9 \text{ Kg/m}^3$$

$$\nu_v = 3.75 \times 10^{-7} \text{ m}^2/\text{s}$$

$$\mu_v = 3.65 \times 10^{-4} \text{ Kg/m s}$$

Thus

$$\begin{aligned}
 h_o &= \left[\frac{6.61 \times 10^{-4}}{9 \times 10^{-3}} \right] (1.02) (779)^{0.45} (2.96)^{1/3} \left[\frac{4.85 \times 10^{-4}}{3.65 \times 10^{-4}} \right]^{0.14} \\
 &\quad \left[\frac{9 \times 10^{-3}}{0.657} \right]^{0.4} \left[\frac{0.037}{0.028} \right]^{0.8} (5.0 \times 10^5)^{0.05} \\
 &= 0.970 \text{ KJ/m}^2 \text{ s K} = 171 \text{ Btu/ft}^2 \text{ hr } ^\circ\text{F}
 \end{aligned}$$

At the Middle Section

The average temperature of cooling water in this section is $49.6^\circ\text{C} = 121.2^\circ\text{F}$

The physical properties at this temperature are as follows:

$$\rho_l = 988.6 \text{ Kg/m}^3$$

$$\nu = 5.53 \times 10^{-7} \text{ m}^2/\text{s}$$

$$\mu = 5.46 \times 10^{-4} \text{ Kg/m s}$$

$$\text{Re} = (9 \times 10^{-3}) (4.03 \times 10^{-2}) / (5.53 \times 10^{-7}) = 656$$

$$\text{Pr}_l = 3.59$$

$$\beta = 4.43 \times 10^{-4} \text{ 1/}^\circ\text{C}$$

$$k = 6.46 \times 10^{-4} \text{ KJ/m s K}$$

$$\Delta T = 86.3 - 49.6 = 36.7^\circ\text{C}$$

$$\begin{aligned}
 \text{Gr} &= (D_{eq}^3 \rho_l^2 \beta g \Delta T) / \mu^2 \\
 &= \frac{[(9 \times 10^{-3}) (988.6)^2 (4.43 \times 10^{-4}) (9.81) (36.7)]}{(5.46 \times 10^{-4})^2} \\
 &= 3.8 \times 10^5
 \end{aligned}$$

$$\text{At } T_{w,o} = 81.5^\circ\text{C},$$

$$\rho_v = 977.6 \text{ Kg/m}^3$$

$$\nu_v = 4.03 \times 10^{-7} \text{ m}^2/\text{s}$$

$$\mu_v = 3.94 \times 10^{-4} \text{ Kg/m s}$$

Thus

$$\begin{aligned}
 h_o &= \left[\frac{6.46 \times 10^{-4}}{9 \times 10^{-3}} \right] (1.02) (656)^{0.45} (3.59)^{1/3} \left[\frac{5.46 \times 10^{-4}}{3.94 \times 10^{-4}} \right]^{0.14} \\
 &\quad \left[\frac{9 \times 10^{-3}}{0.657} \right]^{0.4} \left[\frac{0.037}{0.028} \right]^{0.8} (3.8 \times 10^5)^{0.05} \\
 &= 0.929 \text{ KJ/m}^2 \text{ s K} = 164 \text{ Btu/ft}^2 \text{ hr } ^\circ\text{F}
 \end{aligned}$$

At the Bottom Section

The average temperature of cooling water in this section is $35.3^\circ\text{C} = 95.6^\circ\text{F}$

The physical properties at this temperature are as follows:

$$\rho_1 = 993.6 \text{ Kg/m}^3$$

$$\nu = 7.14 \times 10^{-7} \text{ m}^2/\text{s}$$

$$\mu = 7.10 \times 10^{-4} \text{ Kg/m s}$$

$$\text{Re} = (9 \times 10^{-3}) (4.03 \times 10^{-3}) / (7.14 \times 10^{-7}) = 508$$

$$\text{Pr}_1 = 4.81$$

$$\beta = 3.29 \times 10^{-4} \text{ 1/}^\circ\text{C}$$

$$k = 6.23 \times 10^{-4} \text{ KJ/m s K}$$

$$\Delta T = 82.3 - 35.3 = 47.0^\circ\text{C}$$

$$\begin{aligned}
 \text{Gr} &= (D_{\text{eq}}^3 \rho_1^2 \beta g \Delta T) / \mu^2 \\
 &= \frac{[(9 \times 10^{-3})^3 (993.6)^2 (3.29 \times 10^{-4}) (9.81) (47.0)]}{(7.10 \times 10^{-4})^2}
 \end{aligned}$$

$$= 2.2 \times 10^5$$

$$\text{At } T_{w,o} = 65.2^\circ\text{C},$$

$$\rho_v = 981.5 \text{ Kg/m}^3$$

$$\nu_v = 4.41 \times 10^{-7} \text{ m}^2/\text{s}$$

$$\mu_v = 4.33 \times 10^{-4} \text{ Kg/m s}$$

Thus

$$\begin{aligned}
 h_o &= \left[\frac{6.23 \times 10^{-4}}{9 \times 10^{-3}} \right] (1.02) (508)^{0.45} (4.81)^{1/3} \left[\frac{7.10 \times 10^{-4}}{4.333 \times 10^{-4}} \right]^{0.14} \\
 &\quad \left[\frac{9 \times 10^{-3}}{0.657} \right]^{0.4} \left[\frac{0.037}{0.028} \right]^{0.8} (2.2 \times 10^5)^{0.05} \\
 &= 0.876 \text{ KJ/m}^2 \text{ s K} = 154 \text{ Btu/ft}^2 \text{ hr } ^\circ\text{F}
 \end{aligned}$$

2. Condensate Film Side Heat Transfer Coefficient

For Gravity Control

- Laminar Flow

$$h_c = 0.943 \left[\frac{k_l^3 \rho_l (\rho_l - \rho_v) \lambda g}{\mu_l L (T_{\text{sat}} - T_{w,i})} \right]^{1/4}$$

Turbulent Flow

$$h_c = 0.0089 \text{Pr}_l^{-0.55} \text{Re}_c^{0.35} \text{Pr}_l^{0.2} \left[\frac{k_l^3 \rho_l (\rho_l - \rho_v) g}{\mu_l^2} \right]^{1/3}$$

For Vapor Shear Control

$$h_c = \frac{k_l}{d_i} (0.024) \text{Re}^{0.8} \text{Pr}^{0.44} \left[\frac{\sqrt{(\rho/\rho_m)_i} + \sqrt{(\rho/\rho_m)_o}}{\mu_l^2} \right]$$

Calculate h_c from those equations, and choose the highest one.

At the Top Section

Mass flow rate of condensate in this section

= mass flow rate of first condensate - $(Q_2 + Q_3)/\lambda$

= $1.49 \times 10^{-3} - (0.975 + 1.227)/2250$

= $5.13 \times 10^{-4} \text{ Kg/s}$

$$Re_c = 4(\text{mass flow rate of condensate}) / \pi d_i \mu_l$$

where

$$d_i = \text{inside diameter of the inner column} = 0.025 \text{ m}$$

$$T_{\text{sat}} = 102.6 \text{ } ^\circ\text{C}$$

$$\mu_l = 2.83 \times 10^{-4} \text{ Kg/s}$$

Then

$$Re_c = (4 \times 5.138 \times 10^{-4}) / [\pi (0.025) (2.83 \times 10^{-4})] = 92$$

That means it is in the laminar region

For gravity control

$$h_c = 0.943 \left[\frac{k_l^3 \rho_l (\rho_l - \rho_v) \lambda g}{\mu_l L (T_{\text{sat}} - T_{w,i})} \right]^{1/4}$$

$$T_{\text{sat}} = 102.6 \text{ } ^\circ\text{C}$$

$$\lambda = 2250 \text{ KJ/Kg}$$

$$k_l = 6.82 \times 10^{-4} \text{ KJ/m s K}$$

$$\rho_v = 0.657 \text{ Kg/m}^3$$

$$\rho_l = 956.1 \text{ Kg/m}^3$$

$$Pr_l = 1.76$$

$$T_{w,i} = 213.5 \text{ } ^\circ\text{F} = 100.8 \text{ } ^\circ\text{C}$$

$$L = \text{condensing length} = 0.657 \text{ m}$$

Consequently

$$h_c = 0.943 \left[\frac{(6.82 \times 10^{-4})^3 (956.1) (956.1 - 0.657) (2250) (9.81)}{(2.83 \times 10^{-4}) (0.657) (102.6 - 100.8)} \right]^{1/4}$$

$$= 11.195 \text{ KJ/m}^2 \text{ s K} = 1971 \text{ Btu/ft}^2 \text{ hr } ^\circ\text{F}$$

Vapor shear control

$$x_i = [\text{total mass flow rate} - (Q_2+Q_3)/\lambda] / \text{total mass flow rate}$$

in which

$$\begin{aligned} \text{total mass flow rate} = & \text{mass flow rate of first condensate} + \\ & \text{mass flow rate of second condensate} + \\ & \text{mass flow rate of entrained liquid} \end{aligned}$$

Thus

$$\begin{aligned} x_i &= \frac{\{(1.49 \times 10^{-3} + 0 + 0) - [(0.975 + 1.227)/2250]\}}{1.49 \times 10^{-3}} \\ &= 0.34 \end{aligned}$$

$$\begin{aligned} x_o &= \frac{\text{total mass flow rate} - (Q_1+Q_2+Q_3)/\lambda}{\text{total mass flow rate}} \\ &= \frac{1.49 \times 10^{-3} - [(0.810 + 0.975 + 1.227)/2250]}{1.49 \times 10^{-3}} \\ &= 0.10 \end{aligned}$$

$$\begin{aligned} (\rho/\rho_m)_i &= 1 + \frac{(\rho_l - \rho_v)x_i}{\rho_v} = 1 + \frac{(956.1 - 0.657)(0.34)}{0.657} \\ &= 501.0 \end{aligned}$$

$$\begin{aligned} (\rho/\rho_m)_o &= 1 + \frac{(\rho_l - \rho_v)x_o}{\rho_v} = 1 + \frac{(956.1 - 0.657)(0.10)}{0.657} \\ &= 150.1 \end{aligned}$$

$$\begin{aligned}
 h_c &= \frac{k_l}{d_i} (0.024) (Re_c)^{0.8} (Pr)^{0.43} \left[\frac{\sqrt{(\rho/\rho_m)_i} + \sqrt{(\rho/\rho_m)_o}}{2} \right] \\
 &= \frac{(6.82 \times 10^{-4})}{0.025} (0.024) (92)^{0.8} (1.76)^{0.43} \left[\frac{\sqrt{501.0} + \sqrt{150.1}}{2} \right] \\
 &= 0.540 \text{ KJ/m}^2 \text{ s K}
 \end{aligned}$$

Therefore, this is gravity controlled and $h_c = 11.202 \text{ KJ/m}^2 \text{ s K}$

At the Middle Section

The inner wall temperature in this section = 100.2°C

Mass flow rate of condensate in this section

= mass flow rate of first condensate - Q_3/λ

$$= 1.49 \times 10^{-3} - 1.227/2250$$

$$= 9.46 \times 10^{-4} \text{ Kg/s}$$

$$Re_c = 4(\text{mass flow rate of condensate}) / \pi d_i \mu_l$$

Thus

$$Re_c = (4 \times 9.46 \times 10^{-4}) / [\pi (0.025) (2.83 \times 10^{-4})] = 171, \text{ i.e.,}$$

laminar.

For gravity control

$$\begin{aligned}
 h_c &= 0.943 \left[\frac{k_l^3 \rho_l (\rho_l - \rho_v) \lambda g}{\mu_l L (T_{\text{sat}} - T_{w,i})} \right]^{1/4} \\
 h_c &= 0.943 \left[\frac{(6.82 \times 10^{-4})^3 (956.1) (956.1 - 0.657) (2250) (9.81)}{(2.83 \times 10^{-4}) (2) (0.657) (102.6 - 100.2)} \right]^{1/4} \\
 &= 8.274 \text{ KJ/m}^2 \text{ s K} = 1457 \text{ Btu/ft}^2 \text{ hr } ^\circ \text{F}
 \end{aligned}$$

Vapor shear control

$$\begin{aligned}
 x_i &= [\text{total mass flow rate} - Q3/\lambda] / \text{total mass flow rate} \\
 &= 9.46 \times 10^{-4} / 1.49 \times 10^{-3} = 0.63 \\
 (\rho/\rho_m)_i &= 1 + \frac{(\rho_l - \rho_v) x_i}{\rho_v} = 1 + \frac{(956.1 - 0.657)(0.63)}{0.657} \\
 &= 923.6 \\
 x_o &= 0.34
 \end{aligned}$$

$$(\rho/\rho_m)_o = 501.0$$

$$\begin{aligned}
 h_c &= \frac{k_l}{d_i} (0.024) (Re_c)^{0.8} (Pr)^{0.43} \left[\frac{\sqrt{(\rho/\rho_m)_i} + \sqrt{(\rho/\rho_m)_o}}{2} \right] \\
 &= \frac{(6.82 \times 10^{-4})}{0.025} (0.024) (171)^{0.8} (1.76)^{0.43} \left[\frac{\sqrt{501.0} + \sqrt{923.6}}{2} \right] \\
 &= 1.344 \text{ KJ/m}^2 \text{ s K} = 237 \text{ Btu/ft}^2 \text{ hr } ^\circ\text{F}
 \end{aligned}$$

Therefore, gravity controls, and $h_c = 10.388 \text{ KJ/m}^2 \text{ s K}$

At the Bottom Section

The inner wall temperature in this section = 99.5°C

Mass flow rate of condensate in this section

= mass flow rate of first condensate

$$= 1.49 \times 10^{-3} \text{ Kg/s}$$

$$\begin{aligned}
 Re_c &= 4(\text{mass flow rate of condensate}) / \pi d_i \mu_l \\
 &= (4 \times 1.49 \times 10^{-3}) / [\pi (0.025) (2.83 \times 10^{-4})] = 269
 \end{aligned}$$

That means it is in laminar region

For gravity control

$$h_c = 0.943 \left[\frac{k_l^3 \rho_l (\rho_l - \rho_v) \lambda g}{\mu_l L (T_{sat} - T_{w,i})} \right]^{1/4}$$

$$h_c = 0.943 \left[\frac{(6.82 \times 10^{-4})^3 (956.1) (956.1 - 0.657) (2250) (9.81)}{(2.83 \times 10^{-4}) (3) (0.657) (102.6 - 99.5)} \right]^{1/4}$$

$$= 6.769 \text{ KJ/m}^2 \text{ s K} = 1192 \text{ Btu/ft}^2 \text{ hr } ^\circ\text{F}$$

Vapor shear control

$$x_i = 1$$

$$\left(\frac{\rho}{\rho_m}\right)_i = 1 + \frac{(\rho_l - \rho_v) x_i}{\rho_v} = 1 + \frac{(956.1 - 0.657) (1)}{0.657}$$

$$= 1455.2$$

$$x_o = 0.63$$

$$\left(\frac{\rho}{\rho_m}\right)_o = 923.6$$

$$h_c = \frac{k_l}{d_i} (0.024) (Re_c)^{0.8} (Pr)^{0.43} \left[\frac{\sqrt{(\rho/\rho_m)_i} + \sqrt{(\rho/\rho_m)_o}}{2} \right]$$

$$= \frac{(6.82 \times 10^{-4})}{0.025} (0.024) (2698)^{0.8} (1.76)^{0.43} \left[\frac{\sqrt{1455.2} + \sqrt{923.6}}{2} \right]$$

$$= 2.511 \text{ KJ/m}^2 \text{ s K}$$

Therefore, this is gravity controlled and $h_c = 9.700 \text{ KJ/m}^2 \text{ s K}$

3. Overall Heat Transfer Coefficient from Literature Correlations

$$U_o = \frac{1}{1/h_o + \text{wall resistance} + 0.028/(0.025h_c)}$$

At the Top Section

$$h_o = 0.988 \text{ KJ/m}^2 \text{ s K}$$

$$h_c = 11.195 \text{ KJ/m}^2 \text{ s K}$$

$$\text{wall resistance} = 1.28 \text{ m}^2 \text{ s K/KJ}$$

Thus

$$U_o = \frac{1}{(1/0.988) + 1.28 + [0.028/(0.025*11.195)]}$$

$$= 0.416 \text{ KJ/m}^2 \text{ s K} = 73 \text{ Btu/ft}^2 \text{ hr } ^\circ\text{F}$$

At the Middle Section

$$h_o = 0.946 \text{ KJ/m}^2 \text{ s K}$$

$$h_c = 8.274 \text{ KJ/m}^2 \text{ s K}$$

$$\text{wall resistance} = 1.29 \text{ KJ/m}^2 \text{ s K}$$

Thus

$$U_o = \frac{1}{(1/0.946) + 1.29 + [0.028/(0.025*8.274)]}$$

$$= 0.403 \text{ KJ/m}^2 \text{ s K} = 71 \text{ Btu/ft}^2 \text{ hr } ^\circ\text{F}$$

At the Bottom Section

$$h_o = 0.891 \text{ KJ/m}^2 \text{ s K}$$

$$h_c = 6.769 \text{ KJ/m}^2 \text{ s K}$$

$$\text{wall resistance} = 1.29 \text{ KJ/m}^2 \text{ s K}$$

Thus

$$U_o = \frac{1}{(1/0.891) + 1.29 + [0.028/(0.025*6.769)]}$$

$$= 0.387 \text{ KJ/m}^2 \text{ s K} = 68 \text{ Btu/ft}^2 \text{ hr } ^\circ\text{F}$$

4. Effect of Wall Resistance on Overall Heat Transfer Coefficient

Overall heat transfer coefficient without wall resistance can be calculated as follows:

$$U_{ow} = \frac{1}{(1/h_o) + [0.028/(0.025h_c)]}$$

At the Top Section

$$U_{ow} = \frac{1}{(1/0.988) + [0.028/(0.025*11.195)]}$$

$$= 0.890 \text{ KJ/m}^2 \text{ s K} = 157 \text{ Btu/ft}^2 \text{ hr } ^\circ\text{F}$$

At the Middle Section

$$U_{ow} = \frac{1}{(1/0.946) + [0.028/(0.025*8.274)]}$$

$$= 0.837 \text{ KJ/m}^2 \text{ s K} = 147 \text{ Btu/ft}^2 \text{ hr } ^\circ\text{F}$$

At the Bottom Section

$$U_{ow} = \frac{1}{(1/0.891) + [0.028/(0.025*6.769)]}$$

$$= 0.775 \text{ KJ/m}^2 \text{ s K} = 136 \text{ Btu/ft}^2 \text{ hr } ^\circ\text{F}$$

We found that the overall heat transfer coefficient without wall resistance is about twice the overall heat transfer coefficient with wall resistance.

5. Flooding Point

There are many methods to calculate flooding point. Here we use the Diehl & Koppany and Wallis Methods.

Diehl & Koppany Method

$$V_v^* = F_1 \cdot F_2 (\sigma/\rho_v)^{0.5} \quad \text{if } F_1 \cdot F_2 (\sigma/\rho_v)^{0.5} > 10$$

$$V_v^* = 0.71 [F_1 \cdot F_2 (\sigma/\rho_v)^{0.15}]^{1.15} \quad \text{if } F_1 \cdot F_2 (\sigma/\rho_v)^{0.5} < 10$$

where

V_v^* = superficial flooding velocity of the vapor, ft/s

$$F_1 = [(12d_i/(\sigma/80))]^{0.4} \quad \text{if } [(12d_i/(\sigma/80))] < 1.0$$

$$= 1.0 \quad \text{if } [(12d_i/(\sigma/80))] \geq 1.0$$

$$F_2 = (G_v/G_1)^{0.25}$$

The equation is dimensional, so that it is essential to use the units specified:

$$\rho_v \text{ in lb}_m/\text{ft}^3$$

$$d_i \text{ in ft}$$

$$\sigma \text{ in dyne/cm}$$

Surface tension of water can be found in Perry's Chemical Engineers' Handbook. The correlation is:

$$\sigma = -0.000270661 \cdot T^2 - 0.141961 \cdot T + 75.6907$$

where σ is in dyne/cm and T is in $^{\circ}\text{C}$

At $P = 112.13$ KPa, T_{sat} is 102.6 °C and $\sigma = 58.3$ dyne/cm

G_v = superficial vapor velocity (m/s)

= { mass flow rate of first condensate +
mass flow rate of second condensate +
mass flow rate of entrained liquid } / $\rho_l * A_o$

G_l = superficial liquid velocity (m/s)

= mass flow rate of condensate in that section / $\rho_l * A_o$

Then

$$\frac{G_v}{G_l} = \frac{\text{mass flow rate of vapor in that section}}{\text{mass flow rate of condensate in that section}}$$

d_i = inside diameter of the inner column
= 0.025 m = 0.082 ft

At $P = 112.13$ KPa and $T = 102.6$ °C

$$\rho_v = 0.675 \text{ Kg/m}^3 = 0.041 \text{ lb/ft}^3$$

$$\rho_l = 956.1 \text{ Kg/m}^3$$

Consider at the bottom section because vapor is in at bottom section

Mass flow rate of vapor in this section = 1.49×10^{-3} Kg/s

Mass flow rate of condensate in this section

$$= (Q_1 + Q_2 + Q_3) / \lambda = (0.810 + 0.975 + 1.227) / 2250$$

$$= 1.34 \times 10^{-3} \text{ Kg/s}$$

Consider term $(12d_i) / (\sigma / 80)$

$$(12d_i) / (\sigma / 80) = (12 * 0.082) / (58.3 / 80) = 1.35 > 1.0$$

Then $F_1 = 1.0$

$$F_2 = (G_V/G_L)^{0.25} = (1.49 \times 10^{-3} / 1.339 \times 10^{-3})^{0.25} \\ = 1.027$$

So

$$F_1 \cdot F_2 (\sigma/\rho_V)^{0.5} = 1 \cdot 1.027 \cdot (58.3/0.041)^{0.5} = 38.74 > 10$$

Thus

$$V_V^* = F_1 \cdot F_2 (\sigma/\rho_V)^{0.5} = 38.74 \text{ ft/s} = 11.81 \text{ m/s}$$

Wallis Method

Wallis defines the following non-dimensional velocities,

$$J_V^* = \frac{V_V \rho_V^{1/2}}{[g d_i (\rho_L - \rho_V)]^{1/2}}$$

$$J_L^* = \frac{V_L \rho_L^{1/2}}{[g d_i (\rho_L - \rho_V)]^{1/2}}$$

where V_V and V_L are the superficial vapor and liquid velocities, respectively.

$$N_L = \left[\frac{\rho_L g d_i^3 (\rho_L - \rho_V)}{\mu_L^2} \right]^{1/2}$$

When gravity forces are far more important than viscous forces, N_L is high, and

$$m = 1$$

0.88 < c < 1 for round-edged tubes

c = 0.725 for sharp-edged tubes

When gravity forces can be neglected with respect to

viscous force, N_L is small and

$$m = 5.6 N_L^{-1/2}$$

$c = 0.725$ for round-edged tubes

Flooding points can be correlated by the following formula

$$J_V^{*1/2} + m J_L^{*1/2} = c$$

At $T_{\text{sat}} = 102.6^\circ\text{C}$, $\mu_1 = 6.57 \times 10^{-4} \text{ Kg/m s}$

Thus

$$N_L = \left[\frac{(956.1)(9.81)(0.025)^3(956.1 - 0.675)}{(6.57 \times 10^{-4})^2} \right]^{1/2}$$

$$= 1.8 \times 10^{-4}$$

Since N_L is large and gravity is more important than the viscous force, use $m = 1$. It is a round-edged tube, the approximate value of c from Figure 7 is 0.89.

So,

$$J_V^{*1/2} + J_L^{*1/2} = 0.89$$

By varying values of J_L^* and then calculating J_V^* , we get the curve of J_V^* vs. J_L^* . Since the vapor is in at the bottom section of the reflux condenser, consider only at the entrance or bottom section.

$$V_v = \text{inlet superficial vapor velocity} \\ = 4.624 \text{ m/s}$$

$$J_v^* = \frac{(4.624)(0.657)^{1/2}}{[(9.81)(0.025)(956.1-0.657)]^{1/2}} = 0.245$$

$$V_l = \frac{Q_1+Q_2+Q_3}{\lambda \rho_l A_i} = \frac{1.339 \times 10^{-3}}{(956.1)(\pi/4)(0.025)^2} \\ = 2.854 \times 10^{-3} \text{ m/s}$$

$$J_l^* = \frac{(2.854 \times 10^{-3})(956.1)^{1/2}}{[(9.81)(0.025)(956.1-0.657)]^{1/2}} = 0.006$$

APPENDIX D

ERROR ANALYSIS

Error Analysis

The error propagation analysis is done to evaluate the effect of errors in measurement on the calculated quantities, such as heat duty, wall resistance, and overall heat transfer coefficient. Due to the nature of the properties of the system studied, wall resistance calculations are most susceptible to large errors in calculated quantities.

In general, the propagated error associated with a quantity Y which is dependent on independent variables $X_1, X_2, X_3, \dots, X_n$ is calculated using the following expression:

$$\sigma_Y^2 = \left[\frac{\partial Y}{\partial X_1} \right]^2 \sigma_{X_1}^2 + \left[\frac{\partial Y}{\partial X_2} \right]^2 \sigma_{X_2}^2 + \dots + \left[\frac{\partial Y}{\partial X_n} \right]^2 \sigma_{X_n}^2 \quad (D.1)$$

and

$$\% \text{ error} = (\sigma_Y / Y) \times 100 \% \quad (D.2)$$

where σ_X represents the error associated with the quantity of X_n .

Using the above expression, the errors of the calculated quantities are calculated and were tabulated in the Table III.

TABLE III
ERROR ASSOCIATED WITH THE
CALCULATED QUANTITIES

| Quantities | Average % error |
|----------------------------|-----------------|
| Q, top section | 18 |
| Q, middle section | 17 |
| Q, bottom section | 13 |
| Q, total reflux condenser | 9 |
| Uo, top section | 20 |
| Uo, middle section | 20 |
| Uo, bottom section | 20 |
| Uo, total reflux condenser | 36 |
| Wall resistance | 50 |

Sample Calculations on Error Analysis

Q, top section (= Q₁)

Q₁ was calculated according to the following equation:

$$Q_1 = FW * DEN * c_p * (T4C - T3C)$$

DEN (density of cooling water) was calculated based on the average of the inlet (T3C) and outlet (T4C) temperature which are dependent on the reading temperature. If we assume that c_p is constant, Q₁ will only depend on FW (cooling water flow rate) and inlet/outlet temperature measurement (T4F and T3F). Therefore, error in calculating Q₁ can be evaluated, according to equation G.1, as:

$$\begin{aligned} \sigma_{Q1}^2 &= \sigma_{FW}^2 \{ DEN * c_p * (T4C - T3C) \}^2 \\ &+ \sigma_{T4F}^2 \left\{ \frac{\partial Q1}{\partial T4F} \right\}^2 + \sigma_{T3F}^2 \left\{ \frac{\partial Q1}{\partial T3F} \right\}^2 \end{aligned}$$

Because FW was obtained from the calibration equation, the error is also dependent on the error in the calibration curve (σ_{FW} is 3.15 cc/s, see Appendix A p.80). σ_{T4F} and σ_{T3F} were obtained from the error in the thermocouple calibration curves (about 0.60 °F and 0.68 °F, respectively, see Appendix B p.82).

Fitting equation for cooling water density is:

$$DEN = (-6.857 \times 10^{-5} T^2 + 2.667 \times 10^{-3} T + 62.402) \times 16.0185$$

where DEN is in Kg/m³ and T is evaluated at average cooling water temperature (in °F) or $T = (T3F + T4F)/2$.

$$T4C = (T4F - 32)/1.8 \text{ and } T3C = (T3F - 32)/1.8$$

So

$$\frac{\partial Q1}{\partial T3F} = FW * c_p * 16.0185 \left[(DEN/16.0185)(-1/1.8) + (T4C - T3C) \left(-\frac{6.857 \times 10^{-5}}{2} + \frac{2.667 \times 10^{-3}}{2} \right) \right]$$

$$\frac{\partial Q1}{\partial T4F} = FW * c_p * 16.0185 \left[(DEN/16.0185)(1/1.8) + (T4C - T3C) \left(-\frac{6.857 \times 10^{-5}}{2} + \frac{2.667 \times 10^{-3}}{2} \right) \right]$$

For run no 68:

$$FW = 1.858 \times 10^{-5} \text{ m}^3/\text{s}$$

$$T4C = 66.4 \text{ } ^\circ\text{C}$$

$$c_p = 4.19 \text{ KJ/Kg } ^\circ\text{C}$$

$$T3C = 55.9 \text{ } ^\circ\text{C}$$

$$DEN = 995.8 \text{ Kg/m}^3$$

$$Q1 = 0.810 \text{ KJ/s}$$

$$\frac{\partial Q1}{\partial T3F} = 1.858 \times 10^{-5} * 4.19 * 16.0185 \left[(995.8/16.0185)(-1/1.8) + 10.5 \left(-\frac{6.857 \times 10^{-5}}{2} + \frac{2.667 \times 10^{-3}}{2} \right) \right] = -0.043 \text{ KJ/sK}$$

$$\frac{\partial Q_1}{\partial T_{4F}} = 1.858 \times 10^{-5} * 4.19 * 16.0185 \left[(995.8/16.0185) (1/1.8) + 10.5 \left(\frac{-6.857 \times 10^{-5}}{2} + \frac{2.667 \times 10^{-9}}{2} \right) \right] = 0.043 \text{ KJ/sK}$$

So

$$\sigma_{Q1}^2 = (3.15 \times 10^{-6})^2 (995.8 * 4.19 * 10.5)^2 + (0.60)^2 (0.043)^2 + (0.68)^2 (-0.043)^2 = 0.021$$

$$\sigma_{Q1} = 0.143 \text{ KJ/s}$$

$$\% \text{ Error} = \frac{0.143}{0.810} \times 100 \% = 18 \%$$

The value presented in Table III is the average value of all runs.

σ_{Q2} and σ_{Q3} were calculated in the similar way as σ_{Q1} .

Q. middle section (= Q2)

For run no 68:

$$FW = 1.858 \times 10^{-5} \text{ m}^3/\text{s}$$

$$T_{3C} = 55.9 \text{ }^\circ\text{C}$$

$$c_p = 4.19 \text{ KJ/Kg }^\circ\text{C}$$

$$T_{2C} = 43.3 \text{ }^\circ\text{C}$$

$$DEN = 995.8 \text{ Kg/m}^3$$

$$Q_2 = 0.975 \text{ KJ/s}$$

$$\frac{\partial Q_2}{\partial T_{2F}} = 1.858 \times 10^{-5} * 4.19 * 16.0185 \left[(995.8/16.0185) (-1/1.8) + 12.6 \left(\frac{-6.857 \times 10^{-5}}{2} + \frac{2.667 \times 10^{-9}}{2} \right) \right] = -0.043 \text{ KJ/sK}$$

$$\frac{\partial Q_2}{\partial T_{3F}} = 1.858 \times 10^{-5} * 4.19 * 16.0185 \left[(995.8/16.0185) (1/1.8) + 12.6 \left(\frac{-6.857 \times 10^{-5}}{2} + \frac{2.667 \times 10^{-9}}{2} \right) \right] = 0.043 \text{ KJ/sK}$$

So

$$\sigma_{Q2}^2 = (3.15 \times 10^{-6})^2 (995.8 * 4.19 * 12.6)^2 + (0.68)^2 (0.043)^2 + (0.49)^2 (-0.043)^2 = 0.029$$

$$\sigma_{Q2} = 0.169 \text{ KJ/s}$$

$$\% \text{ Error} = \frac{0.169}{0.975} \times 100 \% = 17 \%$$

Q. bottom section (= Q3)

For run no 68:

$$FW = 1.858 \times 10^{-5} \text{ m}^3/\text{s}$$

$$T2C = 43.3 \text{ }^\circ\text{C}$$

$$c_p = 4.19 \text{ KJ/Kg } ^\circ\text{C}$$

$$T1C = 27.4 \text{ }^\circ\text{C}$$

$$DEN = 995.8 \text{ Kg/m}^3$$

$$Q3 = 1.227 \text{ KJ/s}$$

$$\frac{\partial Q3}{\partial T1F} = 1.858 \times 10^{-5} * 4.19 * 16.0185 \left[(995.8/16.0185) (-1/1.8) + 15.9 \left(-\frac{6.857 \times 10^{-5}}{2} + \frac{2.667 \times 10^{-3}}{2} \right) \right] = -0.043 \text{ KJ/sK}$$

$$\frac{\partial Q3}{\partial T2F} = 1.858 \times 10^{-5} * 4.19 * 16.0185 \left[(995.8/16.0185) (1/1.8) + 15.9 \left(-\frac{6.857 \times 10^{-5}}{2} + \frac{2.667 \times 10^{-3}}{2} \right) \right] = 0.043 \text{ KJ/sK}$$

So

$$\sigma_{Q3}^2 = (3.15 \times 10^{-6})^2 (995.8 * 4.19 * 15.9)^2 + (0.49)^2 (0.043)^2 + (0.51)^2 (-0.043)^2 = 0.045$$

$$\sigma_{Q3} = 0.211 \text{ KJ/s}$$

$$\% \text{ Error} = \frac{0.211}{1.227} \times 100 \% = 17 \%$$

Q, total reflux condenser

$$Q_{TOT} = Q1 + Q2 + Q3 = 3.012 \text{ KJ/s}$$

$$\sigma_{Q_{TOT}}^2 = \sigma_{Q1}^2 + \sigma_{Q2}^2 + \sigma_{Q3}^2 = 0.021 + 0.029 + 0.045 = 0.095$$

$$\sigma_{Q_{TOT}} = 0.308 \text{ KJ/s}$$

$$\% \text{ Error} = \frac{0.308}{3.012} \times 100 \% = 10 \%$$

U_o, top section

$$U_{o,1} = \frac{Q1}{A_o * LMTD1}$$

$$LMTD1 = \frac{T4C - T3C}{\ln \frac{(T_{sat} - T3C)}{(T_{sat} - T4C)}}$$

$$\sigma_{U_{o,1}}^2 = \sigma_{Q1}^2 \left(\frac{\partial U_{o,1}}{\partial Q1} \right)^2 + \sigma_{A_o}^2 \left(\frac{\partial U_{o,1}}{\partial A_o} \right)^2 + \sigma_{LMTD1}^2 \left(\frac{\partial U_{o,1}}{\partial LMTD1} \right)^2$$

$$A_o = \pi d_o L, \text{ therefore } \sigma_{A_o}^2 = \sigma_{d_o}^2 (\pi L)^2 + \sigma_L^2 (\pi d_o)^2$$

$$d_o = 0.028 \text{ m}; \quad \sigma_{d_o} = 0.0005 \text{ m (estimate, based on paralax)}$$

$$L = 0.657 \text{ m}; \quad \sigma_L = 1.6 \times 10^{-3} \text{ m (estimate, based on paralax)}$$

$$\sigma_{A_o}^2 = (0.0005)^2 (\pi \times 0.657)^2 + 1.6 \times 10^{-3} (\pi \times 0.028)^2 = 1.34 \times 10^{-5}$$

$$\sigma_{LMTD1}^2 = \sigma_{T4C}^2 \left(\frac{\partial LMTD1}{\partial T4C} \right)^2 + \sigma_{T3C}^2 \left(\frac{\partial LMTD1}{\partial T3C} \right)^2 + \sigma_{T_{sat}}^2 \left(\frac{\partial LMTD1}{\partial T_{sat}} \right)^2$$

$$\sigma_{T4C} = \sigma_{T4F} / 1.8 = 0.60 / 1.8 = 0.33 \text{ } ^\circ\text{C}$$

$$\sigma_{T3C} = \sigma_{T3F} / 1.8 = 0.68 / 1.8 = 0.38 \text{ } ^\circ\text{C}$$

$$T_{\text{sat}} = -4.658 \times 10^{-4} P^2 + 0.350 P + 69.155$$

$$\sigma_{T_{\text{sat}}}^2 = \sigma_P^2 \left(\frac{\partial T_{\text{sat}}}{\partial P} \right)^2 = \sigma_P^2 \{-2(4.658 \times 10^{-4}) P + 0.350\}^2$$

$$P = 3.3866 P_{\text{atm}} + 6.893 P_{\text{pg}} \quad (P \text{ in KPa})$$

$$\sigma_P^2 = \sigma_{P_{\text{atm}}}^2 \left(\frac{\partial P}{\partial P_{\text{atm}}} \right)^2 + \sigma_{P_{\text{pg}}}^2 \left(\frac{\partial P}{\partial P_{\text{pg}}} \right)^2$$

$$\sigma_{P_{\text{atm}}} = 0.005 \text{ in Hg (estimate based on paralax)}$$

$$\sigma_{P_{\text{pg}}} = 0.25 \text{ psig (estimate based on paralax)}$$

$$\sigma_P^2 = (0.005)^2 (3.3866)^2 + (0.25)^2 (6.893)^2 = 2.97 \text{ (KPa)}^2$$

$$\text{At } P = 112.13 \text{ KPa,}$$

$$\sigma_{T_{\text{sat}}}^2 = 2.97 \{-2 * 4.658 \times 10^{-4} * 112.13 + 0.350\}^2 = 0.054 \text{ (}^\circ\text{C)}^2$$

$$\left(\frac{\partial \text{LMTD1}}{\partial T_{4C}} \right) = \frac{\ln \left[\frac{T_{\text{sat}} - T_{3C}}{T_{\text{sat}} - T_{4C}} \right] - \left[\frac{T_{4C} - T_{3C}}{T_{\text{sat}} - T_{4C}} \right]}{\left[\ln \frac{T_{\text{sat}} - T_{3C}}{T_{\text{sat}} - T_{4C}} \right]^2} = -0.545$$

$$\text{for } T_{\text{sat}} = 102.55 \text{ }^\circ\text{C.}$$

$$\left(\frac{\partial \text{LMTD1}}{\partial T_{3C}} \right) = \frac{-\ln \left[\frac{T_{\text{sat}} - T_{3C}}{T_{\text{sat}} - T_{4C}} \right] + \left[\frac{T_{4C} - T_{3C}}{T_{\text{sat}} - T_{3C}} \right]}{\left[\ln \frac{T_{\text{sat}} - T_{3C}}{T_{\text{sat}} - T_{4C}} \right]^2} = -0.460$$

$$\left(\frac{\partial \text{LMTD1}}{\partial T_{\text{sat}}} \right) = \frac{\frac{(T_{4C} - T_{3C})^2}{(T_{\text{sat}} - T_{4C})(T_{\text{sat}} - T_{3C})}}{\left[\ln \frac{T_{\text{sat}} - T_{3C}}{T_{\text{sat}} - T_{4C}} \right]^2} = 1.005$$

$$\sigma_{\text{LMTD1}}^2 = (0.33)^2 (-0.545)^2 + (0.38)^2 (-0.46)^2 + 0.054 (1.005)^2 = 0.117$$

$$\sigma_{U_{o,1}}^2 = 0.021 \left(\frac{1}{A_o \text{LMTD1}} \right)^2 + 1.34 \times 10^{-5} \left(\frac{-Q1}{\text{LMTD1} A_o^2} \right)^2 + 0.117 \left(\frac{-Q1}{A_o \text{LMTD1}^2} \right)^2$$

For $A_o = 0.058 \text{ m}^2$, $\text{LMTD1} = 41.2^\circ\text{C}$ and $Q1 = 0.810 \text{ KJ/s}$

$$\sigma_{U_{o,1}}^2 = 4.14 \times 10^{-3} \quad \text{or} \quad \sigma_{U_{o,1}} = 0.06 \text{ KJ/m}^2\text{s K}$$

$$U_{o,1} = 0.339 \text{ KJ/m}^2\text{s K}$$

$$\% \text{ Error} = \frac{-0.06}{0.339} \times 100 \% = 18 \%$$

$U_{o, \text{middle section}}$

The same method as in $U_{o,1}$ was used in this calculation.

$$\sigma_{T3C} = 0.38^\circ\text{C}, \quad \sigma_{T2C} = 0.27^\circ\text{C}$$

$$\sigma_{T_{\text{sat}}}^2 = 0.054 (^\circ\text{C})^2$$

$$\frac{\partial \text{LMTD2}}{\partial T_{3C}} = -0.544,$$

$$\frac{\partial \text{LMTD2}}{\partial T_{2C}} = -0.459$$

$$\frac{\partial \text{LMTD}_2}{\partial T_{\text{sat}}} = 1.010$$

$$\sigma_{\text{LMTD}_2}^2 = 0.113 \text{ } (^{\circ}\text{C})^2$$

$$\sigma_{Q_2}^2 = 0.029$$

$$\sigma_{A_o}^2 = 1.34 \times 10^{-5}$$

Therefore,

$$\begin{aligned} \sigma_{U_{o,2}}^2 &= 0.029 \left(\frac{1}{0.058(52.72)} \right)^2 + 1.34 \times 10^{-5} \left(\frac{-0.975}{(52.72)(0.058)^2} \right)^2 \\ &\quad + 0.113 \left(\frac{-0.975}{(0.058)(52.72)^2} \right)^2 \\ &= 3.509 \times 10^{-9} \end{aligned}$$

$$\sigma_{U_{o,2}} = 0.059$$

$$U_{o,2} = 0.319 \text{ KJ/m}^2\text{s K}$$

$$\% \text{ Error} = \frac{0.059}{0.319} \times 100 \% = 19 \%$$

U_o, bottom section

The same method as in U_{o,1} was used in this calculation.

$$\sigma_{T_{2C}} = 0.27 \text{ } ^{\circ}\text{C},$$

$$\sigma_{T_{1C}} = 0.28 \text{ } ^{\circ}\text{C}$$

$$\sigma_{T_{\text{sat}}}^2 = 0.054 \text{ } (^{\circ}\text{C})^2$$

$$\frac{\partial \text{LMTD}_3}{\partial T_{2C}} = -0.550,$$

$$\frac{\partial \text{LMTD}_3}{\partial T_{1C}} = -0.458$$

$$\frac{\partial \text{LMTD}_3}{\partial T_{\text{sat}}} = 1.012$$

$$\sigma_{\text{LMTD}_3}^2 = 0.094 \text{ } (^{\circ}\text{C})^2$$

$$\sigma_{Q_3}^2 = 0.045$$

$$\sigma_{A_o}^2 = 1.34 \times 10^{-5}$$

Therefore,

$$\begin{aligned}\sigma_{U_{o,3}}^2 &= 0.045 \left(\frac{1}{0.058(66.92)} \right)^2 + 1.34 \times 10^{-5} \left(\frac{-1.227}{(66.92)(0.058)^2} \right)^2 \\ &\quad + 0.094 \left(\frac{-1.227}{(0.058)(66.92)^2} \right)^2 \\ &= 3.387 \times 10^{-3}\end{aligned}$$

$$\sigma_{U_{o,3}} = 0.058$$

$$U_{o,3} = 0.316 \text{ KJ/m}^2\text{s K}$$

$$\% \text{ Error} = \frac{0.058}{0.316} \times 100 \% = 18 \%$$

U_o,total reflux condenser

The same method as in U_{o,1} was used in this calculation.

$$\sigma_{T4C} = 0.33 \text{ }^\circ\text{C},$$

$$\sigma_{T1C} = 0.28 \text{ }^\circ\text{C}$$

$$\sigma_{T_{\text{sat}}}^2 = 0.054 \text{ (}^\circ\text{C)}^2$$

$$\frac{\partial \text{LMTDT}}{\partial T4C} = -0.649,$$

$$\frac{\partial \text{LMTDT}}{\partial T1C} = -0.397$$

$$\frac{\partial \text{LMTDT}}{\partial T_{\text{sat}}} = 1.047$$

$$\sigma_{\text{LMTDT}}^2 = 0.119 \text{ (}^\circ\text{C)}^2$$

$$\sigma_{Q_{\text{TOT}}}^2 = 0.095$$

$$\sigma_{A_o}^2 = 1.34 \times 10^{-5}$$

Therefore,

$$\begin{aligned}\sigma_{U_{o,T}}^2 &= 0.095 \left(\frac{1}{0.058(53.32)} \right)^2 + 1.34 \times 10^{-5} \left(\frac{-3.012}{(53.32)(0.058)^2} \right)^2 \\ &\quad + 0.119 \left(\frac{-3.012}{(0.058)(53.32)^2} \right)^2 \\ &= 0.0138\end{aligned}$$

$$\sigma_{U_{o,T}} = 0.117$$

$$U_{o,T} = 0.325 \text{ KJ/m}^2 \text{ s K}$$

$$\% \text{ Error} = \frac{0.117}{0.325} \times 100 \% = 36 \%$$

Wall resistance, at the top section

$$WR = \frac{r_o \ln(r_o/r_i)}{k_w}$$

$$\sigma_{WR}^2 = \sigma_{r_o}^2 \left(\frac{\partial WR}{\partial r_o} \right)^2 + \sigma_{r_i}^2 \left(\frac{\partial WR}{\partial r_i} \right)^2 + \sigma_{k_w}^2 \left(\frac{\partial WR}{\partial k_w} \right)^2$$

$$\sigma_{r_i} = \sigma_{r_o} = 0.0005 \text{ m (estimate)}$$

$$\sigma_{k_w} = 10 \% \text{ of } k_w \text{ (estimated based on reference 24)}$$

$$\text{For } r_o = 0.028 \text{ m, } r_i = 0.025 \text{ m and } k_w = 1.24 \text{ J/m s K}$$

$$\begin{aligned}\sigma_{WR}^2 &= (0.0005)^2 \left\{ \frac{1}{1.24} \left(1 + \ln \frac{0.028}{0.025} \right) \right\}^2 \\ &\quad + (0.0005)^2 \left\{ \frac{0.028}{(0.025)(1.24)} \right\}^2 \\ &\quad + (0.124)^2 \left\{ \frac{-0.028 \ln(0.028/0.025)}{1.24} \right\}^2 = 4.71 \times 10^{-7}\end{aligned}$$

$$\sigma_{WR} = 6.863 \times 10^{-4} \text{ m}^2 \text{ s K/J} = 0.686 \text{ m}^2 \text{ s K/KJ}$$

$$WR = 1.280 \text{ m}^2 \text{ s K/KJ}$$

$$\% \text{ error} = \frac{0.686}{1.280} \times 100 \% = 54 \%$$

2

VITA

Somporn Komolsirikul

Candidate for the Degree of
Master of Science

Thesis: FILMWISE CONDENSATION IN A VERTICAL TUBE
IN COUNTER-CURRENT AND CO-CURRENT FLOW

Major Field: Chemical Engineering

Biographical:

Personal Data: Born in Bangkok, Thailand, June 22,
1967, the daughter of Puttichai and Ratchada
Komolsirikul.

Education: Received Bachelor of Science Degree in
Chemical Engineering from Chulalongkorn
University in March, 1988; completed requirements
for the Master of Science degree at Oklahoma State
University in July, 1991.